1 8 2
3-24-76

Dwr. #2

UCRL-51988

GAS-INITIATED CRACK PROPAGATION IN A POROUS SOLID

MASTER

John H. Pitts

Ph. D. Thesis

January 15, 1976

Prepared for U.S. Energy Research & Development Administration under contract No. W-7405-Eng-48

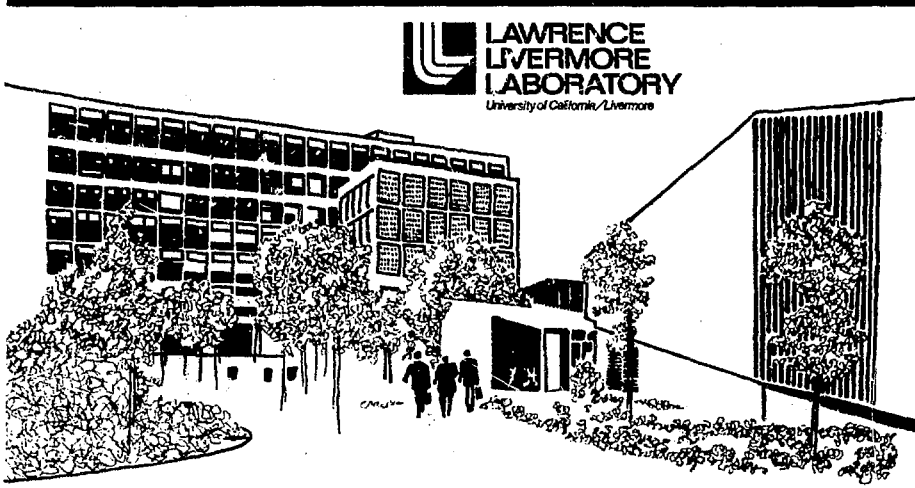

Printed in the United States of America
Available from
National Technical Information Service
U. S. Department of Commerce
5285 Port Royal Road
Springfield, Virginia 22151
Price: Printed Copy $___*; Microfiche $2.25

*Pages	NTIS Selling Price
1-50	$4.00
51-150	$5.45
151-325	$7.60
326-500	$10.60
501-1000	$13.60

Distribution Category
UC-11

LAWRENCE LIVERMORE LABORATORY
University of California Livermore, California 94550

UCRL-51988

GAS-INITIATED CRACK PROPAGATION IN A POROUS SOLID

John H. Pitts

Ph. D. Thesis

Ms. Date: December 31, 1975

Contents

GAS-INITIATED CRACK PROPAGATION IN A POROUS SOLID

Abstract

The propagation of a crack in porous earth formations following an experimental underground nuclear explosion is analyzed. The three-dimensional analysis includes interaction of gas pressure within the crack, permeation of gas into the porous earth formation, deflection of the crack walls, and crack propagation. Effects of permeability, k, from 10^{-6} to 0.1 $(\mu m)^2$ [1 $(\mu m)^2 \approx$ 1 Darcy], initial crack length and width up to 110 and 170 m, and ratio of maximum earth formation resistive pressure to initial driving pressure, $P_{r_{max}}/P_1$, from 0.1 to 0.9 are delineated. Propagation of a crack to the earth's surface following a typical experimental underground nuclear explosion buried at a depth of 500 m occurs only under unlikely conditions, such as when $k = 10^{-4}$ $(\mu m)^2$ and $P_{r_{max}}/P_1 = 0.75$.

Introduction

Safety and environmental considerations require that radioactive contaminants be contained below the earth's surface following an experimental underground nuclear explosion, or following proposed nuclear stimulation of tight subterranean gas reservoirs. To insure that nuclear testing and stimulation can be carried out safely, methods need to be available to determine the flow of radioactive gases through the interstices and cracks of the earth formations. This paper describes one potential release mechanism which involves propagation of a crack in an earth formation through which radioactive gases might vent to the atmosphere.

Consider the experimental underground nuclear explosion shown at the top of Fig. 1. A large amount of energy is released almost instantaneously at the time of the explosion and all matter in the immediate vicinity of the explosion is vaporized. Within a second or two an underground cavity is formed which is filled with radioactive gases at, or slightly above, the earth formation overburden pressure. These radioactive gases permeate the

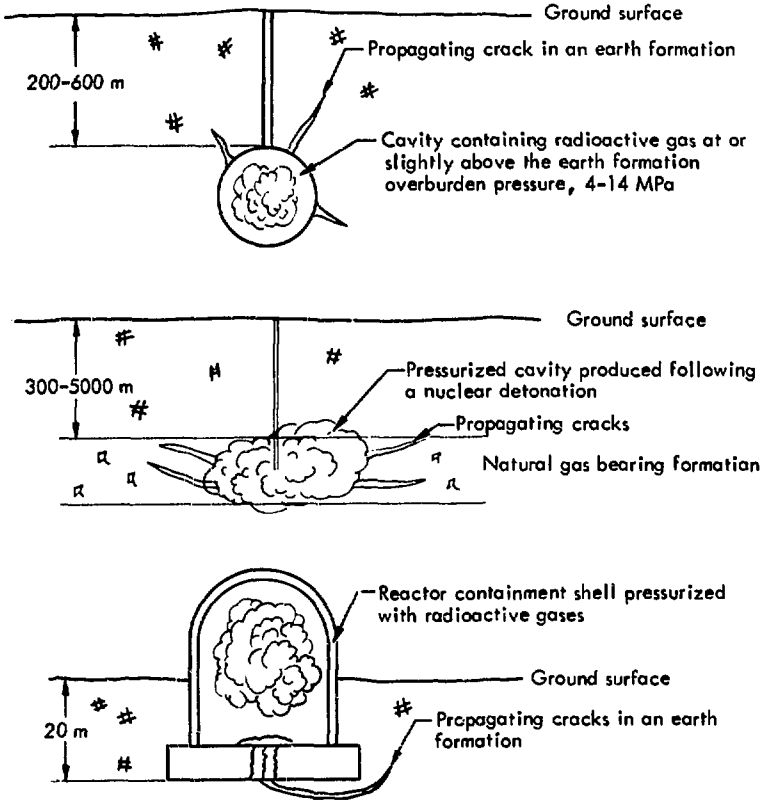

Fig. 1. Three examples of gas-initiated crack propagation.

earth formation and also flow into cracks formed during the same time period as the formation of the underground cavity. Forces due to gas pressure within the cracks may cause the cracks to be enlarged. Should the enlarged cracks propagate to the surface of the earth, they would form open passages through which radioactive contaminants could reach the atmosphere.

A second example of a potential vent to the atmosphere is shown in the middle portion of Fig. 1 where a gas bearing formation is fractured by detonating a nuclear charge. Nuclear fracturing has been carried out on an experimental basis and is being

considered for use with tight and deep formations where it might not be economical to produce natural gas by other means[1,2]. Although we wish to form many large fractures in the gas bearing formation, we need to insure that the fractures do not extend to the surface of the earth and vent radioactive material. Hence, before gas stimulation can be performed safely, the growth pattern of fractures leading to the surface needs to be computed.

A third application involves the analysis of a hypothetical accident in a nuclear power generating station. Should a loss-of-coolant accident ever occur, with subsequent core meltdown, the floor of the containment shell (below the earth's surface) could be cracked by ensuing thermal stresses as shown schematically in the bottom portion of Fig. 1. Radioactive gases from the reactor could be released into the surrounding earth formation through this break in the containment shell. Any cracks present in the earth formation could then be extended to the surface of the earth and form passages through which radioactive gases might reach the atmosphere.

Our objective is to determine the conditions under which a pre-existing crack in a porous earth formation will propagate when exposed to high pressure gas. This apparently is the first study that shows the interaction of gas pressure within the crack, permeation of the gas into the earth formation, deflection of the crack wall, and the phenomenon of crack propagation.

Although three applications have been indicated, our main interest is in containing radioactive contaminants below the earth's surface following an experimental underground nuclear explosion.

At the Nevada Test Site (NTS) of the Lawrence Livermore Laboratory, the most common earth formation in which experimental underground nuclear tests are conducted, is alluvium. This alluvium has a permeability ranging from 10^{-2} to $1(\mu m)^2$ [$1(\mu m)^2$ 1 Darcy][3] and has a negligible tensile strength when compared to the pressures involved in this study[4,5]. The nuclear explosive charge is buried typically between 200 and 600 m below the surface of the earth. Initial temperature variation in the earth formation to this depth is only a few degrees which we neglected. The initial crack thickness is generally on the order of the average grain size of the alluvium formation, which at NTS is about 1 mm. This crack thickness enlarges up to about 150 mm as deflection of the crack walls occurs. Cracks present in the alluvium have lengths[4] of over 40 m.

The literature indicates that relatively little work has been done in the field of gas-initiated crack propagation. Keller, Davis, and Stewart[6] analyzed propagation of small cracks ranging up to a maximum length of 2 or 3 m. They considered a mixture of condensing steam and water and predicted whether a crack would initially grow. Their study did not determine if the crack would reach the surface of the earth and result in the release of radioactive contaminants. Rather, they were able to place a bound on conditions necessary for initial crack growth which could lead to eventual propagation of cracks to the surface of the earth.

Literature is available on hydraulic fracturing as applied to the petroleum industry, e.g. Howard and Fast[1] and Cleary[7]. Hydraulic fracturing involves pressurizing low permeability, petroleum producing formations next to a section of well bore. Hydraulic fracturing differs from nuclear fracturing in that a liquid rather than a gas is used to fracture the formation. Furthermore, in the hydraulic fracturing literature, the complete interaction of pressures within the crack, the flow of fluids, deformation of the earth formation, and extension of the crack has not been included. Therefore, this study also is of interest to the petroleum industry. By changing the equation of state from a gas to a liquid, the propagation of a hydraulic fracture could be predicted.

In the present analysis we consider a porous earth formation, as shown in Fig. 2, where a crack is seen along the left side. The top of the volume is subjected to atmospheric pressure at the ground surface. The bottom of the volume is at the elevation of the underground nuclear explosion. The origin of the coordinate system is in the left front with the "Z" axis vertical. Gas generated by the explosion exerts a driving pressure over a portion of the Z=0 plane bounded by the dashed lines and the "X" and "Y" axes. The X=0 and Y=0 surfaces are planes of symmetry. Other surfaces are positioned at remote distances from the origin so that the pressure gradient perpendicular to these surfaces is zero.

Gas from the explosion permeates the earth formation and simultaneously flows upward in the crack from the Z=0 plane. The resistance to flow in the crack is less than that in the formation. This results in pressures in the crack that are greater than those in the pores of the solid at the same elevation. Thus, gas flows out of the sides of the crack and into the formation from the X=0 plane.

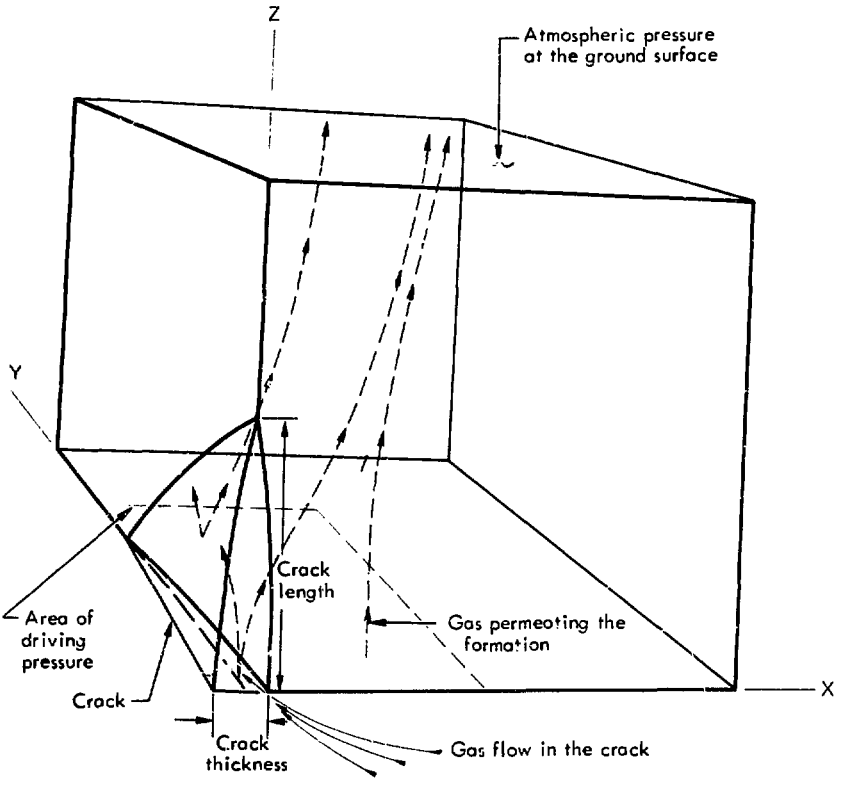

Fig. 2. Model of a propagating crack in a porous earth formation.

The sides of the crack deflect in the "X" direction and extend in the "Y" and "Z" directions. These deflections are produced when the forces due to gas pressure, which tend to open the crack, exceed the resistive pressure forces in the earth formation, which tend to keep the crack closed. The resistive pressure forces, due to the weight of material present above, are transmitted through the solid matrix of the earth formation.

The problem is analyzed in three parts, consisting of deflection of the crack wall, flow of gas in the solid, and flow of gas in the crack. The extent of the crack in

the X=0 plane beyond its initial value consists of the region where the deflection is >0. Deflection of the crack wall is calculated by considering the plane of the crack (X=0) to be the surface of a semi-infinite solid. We find elemental surface deflections caused by a unit load applied in the "X" direction on an elemental area. Total surface deflection is found using superposition. The data of Gerrard and Morgan[8] are used to establish elemental surface deflection away from the area where a unit load is applied. Gerrard and Morgan's data establish a multiplier to reduce the elemental surface deflection with distance away from the loading area. A circle of influence exists beyond which the loads have no effect.

The analysis for gas flow in the porous earth formation follows that of Morrison[9]. The conservation equations are combined with an ideal gas equation of state and placed in dimensionless form. Experimental data are included that verify this portion of the analysis.

The gas flow in the formation is considered isothermal for two reasons. First, in spite of the fact that the initial gas temperature is high, the energy carried by the gas is small in comparison with the heat capacity of the earth formation. Second, the 1 mm average grain size of the alluvium results in a large surface-to-volume ratio which offers rapid heat transfer from the gas to the formation. Consequently, the gas reaches the formation temperature after traveling no more than a few metres.

Gas flow in the crack is calculated by considering fully developed internal flow between closely spaced parallel wall segments[10]. The crack is thickest at the origin and is tapered toward the edges. Up to 200 segments are used to represent the tapered edge of the crack. Changes in crack thickness are gradual so that use of parallel wall segments in the calculation is a good approximation. Transient and acceleration terms present in the complete momentum equations for flow in the crack are neglected. Experimental frictional coefficients dependent on Reynolds number and relative roughness are incorporated.

A solution of the entire problem is obtained by combining the three parts of the analysis into a single, implicit finite-difference iteration procedure. Starting with given crack dimensions and pressures, we calculate a revised crack wall deflection. This calculation also establishes the extent of the crack in the "Y" and "Z" directions. Next we find a

frictional coefficient using the newly calculated dimensions of the crack and known values of pressure. We then determine the gas flow both in the porous earth formation and in the crack. The flow calculations result in pressures at a new time which can be used in the next time iteration to calculate a new crack wall deflection.

Analysis

This section discusses the analysis for deflection of the crack wall, gas flow in the earth formation and gas flow in the crack. The development of equations for the frictional coefficient are included in the analysis for gas flow in the crack.

DEFLECTION OF THE CRACK WALL

The analysis of the "X" direction deflection considers the crack wall to be a portion of the surface of a semi-infinite solid, as shown in Fig. 3. Two opposing forces are present. Forces due to gas pressure in the crack tend to deflect the surface and thereby open the crack while the horizontal resistive pressure forces in the earth formation tend to prevent deflection and keep the crack closed. Also present is a pore pressure equal to the hydrostatic head of fluid in the formation. Since the pores in alluvium at NTS are filled with air to the depth of interest in this study, we take the initial pore pressure throughout the solid to be atmospheric.

Cleary[7] has suggested that the resistive pressure forces are equal to the overburden. This assumption is valid if the earth formation has little strength and is subject to creep, since over geological time, motion would occur in the earth formation until a hydrostatic stress state was reached. On the other hand, if a hydrostatic state is not reached, then a three-dimensional stress state would exist where the resistive pressure forces would be a fraction of the overburden. At NTS, where the earth formation of interest consist of low-strength alluvium, we expect the resistive pressure forces in undisturbed alluvium to be close to overburden. Analytical results are included which show the effect of variations in resistive pressure forces.

To determine crack deflection, we first consider the effect of a force acting on an elemental surface area of a semi-infinite

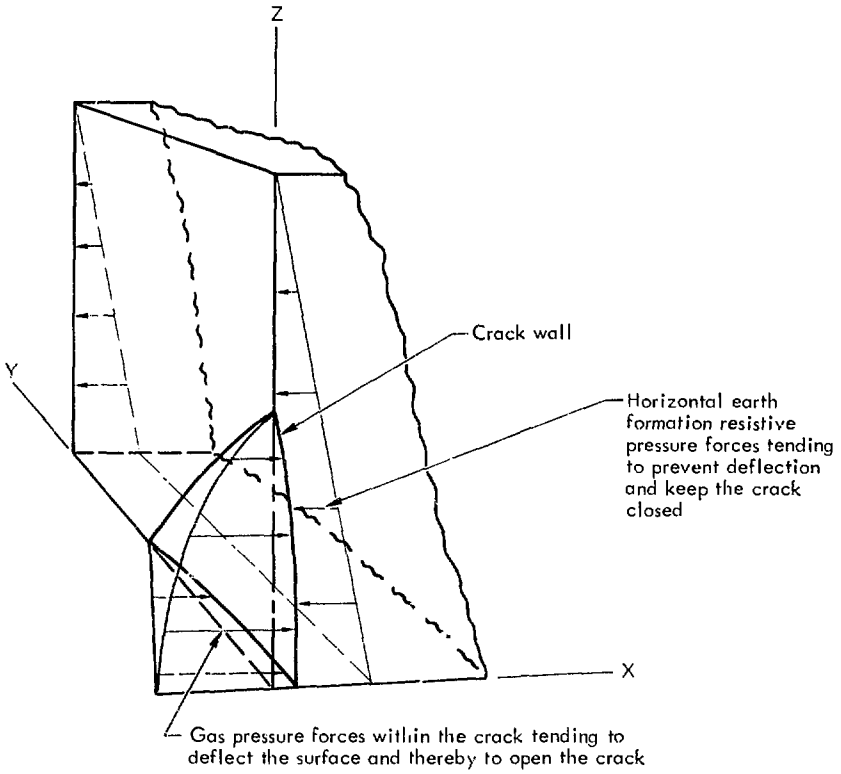

Fig. 3. Pressure forces acting on one wall of the crack.

elastic solid, which is given by Timoshenko and Goodier[11] as

$$p = \frac{(1-\nu^2)\,F}{\pi\,E\,R}\,, \qquad (1)$$

where p is the surface deflection in the "X" direction; ν is Poisson's ratio; E is the modulus of elasticity; F is the force equal to the gas pressure in the crack that is in excess of the initial pore pressure, less the earth formation resistive pressure, and times the elemental area where the pressures are applied; and R is the radius along the crack wall from the elemental area to the point where the deflection is being calculated.

Next, we integrate the force calculated in Eq. (1) over a finite surface area to obtain the deflection due to pressure acting on a portion of the surface. This problem was analyzed in detail by Love[12]. Two difficulties are that the solution is singular at R=0 and that a deflection occurs at any radius however large. When R→0, Timoshenko and Goodier[11] utilized an average deflection under a small surface area. For a square-shaped area this deflection is

$$D_{R\to 0} = \frac{0.95(1-\nu^2)}{E} (P - P_r) \quad A^{\frac{1}{2}} \qquad (2)$$

where P is the gas pressure in the crack, P_r is the earth formation resistive pressure; and A is the surface area of a single grid where the pressure is applied. When the radius becomes large, the data of Gerrard and Morgan[8] can be used to obtain a surface deflection profile. Their data were obtained experimentally for a load applied uniformly over a finite circular area. Extrapolation of Gerrard and Morgan's data is in reasonable agreement with the data of Campen and Smith[13] which show a zero surface deflection beyond a distance equal to about five radii. In other words, a circle of influence exists out to a normalized radius of about five beyond which P and P_r have no influence on the surface deflection.

We converted Gerrard and Morgan's data for a circular surface area loading to an equivalent square surface area loading and obtained coefficients for use in a formula for any radius similar to Eq. (2). That is, a circle of radius $(4/\pi)^{\frac{1}{2}}a$ would be equivalent to a square with a side of 2a. For the finite square area directly below the load the coefficient would be 0.95 and for equivalent radius ratios beyond five the coefficient would be zero. We also normalized the deflection and area using reference length, L, equal to the vertical distance between the Z=0 plane and the ground surface. Pressure and modulus of elasticity were normalized to the difference between the initial gas driving pressure, P_1, and the initial earth formation pore pressure, P_0. The initial earth formation pore pressure is considered constant and equal to the atmospheric pressure.

Finally, we obtain a relationship for the total surface deflection at a point by summing over the entire X=0 plane. This gives

$$\bar{D} = \sum_{\bar{A}} C_G \frac{(1-\nu^2)}{\bar{E}} (\bar{P} - \bar{P}_r) (\bar{A})^{\frac{1}{2}} \qquad (3)$$

where $\bar{D}$ is the normalized total surface deflection and C_G is the Gerrard and Morgan deflection coefficient. The bar above the variables indicates

they are normalized. The summation may be terminated for equivalent radius ratios beyond five since C_G is zero there.

The region where $\bar{D} > 0$ defines the extent of crack propagation and the location of the crack tip. No other criteria are necessary because by definition a crack exists only if its thickness is positive.

Utilization of Eq. (3) implies that the earth formation is elastic during initial loading and therefore that superposition is applicable. Earth formations in general are not elastic and a more complex soil model would improve the accuracy of the calculation. However, the experimental data of Gerrard and Morgan indicate that the initial load-deflection curve for sand is within five per cent of elastic. Further, we were able to make a linear approximation of the stress-strain data for alluvium from NTS[14] between 0 and 12% strain. Actual stress-strain data deviated a maximum of 25% from this linear approximation. This deviation of alluvium from a linear approximation was considered acceptable for the purpose of this study. Therefore the initial loading of alluvium was considered in the analysis to be elastic.

Total deflection, $\bar{D}$, is permitted to increase (but not decrease) in magnitude because in our range of pressures the initial loading causes a reduction of pore volume which does not increase appreciably when the load is reduced[15]. In other words, a reasonable approximation for alluvium at NTS for the range of pressures used in this study is elastic behavior during initial loading with negligible change in deflection during unloading.

We considered two other methods of calculating crack wall deflection. One method is based on an analysis by Sneddon[16] which is used by Keller, Davis, and Stewart[6] and which gives a solution in closed form for deflection of axisymmetric crack shapes. In applying Sneddon's analysis to an underground nuclear explosion, the axis of symmetry is horizontal and the crack length along which propagation would occur is in the radial direction. This radial direction includes both vertical and horizontal rays. We find that the cracks grow more vertically (upward) than horizontally since the earth formation resistive pressure is proportional to the distance below the earth's surface. Thus the axisymmetric assumption limits the results to small lengths of crack propagation. The other method utilized a finite-element computer code developed by Wilson, Farhoomand, and Bathe[17,18] and modified by Tokarz[19]. We used Wilson's analysis

to calculate crack wall deflection in a two-dimensional problem which we analyzed earlier[20]. We found the deflection calculation satisfactory in two dimensions but not readily extendable to three dimensions without requiring excessive computer time. Consequently, neither of these analyses were considered satisfactory for this study.

FLOW IN THE POROUS SOLID

The control volume used for analysis includes both pore space and solid grains. We write the continuity equation as

$$\frac{\partial \rho u_x}{\partial X} + \frac{\partial \rho u_y}{\partial Y} + \frac{\partial \rho u_z}{\partial Z} + \varepsilon \frac{\partial \rho}{\partial t} = 0 \qquad (4)$$

where X, Y, and Z are spatial coordinates; ρ is the gas density; u_x, u_y, and u_z are apparent velocities; ε is the porosity; and t is time.

The apparent velocities equal the volume flow rate passing through a face of the control volume divided by the cross-sectional area of the face, including both void and solid portions. These apparent velocities are different from the actual gas velocities since only a fraction of the control volume is available for occupancy by the gas.

We use Darcy's law[21] for the mementum equations, which are

$$u_x = -\frac{k_x}{\mu} \frac{\partial P}{\partial X} \qquad (5)$$

$$u_y = -\frac{k_y}{\mu} \frac{\partial P}{\partial Y} \qquad (6)$$

$$u_z = -\frac{k_z}{\mu} \frac{\partial P}{\partial Z} \qquad (7)$$

where k_x, k_y, and k_z represent directional permeabilities that are normally determined by experiment, and μ is the gas viscosity. Gravity forces are omitted since they are negligible in comparison to the pressure forces.

An ideal gas equation of state is used since this is a good approximation for non-condensible gases at ambient temperature and pressures[22] up to 10 MPa, which are the maxima of interest in this study. The gas equation of state is written as

$$\rho = \frac{P}{R\,T} \qquad (8)$$

where R is the gas constant and T is the absolute temperature of the gas which we consider constant.

Combining Eqs. (4) through (8) gives the equation

$$\bar{k}_x \frac{\partial^2 F}{\partial \bar{X}^2} + \bar{k}_y \frac{\partial^2 F}{\partial \bar{Y}^2} + \bar{k}_z \frac{\partial^2 F}{\partial \bar{Z}^2} = F^{-\frac{1}{2}} \frac{\partial F}{\partial \tau} \qquad (9)$$

where the quantities with a bar represent normalized variables and

$$F = \left(\bar{P} + \frac{1}{N-1}\right)^2 \qquad (10)$$

$$N = P_1/P_0 \qquad (11)$$

and

$$\tau = \frac{k_0(P_1-P_0)t}{\varepsilon \mu L^2} \qquad (12)$$

Values of $\bar{k}_x$, $\bar{k}_y$, and $\bar{k}_z$ are made dimensionless using a constant reference permeability, k_0.

Eq. (9) is differenced using an implicit method because the spatial derivatives taken individually with the time derivative form a parabolic equation. We use Brian's method[23-25] since this reduces to the alternating-direction implicit method in two spatial dimensions identical to the "Y" and "Z" directions difference algorithm used for calculating flow in the crack. The coefficient on the right hand side of Eq. (9) is evaluated using values of F at an average of the old and new times until convergence is obtained.

Increased accuracy for a given number of grid points is achieved by using a variable grid spacing for the "X" direction based on Blottner's grid-stretching relationship[26,27]. Blottner's relationship is

$$X = X_0 \frac{(\kappa^{i/I}-1)}{(\kappa^{1/I}-1)} \qquad i = 1,2....I \quad (13)$$

where X_0 is the total length in the "X" direction; κ is a variable normally between 1.5 and 2.718 (i.e. the value of e), and I is the number of spatial intervals in the "X" direction.

FLOW IN THE CRACK

The crack is divided into parts and the analysis considers internal flow between two parallel porous wall segments through which the gas permeates the earth formation. The continuity equation may be written as

$$\frac{\partial \rho u_x}{\partial X} + \frac{\partial \rho u_y}{\partial Y} + \frac{\partial \rho u_z}{\partial Z} + \frac{\partial \rho}{\partial t} = 0 \; . \qquad (14)$$

We establish a control volume so that a single finite difference mesh spans one half the crack thickness and takes advantage of a plane of symmetry at the crack centerline across which there is no mass flow. Such a control volume prevents the determination of a velocity profile in the "X" direction within the crack. However, this information is not germane to our analysis. The momentum equations take on a different form in the "X" direction than in the "Y" and "Z" directions. Flow through the walls of the crack in the "X" direction is governed by the pressure distribution in the

adjacent earth formation so that Darcy's law is applicable. Flow in the "Y" and "Z" directions is approximated by the momentum equation for fully developed internal flow[10] that is rearranged for an explicit solution of the velocity. The momentum equations used are

$$u_x = -\frac{k_x}{\mu}\frac{\partial P}{\partial X} \qquad (15)$$

$$u_y = \pm\left(\left|\frac{4d_c}{\lambda\rho}\frac{\partial P}{\partial Y}\right|\right)^{1/2} \qquad (16)$$

$$u_z = \pm\left(\left|\frac{4d_c}{\lambda\rho}\frac{\partial P}{\partial Z}\right|\right)^{1/2} \qquad (17)$$

where d_c is the crack thickness in the "X" direction and λ is a frictional coefficient.

The plus sign in Eqs. (16) and (17) is used when the pressure gradient is <0 and the minus sign when the pressure gradient is >0. The flow may be either laminar or turbulent. These different flow conditions are accounted for in the calculation of λ which is dependent on Reynolds number and the relative roughness of the crack walls.

We took computed results and used these to determine the magnitude of the neglected transient and acceleration terms in the "Y" and "Z" direction momentum equations. The magnitude of these neglected terms was then compared with the included pressure gradient term. This comparison shows the neglected terms to be less than 10% of the included terms except at times less than about one eighth of the total problem time. Even at these early times the neglected terms are probably negligible since the actual driving pressure is applied over a short period of time rather than the instantaneous fashion we have used mathematically.

Application to transient conditions of a frictional coefficient, λ, evaluated under steady flow conditions, has been used by several authors. Ginzburg[28] assumed that the resistance properties established for steady flow are preserved for transient flow. Petrova[29] also determined the magnitude of the frictional coefficient using steady flow conditions. Yeremenko and Markov[30] used Prandtl's mixing length hypothesis with a linear variation in shear stress to obtain mathematically variations in frictional coefficients from their steady state values. Yeremenko and Markov expanded the shear stress of Prandtl's mixing length hypothesis in the form of a polynominal based on open channel flow. They showed quantitative increases in frictional coefficient for accelerating flow using an unsteady flow parameter, δ_0.

Unfortunately, no method of determining δ_0 is indicated without knowledge of the velocity distribution in the flow channel. This velocity distribution has been analyzed in the laminar flow regime[31] but in general is unknown. Further studies relating the effects of acceleration on frictional coefficient are needed but in their absence we use the values corresponding to steady flow.

An ideal gas equation of state,

$$\rho = \frac{P}{R\,T}\,, \qquad (18)$$

is again taken under isothermal conditions so that Eqs. (15) through (18) may be combined using normalized variables and neglecting gravity to give

$$-\bar{k}_{cx}\frac{\partial F}{\partial \bar{X}} \pm \frac{\partial}{\partial \bar{Y}}\left(\bar{k}_{cyz}\left(\left|\frac{\partial F}{\partial \bar{Y}}\right|\right)^{\frac{1}{2}}\right) \pm \frac{\partial}{\partial \bar{Z}}\left(\bar{k}_{cyz}\left(\left|\frac{\partial F}{\partial \bar{Z}}\right|\right)^{\frac{1}{2}}\right) + \frac{\partial \bar{P}}{\partial \tau} = 0 \qquad (19)$$

where

$$\bar{k}_{cx} = \frac{\varepsilon\, L\, \bar{k}_x}{d_c} \qquad (20)$$

$$\bar{k}_{cyz} = \frac{\varepsilon\, \mu}{(P_1 - P_0)k_0}\left(\frac{2d_c\, L\, R\, T}{\lambda}\right)^{\frac{1}{2}}. \qquad (21)$$

The reference permeability, k_0, is set so that the initial value of $\bar{k}_{cyz}$ is unity at the origin.

Equation (19) may be placed in an efficient and convenient form for numerical solution by differentiating the "Y" and "Z" terms which, after rearranging and using Eq. (10), yields

$$\bar{k}_{cx}\frac{\partial F}{\partial \bar{X}} + \left(\frac{\partial F}{\partial \bar{Y}}\Big/\left(\left|\frac{\partial F}{\partial \bar{Y}}\right|\right)^{\frac{1}{2}}\right)\frac{\partial \bar{k}_{cyz}}{\partial \bar{Y}} + \left[\bar{k}_{cyz}\Big/2\left(\left|\frac{\partial F}{\partial \bar{Y}}\right|\right)^{\frac{1}{2}}\right]\frac{\partial^2 F}{\partial \bar{Y}^2} + \left(\frac{\partial F}{\partial \bar{Z}}\Big/\left(\left|\frac{\partial F}{\partial \bar{Z}}\right|\right)^{\frac{1}{2}}\right)\frac{\partial \bar{k}_{cyz}}{\partial \bar{Z}} + \left[\bar{k}_{cyz}\Big/2\left(\left|\frac{\partial F}{\partial \bar{Z}}\right|\right)^{\frac{1}{2}}\right]\frac{\partial^2 F}{\partial \bar{Z}^2} = \frac{1}{2}F^{-\frac{1}{2}}\frac{\partial F}{\partial \tau}. \qquad (22)$$

The terms in Eq. (22) containing $\partial \bar{k}_{cyz}/\partial \bar{Y}$ and $\partial \bar{k}_{cyz}/\partial \bar{Z}$ are calculated explicitly since they vary mainly with spatial location and are nearly constant with time. The terms in square brackets make Eq. (22) nonlinear. If the "X" direction spatial derivative dominates over the "Y" and "Z" direction derivatives of F, the equation becomes hyperbolic in nature. An explicit differencing technique would then be necessary to prevent artificial numerical damping[32]. If either the "Y" or "Z" direction derivatives of F dominate, the equation becomes parabolic and an implicit solution

is most efficient. Because dominance by any one spatial derivative may occur, we use an operator splitting technique[33] to solve Eq. (22). This increases the speed of computation because the stability inherent with implicit differencing may be used to advantage. Eq. (22) is broken into two separate equations

$$\bar{k}_{cx} \frac{\partial F}{\partial \bar{X}} = \frac{1}{2} F^{-\frac{1}{2}} \frac{\partial F}{\partial \bar{\tau}} \qquad (23a)$$

$$\left(\frac{\partial F}{\partial \bar{Y}} \Big/ \left(\left| \frac{\partial F}{\partial \bar{Y}} \right| \right)^{\frac{1}{2}} \right) \frac{\partial \bar{k}_{cyz}}{\partial \bar{Y}} +$$

$$\left[\bar{k}_{cyz} \Big/ 2 \left(\left| \frac{\partial F}{\partial \bar{Y}} \right| \right)^{\frac{1}{2}} \right] \frac{\partial^2 F}{\partial \bar{Y}^2} +$$

$$\left(\frac{\partial F}{\partial \bar{Z}} \Big/ \left(\left| \frac{\partial F}{\partial \bar{Z}} \right| \right)^{\frac{1}{2}} \right) \frac{\partial \bar{k}_{cyz}}{\partial \bar{Z}} +$$

$$\left[\bar{k}_{cyz} \Big/ 2 \left(\left| \frac{\partial F}{\partial \bar{Z}} \right| \right)^{\frac{1}{2}} \right] \frac{\partial^2 F}{\partial \bar{Z}^2} = \frac{1}{2} F^{-\frac{1}{2}} \frac{\partial F}{\partial \bar{\tau}} \qquad (23b)$$

with Eq. (23a) first solved repeatedly in an explicit fashion using a small time step to assure stability. The resulting new values of F from Eq. (23a) are used as initial values to solve Eq. (23b) which is solved by the alternating-direction implicit method[23]. The total time increment in solving both Eqs. (23a) and (23b) is kept identical.

Calculational Method

The problem posed in this study is solved numerically using nearly the entire small core memory of a Control Data Corporation* 7600 computer. Although use of just the small core memory results in faster speed, the calculations are still time consuming. The 65,000 word capacity of the small core memory permitted the inclusion of about 3000 spatial nodes. A larger number of spatial nodes could have been included but at a sacrifice in the speed of computation. Typical computer run times using just the small core memory range from 15 minutes to one hour. The total computer time to generate the results for this study was about 50 hours.

Both the crack wall deflection and the frictional coefficient are

*Reference to a company or product name does not imply approval or recommendation of the product by the University of California or the U.S. Energy Research & Development Administration to the exclusion of others that may be suitable.

found at each node within the crack from the governing equations. The bulk of the calculations in each time step are required to determine the pressure function, F, in the porous solid and in the crack. At each node we select the applicable governing equation. The calculation of F at the new time step is performed in three parts. First, intermediate values of F are found using Eq. (23a) if the node is within the crack or, if the node is in the porous solid, by setting up a matrix with the "X" direction calculations implicit. These first intermediate values of F are determined for each node before the calculations are continued. Next, we use the first intermediate values of F to determine a second intermediate value of F at each node by considering the "Y" direction calculations to be implicit Finally, the value of F at the end of the time step is determined at each node using the second intermediate values of F and by considering the "Z" direction calculations to be implicit. In this fashion, the calculations for nodes in the crack are interspersed with calculations for nodes in the solid.

The governing equations are nonlinear so that stability is not assured even though the differencing is implicit unless the time step is kept below an upper bound. This upper bound was determined by trial calculations. Values of pressure need only be determined for calculation of the crack wall deflection and for printout of the results. We find that results are independent of variations in the time step over a factor of one hundred as long as stability is maintained. This is an indication that writing the governing equations in terms of F was a judicious choice.

Up to a point, results are also independent of changes in the "Y" and "Z" direction spatial mesh size. However, a decrease of the "X" direction spatial mesh size by a factor of 100 typically was found to increase the time for crack propagation to the surface of the earth by 20%. This is due to the dependence of gas permeation into the porous solid from the crack on the pressure function derivative, the approximation of which improves as the mesh size is reduced. Because our interest is in prevention of crack propagation, selection of a given "X" direction spatial mesh size acts as a conservative bound on the time required for crack propagation. That is, inclusion of a finer grid spacing has the effect of increasing crack propagation time. If no propagation occurs under the selected "X" direction mesh size, then a reduction in

mesh size would only confirm that the crack will not propagate. Although it might appear desirable to continually decrease the "X" direction grid size, a limit is reached where the CDC 7600 small core memory is exceeded if the necessary spatial distances are maintained. Computer run time would then increase beyond our allowable budget. The computer program consists of a main portion used for input and output and which updates necessary variables prior to calling three calculational subroutines. These three subroutines determine the crack wall deflection, frictional coefficient, and flow both in the crack and in the porous solid. A typical real-time step was 0.005s.

Experimental Verification

The primary application of this study is to assure the safety of underground nuclear explosions. Experimental verification by means of a underground nuclear explosion with subsequent release of contaminants to the atmosphere is in conflict with this study's basic purpose of preventing the release of contaminants. Full scale tests using high explosives are costly since enough explosive must be used to propagate the crack a significant distance. Perhaps some laboratory scale model of the complete analysis is possible; however, one is concerned about the accuracy of measuring the location of a propagating crack in an earth formation on a reduced scale. Consequently, experimental verification of the complete analysis does not appear feasible.

We found experimental data in the literature for the frictional coefficient used to calculate flow in the crack. We also found experimental data in the literature relating load, surface deflection, and distance away from the point of load application which could be used to determine deflection of the crack wall. Data necessary to adequately verify the nonlinear, transient gas flow in the solid was not found in the literature so we constructed an experimental facility and generated the required information. Each portion of this analysis then is either experimentally verified or based on experimental results from the literature.

The experimental test apparatus constructed to obtain data for transient gas flow in a porous solid consisted of a 0.3 m diameter,

4.6 m long steel pipe filled with Overton sand as shown schematically in Fig. 4. Overton sand has a permeability of 20 $(\mu m)^2$, which is within the range of permeability for alluvium at NTS, and was selected rather than alluvium formation because of the ease in installation and because no economical means exists to obtain samples of alluvium formation at depths over a hundred meters of the size necessary for our tests without significantly changing its permeability and other flow properties. Dry nitrogen was forced through the column of sand by using a pneumatically operated valve controlled by an analog computer. Flow rate was determined by measuring the gas pressure on each side of sharp edged orifices placed in the inlet line. Measurements of gas pressure in the column of sand were made as a function of time at eight axial locations.

Pressure was obtained with strain-gage type pressure transducers having an accuracy of 0.1% of full scale. Readout of pressure was performed on strip chart recorders capable of resolving pressures to 2% of the 3.5 bar inlet pressure. The facility was designed to permit use of a mixture of steam and nitrogen; however, these data are not applicable to the present study.

Each test was conducted by first establishing the approximate initial flowrate using a bypass line. An orifice was installed in the bypass line to simulate the initial resistance of the column of sand. At the appropriate time a three-way, full-flow valve was actuated that switched flow from the bypass line to the line leading to the column of sand. A zero time was established when the pressure tranducer at the inlet to the column of sand recorded the resulting step change in pressure.

A comparison of these data with the theoretical results which are used to predict the non-linear transient gas flow in the porous solid is shown in Fig. 5. The theoretical results for selected times are indicated as solid lines with the experimental data points related by the various symbols. Agreement is felt to be excellent thereby confirming the accuracy of the analysis for gas flow in the porous solid. The analysis for the "X" direction gas flow out of the sides of the crack has the same form as gas flow in the porous solid since it is governed by the pressure distribution in the porous solid.

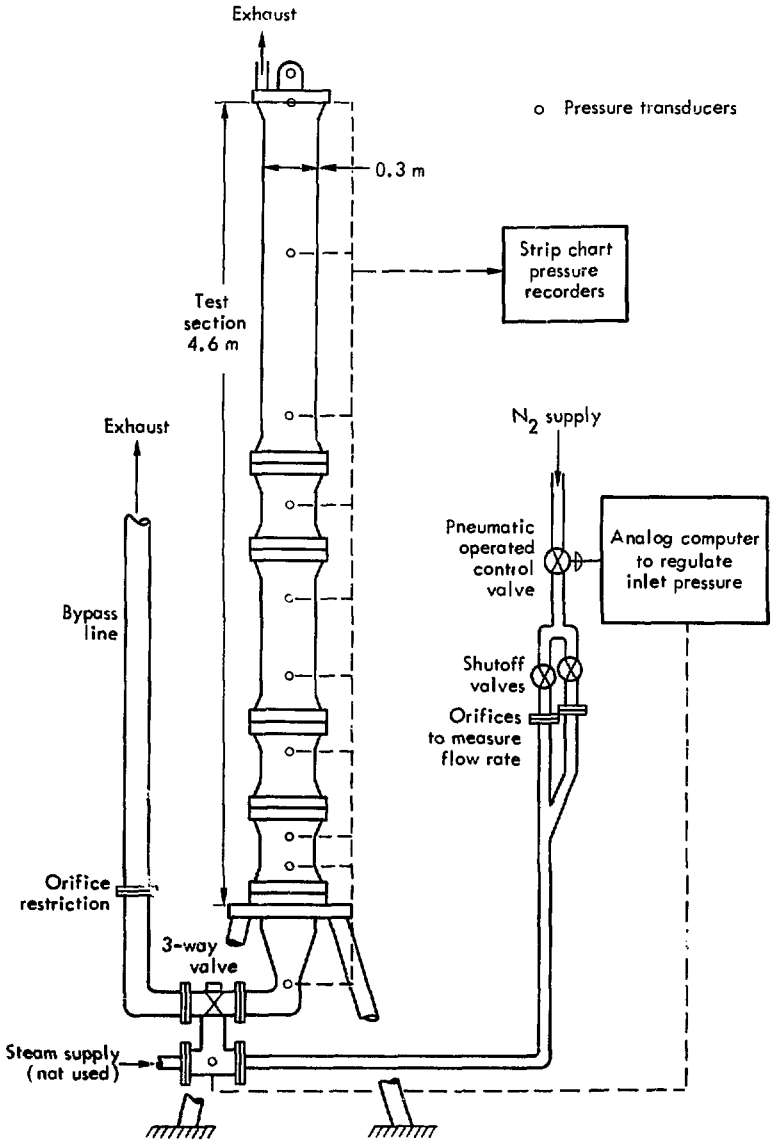

Fig. 4. Test apparatus for measuring transient gas flow in a porous solid.

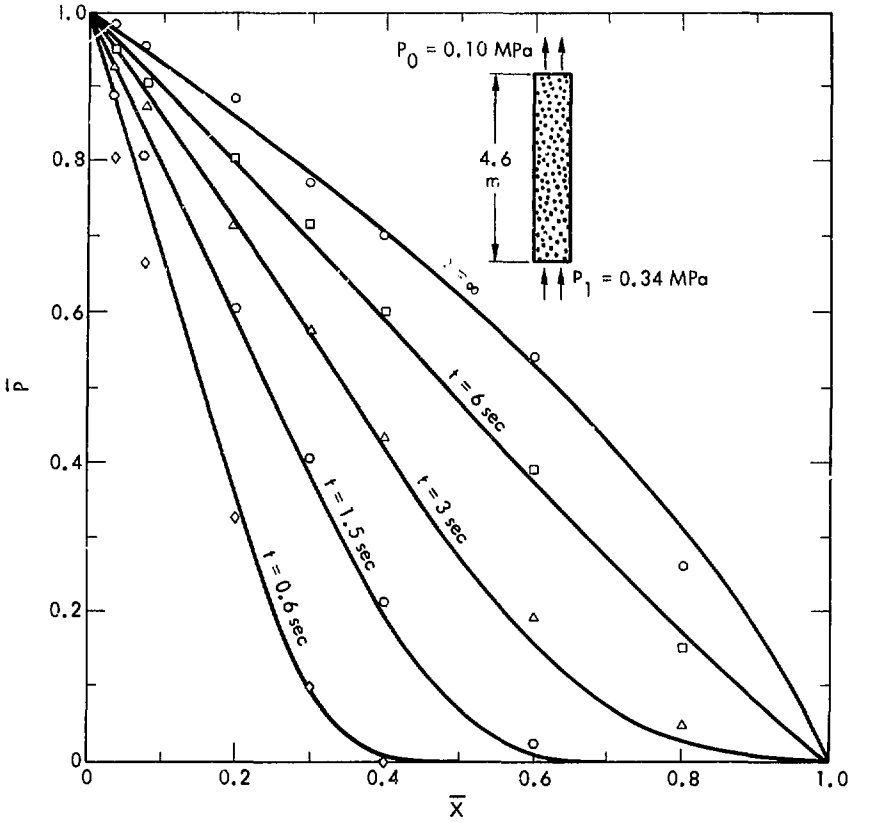

Fig. 5. Comparison between theoretical and experimental results for nitrogen flow through a column of 20 $(\mu m)^2$ permeability Overton sand.

Results

Results were generated using the parameters shown in Table 1 for a proposed underground nuclear test. A hypothetical crack with initial length and width up to their maximum feasible values of 110m and 170m, respectively, was incorporated since this presented an upper bound on possible propagation of the crack. An exponential decay of the driving pressure was included to approximate the expected conditions of the proposed test. This reduces the driving pressure to about 95% of its initial value in 60 seconds. The exponential decay continues for perhaps 10 minutes, after which the pressure decreases abruptly. This abrupt decrease in pressure occurs as the formation starts to fall into the cavity void space and rapidly cools the gases present there.

Table 1

Parameters from a Proposed Underground Nuclear Test Use for Generating Results

Distance to surface of the earth	- 530 m
Initial crack length	- 30 to 110 m
Initial crack width	- 60 to 170 m
Maximum initial crack thickness	- 10 to 50 mm
Permeability of the formation	- 10^{-6} to 1 $(\mu m)^2$
Porosity of the formation	- 0.3
Poisson's ratio of the formation	- 0.25
Modulus of elasticity of the formation	- 3.5 GPa
Initial driving pressure	- 10 MPa
Gas viscosity	- 2.4×10^{-5} Pa•s

A parametric study was completed to assure that radioactive contaminants would be contained below the surface of the earth if the proposed test were actually conducted. Figure 6 shows results for maximum feasible values of initial crack length and width. Time for crack propagation to the surface of the earth is seen to increase as permeability and the ratio of maximum resistive pressure, $P_{r_{max}}$, to initial driving gas pressure, P_1, increases. Because the driving pressure decays with time, each curve approaches an asymptote. That is, propagation will occur in the first few minutes if it occurs at all. Maximum penetration of cavity gases into the formation beyond the crack tip was found to be less than 1% of the distance to the surface of the earth. For the proposed test, the permeability

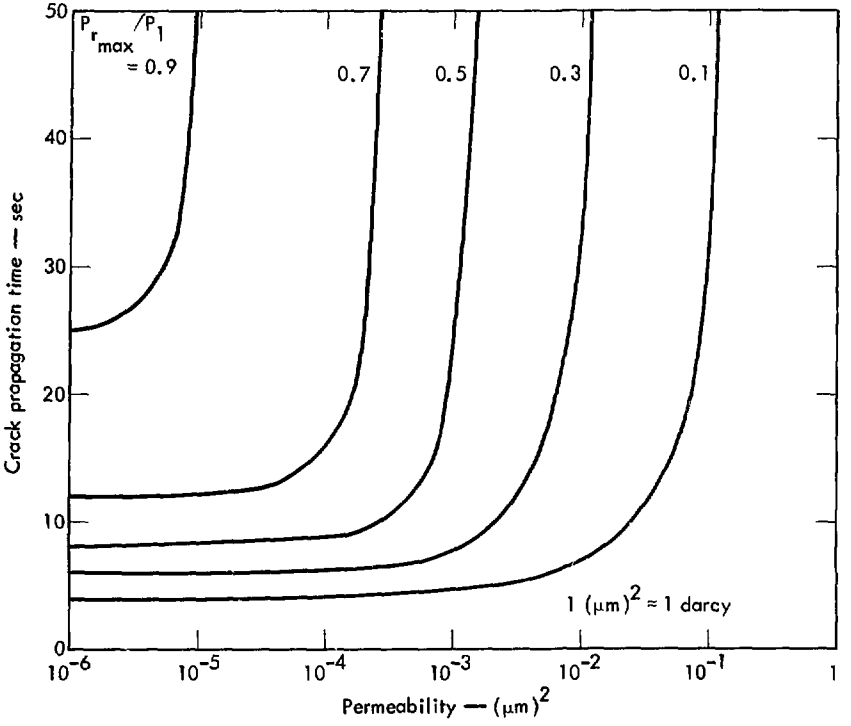

Fig. 6. Crack propagation time vs permeability for various ratios of maximum resistive pressure to initial driving pressure.

of the earth formation ranges between 10^{-2} and 1 $(\mu m)^2$. The expected ratio of $P_{r_{max}}/P_1$ is close to unity with the lowest feasible value equal to 1/3. Under these conditions we find that a crack would not propagate to the surface of the earth and therefore no radioactive material would be released into the atmosphere should the proposed test be conducted.

For any given set of parameters, there is a permeability large enough to prevent crack propagation. That is, gas flowing into the crack from the source permeates the earth formation so rapidly that pressures inside the crack do not exceed the

resistive pressure forces of the earth formation which tend to prevent crack propagation. As the permeability is decreased, the crack propagates a short distance and stops. This is due to a reduction in gas pressure inside the crack as propagation occurs. Initially the gas flowing into the crack from the source cannot be dissipated into the earth formation fast enough to prevent propagation. As the crack grows, the area of the crack walls through which gas permeates the earth formation increases thereby decreasing the resistance to gas flow out of the crack. The resistance to gas flow inside the crack remains more nearly constant, increasing as the length of the crack increases and decreasing as the flow area inside the crack increases. The net effect is to reduce gas pressure inside the crack.

With additional decreases in permeability, the crack propagates farther until a magnitude of permeability is reached where the crack just propagates to the surface of the earth. Further decreases in permeability shorten the time necessary for crack propagation. This is seen in Fig. 7 where the normalized crack tip location along the "Z" axis is presented as a function of time for three values of permeability near that which causes the crack to just reach the surface of the earth. The slope of the curves represent the speed of propagation which is rapid at first decreasing with time as the resistance for gas to permeate the earth formation decreases. Near the surface of the earth the resistive pressure forces of the formation, which are proportional to the depth below the surface, decrease faster than the pressure near the tip of the crack. Hence, for those cases where the crack reaches the surface of the earth, the speed of propagation increases at late times. For the middle curve on Fig. 7, the minimum speed is about 15% of the maximum speed.

Figure 8 shows the variation of crack tip location on the "Z" axis vs time for several initial crack sizes. The length and width values selected correspond to multiples of the spatial zone size. A crack with initial length and width of 30 m by 30 m travels rapidly until it reaches the length and width of an initially larger crack. Beyond this time the speed of crack propagation for both cracks is nearly the same. Hence a variation in crack length and width by a factor of four results in a change in propagation time of only 15%. The maximum initial crack thickness chosen at the origin

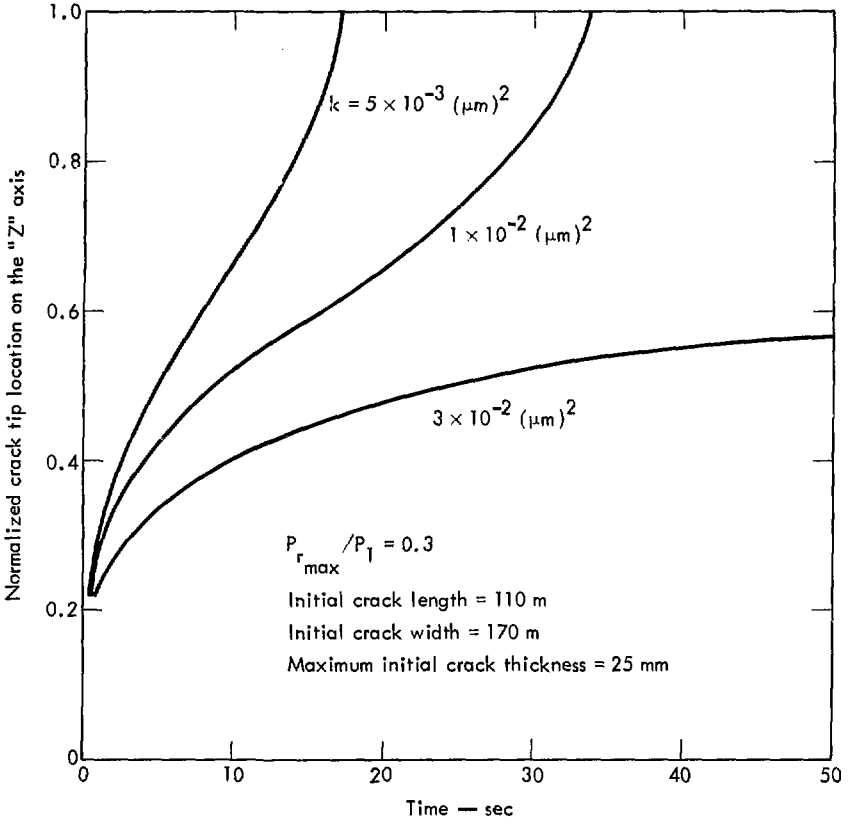

Fig. 7. Crack-tip location on the "Z" axis vs time for three magnitudes of permeability near that required for the crack to just reach the surface of the earth.

is less than 10% of the crack thickness at the origin after deflection occurs so that changes in initial crack thickness by a factor of four affect the crack propagation time by less than 25%.

The initial shape of the crack in the "Y" and "Z" directions was chosen to be rectangular. Figure 9 indicates that the crack becomes fan shaped as propagation occurs. The crack grows more vertically than

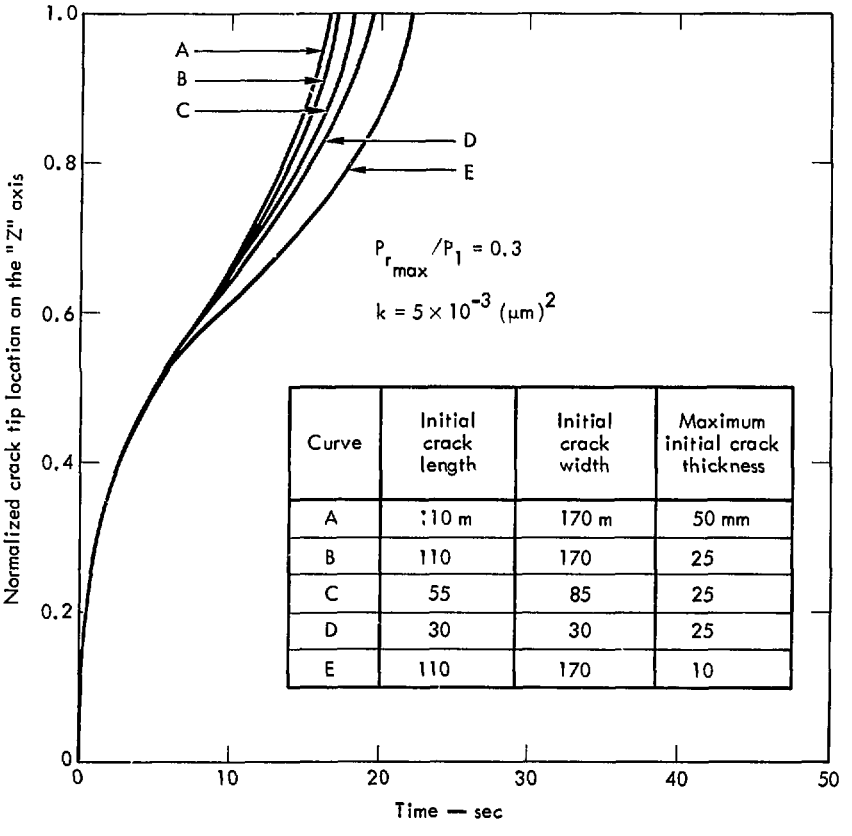

Curve	Initial crack length	Initial crack width	Maximum initial crack thickness
A	110 m	170 m	50 mm
B	110	170	25
C	55	85	25
D	30	30	25
E	110	170	10

Fig. 8. Crack-tip location on the "Z" axis vs time for several initial crack sizes.

horizontally because the earth formation resistive pressure, P_r, which tends to prevent crack deflection, is proportional to depth below the surface.

Because gas pressure at the crack tip in the region near the horizontal depends mainly on the distance from the pressure source to the crack tip, equal crack wall deflection, or crack thickness, occurs at a larger distance from the pressure source above the horizontal where P_r is less than its value on

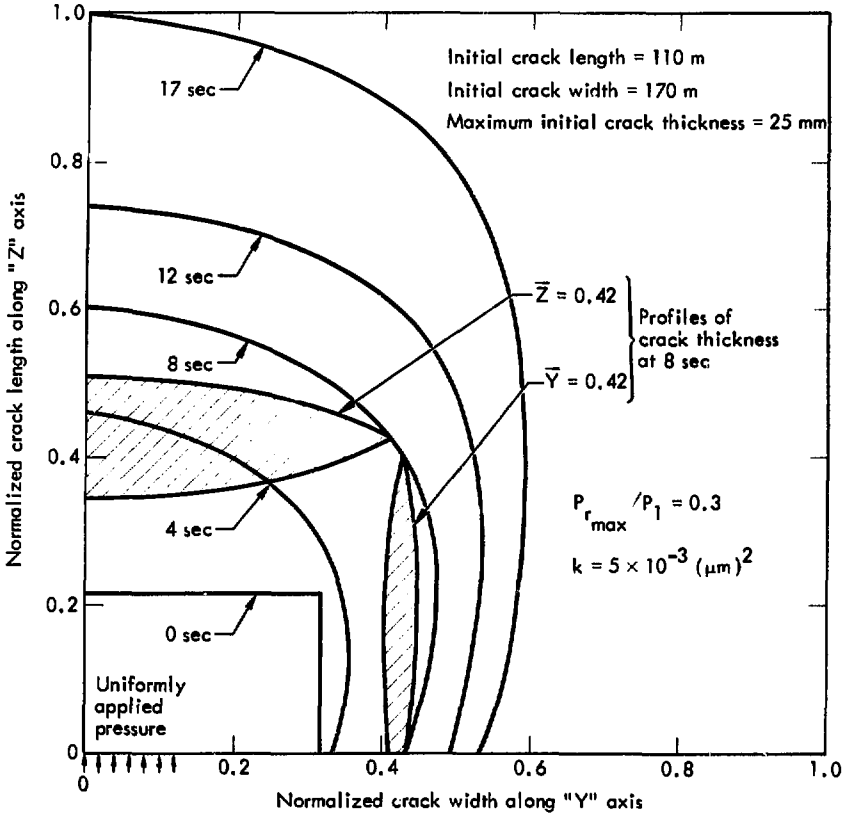

Fig. 9. Crack length vs width at various times. Also shown are profiles of crack thickness at 8 seconds for $\bar{Y}$ = 0.42 and $\bar{Z}$ = 0.42.

the horizontal. Hence, the locus of the crack tip is convex to the right. The cross hatched areas in Fig. 9 show profiles of crack thickness for constant values of "Y" and "Z" at 8 seconds. The scale of the cross hatched areas is different than the rest of the graph with the maximum thickness for Y = 0.42 equal to 20 mm and for Z = 0.42 equal to 85 mm.

Figs. 10 and 11 show the variation of crack thickness and normalized pressure as a function

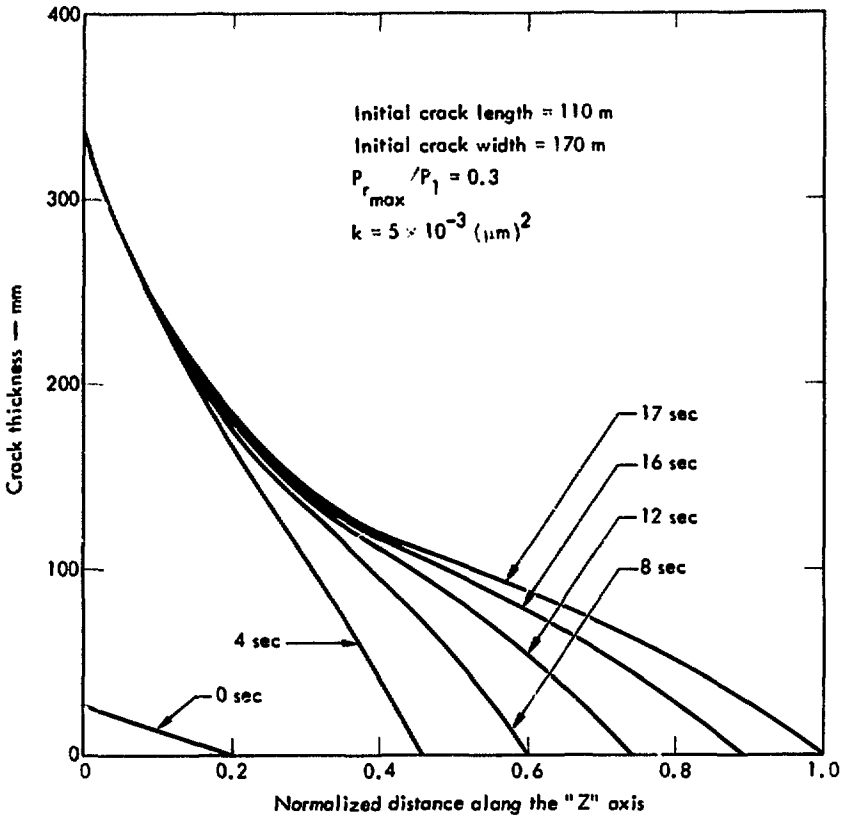

Fig. 10. Crack thickness vs normalized distance along "Z" axis for various times.

of distance along the "Z" axis for various times. Both graphs are interrelated. Initial crack thickness was taken as linear with distance as shown by the lower left curve of Fig. 10. As gas flows into the crack, the crack thickness and pressure increase. The increased crack thickness reduces the resistance to gas flow and allows for further increase in pressure within the crack. A complex variation of crack thickness and pressure with distance along the "Z" axis develops

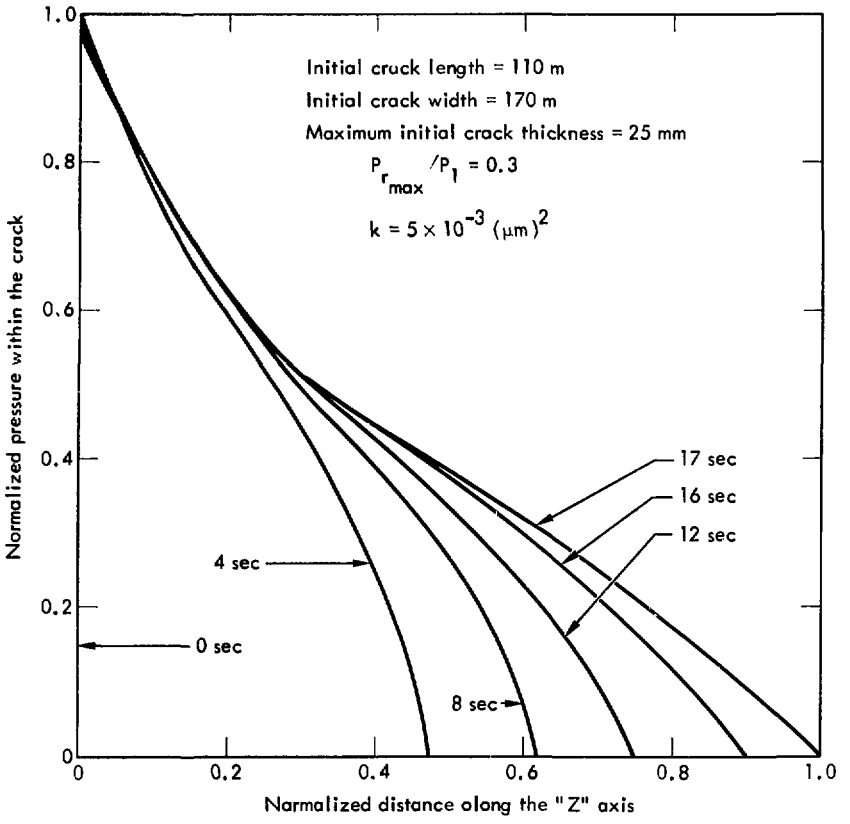

Fig. 11. Normalized pressure within the crack vs normalized distance along the "Z" axis for various times.

as time elapses. The concave upward shape near the left side of the curves in both graphs is characteristic of a channel with porous walls. The crack thickness and pressure are depressed due to loss of gas through the walls of the crack into the earth formation. Near the crack tip the curves become concave downward. Here the crack thickness becomes small and the resistance to gas flow inside the crack increases. Consequently, gas flow into the formation is less important in comparison to gas flow inside the crack near the crack tip than it is near the "Z" axis.

Conclusion

To our knowledge, this is the first study that shows the interaction of gas pressure within a crack, permeation of gas into a porous earth formation, deflection of the crack wall, and the phenomenon of crack propagation. One other analysis by Keller, Davis, and Stewart[6] determined if a small crack of length up to 75 mm would initially grow but not if propagation would continue. Although conditions were different, results that can be compared are in reasonable agreement.

Crack propagation to the surface of the earth following an underground explosion occurs as shown in Fig. 6 and the parameters of Table 1 only under unlikely conditions. For example, if the permeability is 3×10^{-4} $(\mu m)^2$ and the ratio of maximum earth formation resistive pressure due to overburden to initial driving pressure is 0.7, the crack would reach the surface of the earth in 50 to 60 seconds.

Normally, the permeability of the earth formation at the Nevada Test Site where experimental underground nuclear explosions are conducted ranges between 10^{-2} and 1 $(\mu m)^2$. The corresponding value of maximum earth formation resistive pressure is close to the initial driving pressure so that crack propagation to the surface of the earth is not anticipated. Conditions of each test may be checked with this analysis to assure radioactive contaminants are contained below the surface of the earth following an underground nuclear explosion.

Nomenclature

A	- Surface area of pressure application
$\bar{A}$	- Normalized area equal to A/L^2
a_{eq}	- Equivalent radius of a square area of sides 2a
C	- Dimensionless constant used in deriving Darcy's law
C_G	- Gerrard and Morgan deflection coefficient
d	- Characteristic length approximating the grain size
d_c	- Crack thickness in "X" direction which is half of the hydraulic diameter, d_h
d_h	- Hydraulic diameter equal to four times the flow area divided by the wetted perimeter
d_p	- Average particle size of grains in the earth formation
D	- Deflection of the crack boundary in the "X" direction due to a point force or pressure acting on a small area
D	- Total deflection of the crack boundary in the "X" direction
$\bar{D}$	- Normalized total surface deflection equal to D/L
dX, dY, dZ	- Elemental distances in the "X", "Y", & "Z" directions
dN	- Elemental distance in the direction of the total velocity vector within the crack
E	- Modulus of elasticity of the earth formation
$\bar{E}$	- Normalized modulus of elasticity equal to $E/(P_I - P_O)$
F	- Pressure function equal to $\left(\bar{P} + \frac{1}{N-1}\right)^2$
F	- Force equal to gas pressure in the crack less the resistive pressure, times the area of application
g	- Acceleration of gravity
i,j,k	- Spatial indices
I	- Number of spatial intervals in the "X" direction used in Blottner's grid stretching relationship
k_x, k_y, k_z	- Directional permeabilities for gas in the "X", "Y", & "Z" directions

$\bar{k}_x, \bar{k}_y, \bar{k}_z$ - Dimensionless permeabilities equal to $\bar{k}_x = \frac{k_x}{k_0}$, $\bar{k}_y = \frac{k_y}{k_0}$, $\bar{k}_z = \frac{k_z}{k_0}$

$\bar{k}_{cx}$ - Normalized effective permeability for "X" direction gas flow in the crack defined by Eq. (20)

$\bar{k}_{cyz}$ - Normalized effective permeability for the "Y" and "Z" direction gas flow in the crack defined by Eq. (21)

k_s - Average gain size (diameter) of particles in the crack wall

k_0 - Reference permeability set equal to the initial equivalent permeability in the crack at the origin and calculated using Eq. (21).

L - Vertical distance between the Z=0 plane and the ground surface

N - Pressure ratio, equal to P_1/P_0

NTS - Nevada Test Site near Las Vegas, Nevada

P - Gas pressure

P_r - Earth formation resistive pressure

P_0 - Initial earth formation pore pressure

P_1 - Initial gas driving pressure

$\bar{P}$ - Normalized gas pressure equal to $(P-P_0)/(P_1-P_0)$

$\bar{P}_r$ - Normalized resistive pressure equal to $(P_r-P_0)/(P_1-P_0)$

Q - Volume flow rate

r - Radius from load area used in calculating the Gerrard and Morgan deflection coefficient, C_G.

R - Radius measured along the crack wall from the elemental area of force application to the point where the deflection is being calculated

R - Gas constant

Re - Reynolds number, $Re = V d_h \rho/\mu g$.

t - Time variable

T - Absolute temperature of the gas

u_x, u_y, u_z - Apparent velocities in "X", "Y", & "Z" directions equal to volume flow rate per unit cross-sectional area

$\tilde{u}$ - Magnitude of the total apparent velocity vector, $\tilde{u} = \left(u_x^2 + u_y^2 + u_z^2\right)^{\frac{1}{2}}$

u,v,w - Actual velocities equal to $u = u_x/\varepsilon$, $v = u_y/\varepsilon$, $w = u_z/\varepsilon$

V - Total velocity vector in the crack

X,Y,Z - Spatial coordinates

$\bar{X},\bar{Y},\bar{Z}$ - Normalized spatial coordinates equal to $\bar{X} = X/L$, $\bar{Y} = Y/L$, $\bar{Z} = Z/L$

$\hat{X},\hat{Y},\hat{Z}$ - Terms due to body forces acting on an elemental volume which are used in deriving Darcy's law

X_0 - Total length in the "X" direction

ξ_0 - Yeremenko and Markov's unsteady flow parameter

$\delta_x^2,\delta_y^2,\delta_z^2$ - Finite difference forms of the second derivative

ε - Porosity of the earth formation

ε_t - Turbulent eddy viscosity

κ - Variable in Blottner's grid stretching relationship normally ranging from 1.5 to $e = 2.718$

λ - Frictional coefficient

λ_l - Laminar flow frictional coefficient

λ_{Lame} - Lamé constant in the earth formation

λ_t - Turbulent flow frictional coefficient

μ - Gas viscosity

μ_{Lame} - Lamé constant in the earth formation

ν - Poisson's ratio of the earth formation

ρ - Gas density

ρ_s - Bulk density of the earth formation

τ - Dimensionless time equal to $k_0(P_1-P_0)t/\varepsilon\mu L^2$

τ_l - Laminar shear stress

τ_t - Turbulent shear stress

τ_w - Wall shear stress

Acknowledgments

Messrs. W. Arnold, V. Karpenko, and C. Walter of the Lawrence Livermore Laboratory authorized and supported this research. Professors H. Brandt, H. Dwyer, and A. McKillop of the University of California at Davis gave technical guidance throughout the project.

References

1. G. C. Howard, and C. R. Fast, Hydraulic Fracturing, (Society of Petroleum Engineers of AIME, New York, 1970).

2. M. E. Hanson, B. K. Crowley, and J. S. Kahn, Massive Hydraulic Fracturing: Identification of Critical Technical Issues for Application in Increasing Gas Production in the Western United States, Lawrence Livermore Laboratory, Rept. UCRL-51751, (1975).

3. R. Rozsa, D. Snoeberger, and J. Baker, Permeability of a Nuclear Chimney and Surface Alluvium, Area 2, ERDA NTS, Lawrence Livermore Laboratory Rept. UCID-16722, (1975).

4. E. Teller, W. K. Talley, G. H. Higgins, and G. W. Johnson, The Constructive Uses of Nuclear Explosives (McGraw-Hill, New York, 1968) p. 162, Chapter 4.

5. I. K. Lee, Soil Mechanics, Selected Topics, (American Elsevier, New York, 1968) pp 36-38.

6. C. E. Keller, A. H. Davis, and J. N. Stewart, Jr., The Calculation of Steam Flow and Hydraulic Fracturing in a Porous Medium with the KRAK Code, Los Alamos Scientific Laboratory, Rept. LA-5602-MS, (1974).

7. J. M. Cleary, Hydraulic Fracture Theory, State of Illinois Division of Geological Survey, Urbana, Illinois, Circulars 251, 252, and 281, (1958, 1959).

8. C. M. Gerrard, and J. R. Morgan, "Initial loading of a Sand Layer Under a Circular Pressure Membrane," Geotechnique, Vol. 22, (1972,) pp 635-661.

9. F. A. Morrison, Jr., "Transient Gas Flow in a Porous Column," I&EC Fundamentals, Vol. 11. (1972) pp 191-197.

10. H. Schlichting, Boundary-Layer Theory, (McGraw-Hill, New York 6th Edition, 1968).

11. S. P. Timoshenko, and J. N. Goodier, Theory of Elasticity, (McGraw-Hill, New York, 3rd Edition, 1970) p 402ff.

12. A. E. H. Love, "The Stress Produced in a Semi-Infinite Solid by Pressure on Part of the Boundary," Trans. Royal Soc. of London, Series A, Vol. 228, 1929, pp 377-420.

13. W. H. Campen, and J. R. Smith, Use of Load Tests in the Design of Flexible Pavements, ASTM Special Technical Publication No. 79, (1947), pp 51-64.

14. H. Brandt, H. Chu, and J. Scott, Triaxial Tests of Alluvium, Final Report for Contract 648205, University of California at Davis, published as Lawrence Livermore Laboratory Rept., UCRL-13666, (1975).

15. B. Bonner, A. Abey, H. Heard, and R. Schock, High Pressure Mechanical Properties of Merlin Alluvium, Lawrence Livermore Laboratory Rept, UCRL-51252, (1972).

16. I. N. Sneddon, "The Distribution of Stress in the Neighbourhood of a Crack in an Elastic Solid," Proc. Royal Soc. of London, Series A, Vol. 187, 1009, (1946), pp 229-260.

17. E. L. Wilson, I. Farhoomand, and K. J. Bathe, "Nonlinear Dynamic Analysis of Complex Structures," Earthquake Engineering and Structural Dynamics, Vol. 1, (1973), pp 241-252.

18. I. Farhoomand, Nonlinear Dynamic Stress Analysis of Two-Dimensional Solids, Ph.D. Dissertation, University of California, Berkeley, (1970).

19. F. J. Tokarz, User's Manual of NTEDYNS, A Nonlinear Finite Element Code for Analyzing the Response of Underground Structures Subjected to Ground Shock, Lawrence Livermore Laboratory Rept. UCID-20027, Rev. 1, (1971).

20. J. H. Pitts, Gas-Initiated Crack Propagation in a Porous Solid - A Progress Report, Lawrence Livermore Laboratory Rept, UCID-16236, (1973).

21. R. J. M. DeWeist, Flow Through Porous Media, (Academic Press, New York, 1969), pp 5-6.

22. W. H. Giedt, Thermophysics, (Van Nostrand, New York, 1971), pp 394-401, and 574-575.

23. B. Carnahan, H. A. Luther, and J. O. Wilkes, Applied Numerical Methods, (John Wiley and Sons, New York, 1969).

24. P. J. Roache, Computational Fluid Dynamics, (Hermosa, Albuquerque, N.M., 1972).

25. P. L. T. Brian, "A Finite-Difference Method of High-Order Accuracy for the Solution of Three-Dimensional Transient Heat Conduction Problems," AICHE Journal, Vol. 7, (1961), pp 367-370.

26. F. G. Blottner, "Variable Grid Scheme Applied to Turbulent Boundary Layers," in Computer Methods in Applied Mechanics and Engineering, Vol. 4, (1974), pp 179-194.

27. T. Cebeci, and A. M. O. Smith, "A Finite-Difference Method for Calculating Compressible Laminar and Turbulent Boundary Layers," ASME J. Basic Engineering, Vol 92, (1970), pp 523-535.

28. I. P. Ginzburg, Applied Fluid Mechanics, National Sciences Foundation translation, (1958), p 72.

29. O. N. Petrova, "Pressure and Flow Distribution Along a Pipeline in Unsteady Flow," International Chemical Engineering, Vol. 11, 2, 1971), pp 242-243.

30. Ye. V. Yeremenko, and S. B. Markov, "On Calculation of Averaged Velocities and Resistance in Unstable [Transient] Turbulent Flow in a Pressurized Rough Channel," Fluid Mechanics-Soviet Research, Vol. 1, 5, (1972), pp 48-58.

31. J. R. Doughty, "Parallel Porous Plate Channel Flow Characteristics Resulting from Nonuniform Entry Velocity Profiles," Journal of Fluids Engineering, Vol. 97, (1975), pp 78-81.

32. F. B. Hildrebrand, Finite Difference Equations and Simulations, (Prentice Hall, New York, 1968), Chapt. 3.

33. N. N. Yanenko, The Method of Fractional Steps, (Springer-Verlag, 1971), Chapt. 2.

Appendix A - Derivation of the Governing Equations

Included are the detailed analyses for determining crack wall deflection and gas flow with in a porous solid such as an earth formation and in the crack. Gas flow in the crack uses a correlation for frictional coefficient, λ, which is also discussed. In the appropriate portions of this appendix, alternate methods of solution are mentioned along with the reasons for using the particular method selected.

DEFLECTION OF THE CRACK WALL

Total deflection of the crack wall in the "X" direction will normally exceed the initial crack thickness. We must account for this deflection to predict the "Y" and "Z" direction flow of gas in the crack accurately since the governing equation (Eq. 19) is dependent on crack thickness.

Referring to Fig. 3, consider the right hand crack wall to be a portion of the surface of a semi-infinite solid. Deflection of the crack wall in the "X" direction results from two opposing forces as explained in the analysis section. The gas pressure in the crack exerts a force that tends to deflect the crack wall in the "X" direction. The horizontal earth formation resistive pressure results in a force which tends to prevent deflection and keep the crack closed. Any deflection of the crack wall beyond its initial position is then the resultant of these two effects.

In calculating the deflection of the crack wall, the magnitude of the gas pressure in the crack is taken to be that in excess of the initial pore pressure in the earth formation. At NTS, the pores of the earth formation are filled with air to the depths of interest of this study so that the initial pore pressure is atmospheric.

The horizontal earth formation resistive pressure is due to the overburden, or weight of material above, and is transmitted through the solid grains of the earth formation. If the earth formation has little strength and is subject to creep over geological times, then the horizontal resistive pressure will be close in magnitude to the overburden which is about 20 kPa/m of depth. Alluvium soil at the Nevada Test Site falls near to this category. Alternately, if a hydrostatic state is not reached, then a three-dimensional stress state would exist where resistive pressure forces are a fraction of the

overburden. For example, if there has been no horizontal strain, the magnitude of this fraction is determined from Hooke's law to be $1-\nu/\nu$.

Total deflection in the "X" direction is found by applying the technique of superposition. We first determine deflection due to force applied at a point on the surface of a semi-infinite solid as shown in Fig. A-1 part a. Following the analysis developed by Bousinesq [A-1] and outlined by Timoshenko and Goodier[11], deflection in the "X" direction caused by an applied force on the surface of a semi-infinite solid is

$$D(Y,Z) = \frac{(1-\nu^2)\ F\ (Y',Z')}{\pi\ E\ R} \qquad \text{(A-1)}$$

where here the deflection, D, acts at coordinates (Y,Z) and the force F, acts at coordinates (Y',Z').

The applied force is considered equal to the difference between the gas pressure in the crack that is in excess of the initial pore pressure, and the earth formation resistive pressure, times a small area of application as shown in Fig. A-1 part b. The calculated deflection of Eq. (A-1) then becomes

$$D(Y,Z) = \frac{(1-\nu^2)\ (P-P_r)dY'dZ'}{\pi\ E\ R} \qquad \text{(A-2)}$$

where P_r is the earth formation resistive pressure; and dY', dZ' is the area over which the pressures are applied. Integrating the deflection calculated in Eq. (A-2) over a finite area of surface gives a solution for the total

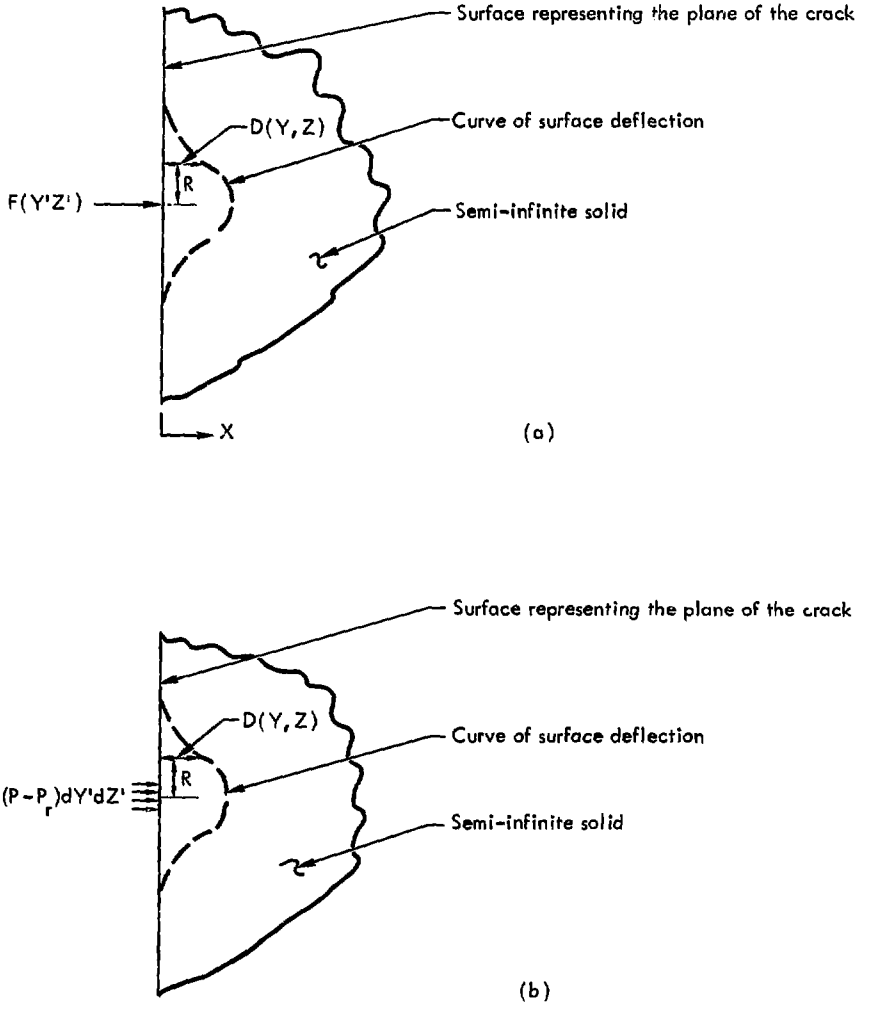

Fig. A-1. Part a. Surface deflection due to a force applied to a point on a semi-infinite solid. (See Eq. (A-1)). Part b. Surface deflection due to a pressure applied over a small area of surface. (See Eq. (A-2)).

deflection, D, at coordinates (Y,Z) due to pressure acting on a portion of the boundary*

$$D(Y,Z) = \frac{(1-\nu^2)}{\pi E} \iint \frac{(P-P_r)\, dY'dZ'}{\sqrt{(Y-Y')^2 + (Z-Z')^2}} \qquad \text{(A-3)}$$

The deflection at the coordinates (Y',Z') as calculated by Eq. (A-3) is singular. At this position, the average deflection under a small area is used since in reality the pressures are applied not at a point but over a small area. Timoshenko and Goodier[11] have calculated average surface deflections for various rectangles subjected to a uniform pressure. In the special case of a square, which is convenient for our coordinate mesh spacing,

$$D(Y',Z')_{\text{Average}} = \frac{0.95(1-\nu^2)}{E} (P-P_r) (A)^{\frac{1}{2}} \qquad \text{(A-4)}$$

Total deflection at any point (Y,Z) due to pressure applied over part of the boundary of a semi-infinite solid may be calculated by using Eqs. (A-3) and (A-4).

---

*The form of Eq. (A-3) may be placed into that derived by Love[12] if relationships between E and ν and the Lamé constants $\mu_{Lamé}$ and $\lambda_{Lamé}$ are used. Taking

$$E = 2\, \mu_{Lamé}\, (1 + \nu)$$

$$\nu = \frac{\lambda_{Lamé}}{2(\lambda_{Lamé} + \mu_{Lamé})}$$

gives

$$\frac{1-\nu^2}{E} = \frac{(1-\nu)(1+\nu)}{2\, \mu_{Lamé}\, (1+\nu)} = \frac{\lambda_{Lamé} + 2\, \mu_{Lamé}}{4\, \mu_{Lamé}\, (\lambda_{Lamé} + \mu_{Lamé})}$$

The right hand side of the above equation is the form used by Love.

The nature of the calculated deflection is such that a pressure applied over one region of the surface results in deflections over all areas of the surface. Deflections approach zero only as the radius approaches infinity. This is a result of the assumption that the medium is elastic. Actual data shows that an elastic analysis gives reasonable results for initial loading near the point of load application but over-predicts the surface deflections as the distance away from the load increases.

Fig. A-2 indicates the variation of surface deflection with distance from the point of load application. The theoretical curve is shown for an elastic material calculated using Timoshenko and Goodier's[11] analysis for a circular loading area. It may be seen to give deflections larger than the experimental data of Gerrard and Morgan[8] away from where the load is applied. Gerrard and Morgan have developed more accurate theoretical solutions however these solutions still overpredict the data away from the area of load application.

The data of Gerrard and Morgan is extrapolated to zero at a radius of five in conformance with data of Campen and Smith.[13] The magnitude of deflection at the centerline of the uniform pressure loading area predicted by Timoshenko and Goodier agrees with Gerrard and Morgan's experimental data if an elastic modulus of about 6.9 MPa is incorporated. Gerrard and Morgan reference data from triaxial tests by Holden[A-2] for their soil where the elastic modulus ranges from 3.4 to 10.3 MPa. Holden's data confirms that the experimental deflections near the uniform pressure loading area agree with the theory and only differ at locations away from the loading area.

Waterways Experiment Station[A-3] reports other data below the surface but off the axis of the point of load application. Extrapolation of this data to the surface gives a result that is also overpredicted by theory.

We felt the more accurate and easier method of determining surface deflection was to utilize Gerrard and Morgan's data directly. The computer program used for this dissertation incorporates a square grid in the Y-Z plane. We converted these squares to equivalent circles by equating areas. This is, a square with sides of 2a would be considered equivalent to a circle of radius $(4/\pi)^{\frac{1}{2}}a$. Deflection at coordinates (Y,Z) due to a uniform pressure applied over an elemental area at coordinates (Y',Z') is found using the formula

$$D(Y,Z) = C_G \frac{(1 - \nu^2)}{E} (P-P_r) (\Delta Y' \Delta Z')^{\frac{1}{2}}. \qquad (A-5)$$

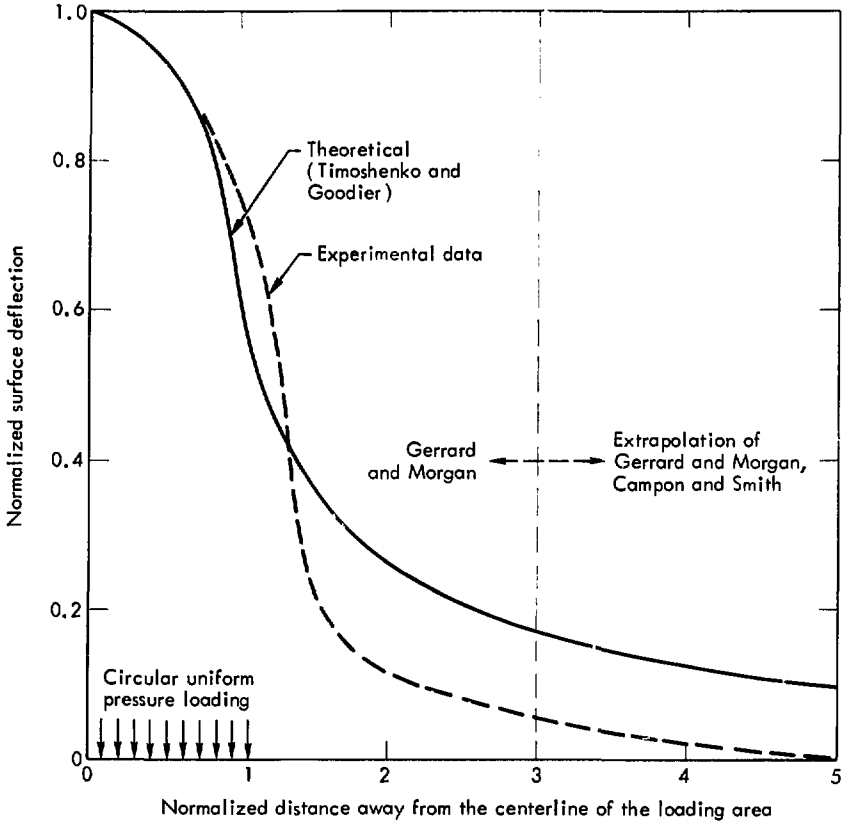

Fig. A-2. Profile of surface displacements.

The Gerrard and Morgan deflection coefficient, C_G, is set equal to 0.95 if the point where the deflection is calculated is below the loading area in conformance with Eq. (A-4). The coefficient would be zero for normalized radii beyond five. Table A-1 shows these coefficients for a square coordinate grid. The coefficients define a circle of influence around the location of uniform pressure load application beyond which the load has no effect on deflection.

Table A-1 - Gerrard and Morgan Deflection Coefficients for Uniform Pressure Loading of a Square Area with Sides Equal to 2a.

		"Y" Direction		
Mesh No.		1	2	3
"Z" Direction	1	$r/a_{eq} = 0$	1.77	3.55
		$C_G = 0.95$	0.30	0.05
	2	$r/a_{eq} = 1.77$	^.51	3.96
		$C_G = 0.30$	0.10	0.02
	3	$r/a_{eq} = 3.55$	3.96	5.01
		$C_G = 0.05$	0.02	0.002

r/a_{eq} - normalized distance from the center of the mesh indicated, to the center of mesh (1,1). Mesh (1,1) is the area subjected to uniform pressure loading.

$$a_{eq} = \left(\frac{4}{\pi}\right)^{\frac{1}{2}} a.$$

C_G - Gerrard and Morgan Deflection Coefficient for use in Eq. (A-5 to A-7).

The total deflection, D, at a point is found using superposition by summing the component deflections for all non-zero C_G using the following equation.

$$D(Y,Z)_{total} = \sum C_G \frac{(1 - \nu^2)}{E} (P-P_r) (\Delta Y' \Delta Z')^{\frac{1}{2}} \qquad \text{(A-6)}$$

Equation (A-6) is put in dimensionless form

$$\overline{D}(\overline{Y},\overline{Z}) = \sum C_G \frac{(1 - \nu^2)}{\overline{E}} (\overline{P}-\overline{P}_r) (\Delta \overline{Y}' \Delta \overline{Z}')^{\frac{1}{2}} \qquad \text{(A-7)}$$

by dividing D, Y, and Z by a reference length and, $(P-P_r)$ and E by a reference pressure. We use the length of the "Z" axis and the initial driving pressure less the initial pore pressure as reference values. The bars above the variables indicate they are normalized. The crack includes all nodes where tne total deflection is positive. The extent of crack propagation is determined automatically by examining the region of positive total deflection.

The use of superposition is justified by examination of experimental data as indicated in the analysis section. Because alluvium at NTS has negligible strength in tension when compared to the gas pressures present,[4] the crack is actually formed more by parting of the surfaces along the plane of the crack rather than failure of the alluvium material. Even if the alluvium had appreciable strength, the crack could propagate along microfissures developed during the explosion so that formation of the crack would still be by parting of the surfaces. The application of superposition to our study is appropriate since the parting of the crack surfaces is similar to initial deflection of the earth materials which have experimentally exhibited elastic behavior.

An alternate means of predicting deflection for axisymmetric crack shapes was developed by Sneddon.[16] Sneddon incorporates a radially varying pressure within the crack with zero deflection beyond the crack as a boundary condition. A solution involving integration over the crack is developed for an elastic solid. In applying the solution, the axis of symmetry is horizontal and the length of the crack is in the radial direction. The crack contains both vertical and horizontal rays.

Unfortunately, the solution has several drawbacks for our particular application. First, cracks grow more vertically than horizontally since the overburden pressure decreases with depth. Hence, the axisymmetric assumption limits the use of results to small lengths of crack propagation. Second, the boundary condition of zero deflection at and beyond the crack tip is imposed in such a fashion that a separate criteria is required to determine propagation. In the method we utilize, deflection is based on pressures within a circle of influence and the extent of the crack is determined automatically. Third, the form of the integral is inconvenient for incorporation experimental data such as Gerrard and Morgan's[8] and as such is difficult to improve based on actual observation.

Another means of predicting deflection is with the use of a finite element analysis using a computer code such as that developed by Wilson, Farhoomand, and Bathe.[17-19] We used a modification of this code for the solution to a two-dimensional problem[20] analyzed earlier where the crack grew only in the "Z" direction and contained a cross section independent of "Y". Extension of the analysis to three dimensions was possible but prediction of the deflection would be time consuming. Since the deflection is calculated repeatedly along with flow in the crack and in the porous solid, limitations on computer time appear to make this method unfeasible for a three-dimensional analysis.

FLOW IN THE POROUS SOLID

We consider a porous solid such as an earth formation on a macroscopic basis and establish a control volume for analysis that contains both pore space and solid grains as shown in Fig. A-3. A continuity equation is developed by equating the net influx of mass to the time change of mass within the control volume. Apparent velocities u_x, u_y, and u_z are defined as the volume flow rate across a face of the control volume divided by the total cross-sectional area, including both voids and solid. These apparent velocities are different from the actual velocities since a portion of the control volume is occupied by solid grains. Conversion to the actual velocities may be made by dividing the apparent velocities by the porosity. The continuity equation is written as

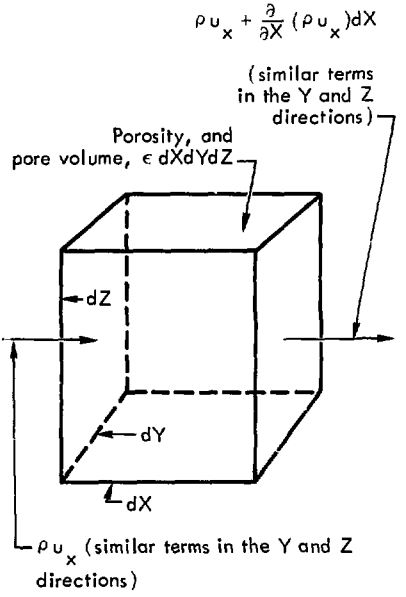

Fig. A-3. Control volume used for derivation of flow through the porous solid.

$$\left[\rho u_x + \frac{\partial}{\partial X}(\rho u_x)dX\right] dYdZ - \rho u_x\, dYdZ$$
$$+ \left[\rho u_y + \frac{\partial}{\partial Y}(\rho u_y)\, dY\right] dXdZ - \rho u_y\, dXdZ$$
$$+ \left[\rho u_z + \frac{\partial}{\partial Z}(\rho u_z)\, dZ\right] dXdY - \rho u_z\, dXdY$$
$$+ \epsilon \frac{\partial \rho}{\partial t} dXdYdZ = 0 \qquad \text{(A-8)}$$

or

$$\frac{\partial}{\partial X}(\rho u_x) + \frac{\partial}{\partial Y}(\rho u_y) + \frac{\partial}{\partial Z}(\rho u_z) + \epsilon \frac{\partial \rho}{\partial t} = 0. \qquad \text{(A-9)}$$

We may apply a similar control volume and develop the Navier-Stokes equations using the actual gas velocities u, v, and w. Full development of the Navier-Stokes equations are shown by Schlichting (Ref. 10, Chapt. 3). For brevity, only the "Z" direction equation with constant viscosity is shown below where $\hat{Z}$ is a term due to the net body force acting on the elemental volume.

$$\rho u \frac{\partial w}{\partial X} + \rho v \frac{\partial w}{\partial Y} + \rho w \frac{\partial w}{\partial Z} + \rho \frac{\partial w}{\partial t} = \hat{Z} - \frac{\partial P}{\partial Z} + \mu \left\{ \frac{\partial^2 w}{\partial X^2} + \frac{\partial^2 w}{\partial Y^2} + \frac{\partial^2 w}{\partial Z^2} + 1/3 \left(\frac{\partial^2 u}{\partial X \partial Z} + \frac{\partial^2 v}{\partial Y \partial Z} + \frac{\partial^2 w}{\partial Z^2} \right) \right\} . \qquad \text{(A-10)}$$

Velocities of interest in flow through porous solids are very slow so that Stoke's approximation may be applied (Ref. 10, p 104ff). That is, we can neglect inertia terms which contain multiples of two velocities, in comparison with those which contain a single velocity. Since the time variable is on the order of Z/w, the last term on the left of Eq. (A-10) contains an equivalent of a multiple of two velocities also. Under Stoke's approximation, then, the left side of Eq. (A-10) is zero. In terms of the apparent velocities, this gives

$$\hat{Z} - \frac{\partial P}{\partial Z} + \frac{\mu}{\varepsilon} \left\{ \frac{\partial^2 u_z}{\partial X^2} + \frac{\partial^2 u_z}{\partial Y^2} + \frac{\partial^2 u_z}{\partial Z^2} + 1/3 \left(\frac{\partial^2 u_x}{\partial X \partial Z} + \frac{\partial^2 u_y}{\partial Y \partial Z} + \frac{\partial^2 u_z}{\partial Z^2} \right) \right\} = 0 \qquad \text{(A-11)}$$

Exact representation of the fluid passing through the solid is not practical because of the multitude of tortuous flow paths which exist. Instead, we view the problem on a macroscopic basis, treating the statistical nature of flow. We assume that

$$\frac{\partial^2 u_z}{\partial X^2} + \frac{\partial^2 u_z}{\partial Y^2} + \frac{\partial^2 u_z}{\partial Z^2} + 1/3 \left(\frac{\partial^2 u_x}{\partial X \partial Z} + \frac{\partial^2 u_y}{\partial Y \partial Z} + \frac{\partial^2 u_z}{\partial Z^2} \right) = - C \frac{u_z}{d^2} \qquad \text{(A-12)}$$

where d is a characteristic length approximating the grain size and C is a dimensionless constant. This approximation has been used by other investigators,[21,A-4] has been verified experimentally, and is dimensionally correct. If we define a permeability

$$k_z = \frac{\varepsilon d^2}{C} \tag{A-13}$$

and set the body force term equal to that due to gravity ($Z = -\rho g$)*, then substituting Eq. (A-12) and (A-13) into (A-11) results in

$$u_z = -\frac{k_z}{\mu}\left(\frac{\partial P}{\partial Z} + \rho g\right). \tag{A-14}$$

The value of permeability, k_z, is determined for each formation normally by experiment and in addition to the above effects contains such items as tortuosity, surface roughness, etc. Equation (A-14) is Darcy's law. For conditions at the Nevada Test Site the value of ρg is negligible with respect to the minimum expected "Z" direction pressure gradient, leaving**

$$u_z \approx -\frac{k_z}{\mu}\frac{\partial P}{\partial Z}. \tag{A-15}$$

We can obtain similar expressions for the "X" and "Y" directions, but in these cases the values of body forces $\hat{X}$ and $\hat{Y}$ are identically equal to zero leaving

$$u_x = -\frac{k_x}{\mu}\frac{\partial P}{\partial X} \tag{A-16}$$

$$u_y = -\frac{k_y}{\mu}\frac{\partial P}{\partial Y}. \tag{A-17}$$

---

*In the appendices of this report we include the acceleration of gravity, g, along with the density so that the equations are similar to those used in the computer program, CHASM, where g is required for consistency of units.

**The driving pressure is on the order of the overburden of the earth formation, so the pressure gradient is approximately equal to the specific weight of the earth formation. That is, $\partial P/\partial Z \approx \rho_s g$ where ρ_s is the density of the earth formation. $\partial P/\partial Z$ ranges between 1.7 and 1.9 g/cc for soils of interest. The value of ρg used in Eq. (A-14) for air is ~.13 g/cc, a negligible value compared to $\partial P/\partial Z$.

Darcy's Law is verified experimentally for Reynolds number,* Re, less than unity but data deviate from this relation as fluid velocity increases. A modification called Forchheimer's relation, which includes a velocity squared term, adequately predicts experimental data up to Re > 1000.[A-5,A-6] This added complication is not necessary for the present investigation because flow in the earth formation is within the regime of Darcy's law.

The equation of state used with the analysis is that of an ideal gas at constant temperature

$$\rho = \frac{P}{R\,T} \,. \tag{A-18}$$

The constant temperature assumption circumvents the need for an energy equation and is valid since the gas reaches the temperature of the earth formation after having traveled normally less than one per cent of the "Z" direction total length into the earth formation. This rapid change to a constant temperature occurs because the heat capacity of the earth formation is large in comparison to the amount of energy transported into the earth formation by the gas and because the average grain size of alluvium soil at NTS is small (about 1 mm). A small average grain size results in a large surface area to volume ratio of the particles that enhances heat transfer.

The viscosity of the gas is a strong function of temperature and only a weak function of pressure so that it is appropriate to consider viscosity constant also. Substituting Eqs. (A-15)-(A-18) into Eq. (A-9) gives

$$\frac{\partial}{\partial X}\left(\frac{P}{R\,T}\,\frac{k_x}{\mu}\,\frac{\partial P}{\partial X}\right)+\frac{\partial}{\partial Y}\left(\frac{P}{R\,T}\,\frac{k_y}{\mu}\,\frac{\partial P}{\partial Y}\right)+\frac{\partial}{\partial Z}\left(\frac{P}{R\,T}\,\frac{k_z}{\mu}\,\frac{\partial P}{\partial Z}\right)=\varepsilon\,\frac{\partial\,\frac{P}{R\,T}}{\partial t}\,, \tag{A-19}$$

which for constant temperature and viscosity becomes

$$\frac{\partial}{\partial X}\left(k_x\,P\,\frac{\partial P}{\partial X}\right)+\frac{\partial}{\partial Y}\left(k_y\,P\,\frac{\partial P}{\partial Y}\right)+\frac{\partial}{\partial Z}\left(k_z\,P\,\frac{\partial P}{\partial Z}\right)=\varepsilon\,\mu\,\frac{\partial P}{\partial t}\,. \tag{A-20}$$

---

*Here Reynolds number is defined as, $Re = \tilde{u} d_p \rho/\mu g$ where $\tilde{u}$ is the magnitude of the total apparent velocity vector and d_p is the average particle size of the grains in the earth formation.

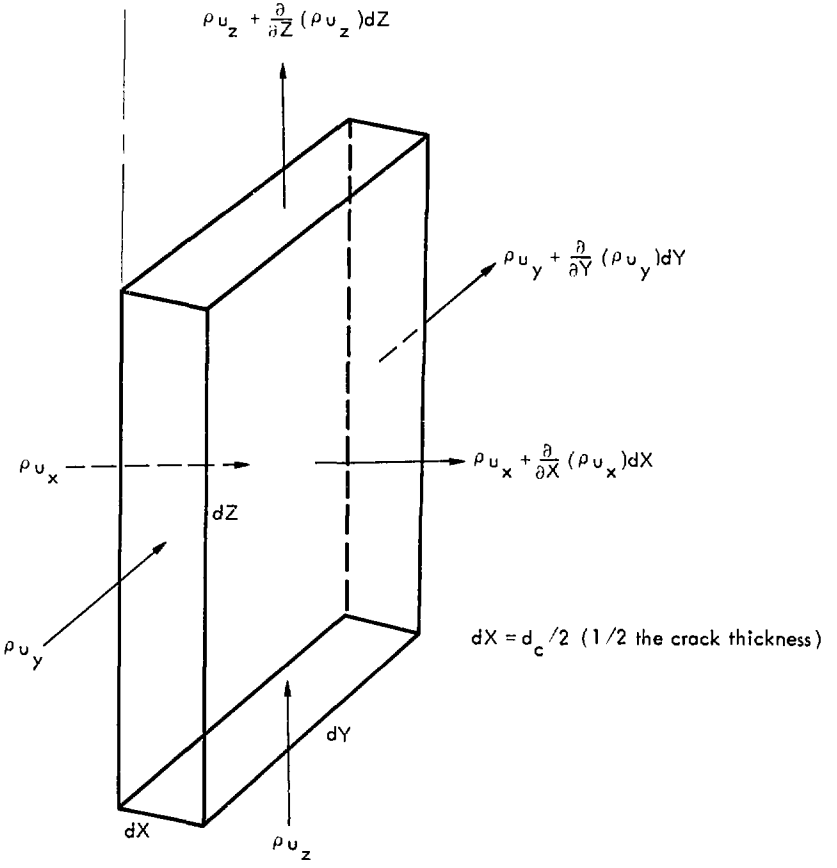

Fig. A-4. Control volume used to derive equations governing gas flow inside the crack.

If we consider P_0, the initial pore gas pressure, and P_1, the initial driving pressure at time zero, we may define a dimensionless pressure

$$\overline{P} = \frac{P - P_0}{P_1 - P_0} , \qquad \text{(A-21)}$$

so that

$$P = \overline{P}(P_1 - P_0) + P_0 \quad . \tag{A-22}$$

Eq. (A-20) then becomes

$$(P_1-P_0)^2 \left\{ \frac{\partial}{\partial X}\left[k_x \left(\overline{P} + \frac{P_0}{P_1-P_0} \right) \frac{\partial}{\partial X}\left(\overline{P} + \frac{P_0}{P_1-P_0} \right) \right] + \frac{\partial}{\partial Y}\left[k_y \left(\overline{P} + \frac{P_0}{P_1-P_0} \right) \frac{\partial}{\partial Y}\left(\overline{P} + \frac{P_0}{P_1-P_0} \right) \right] + \frac{\partial}{\partial Z}\left[k_z \left(\overline{P} + \frac{P_0}{P_1-P_0} \right) \frac{\partial}{\partial Z}\left(\overline{P} + \frac{P_0}{P_1-P_0} \right) \right] \right\} = \varepsilon \mu (P_1-P_0) \frac{\partial}{\partial t}\left[\overline{P} + \frac{P_0}{P_1-P_0} \right] \quad . \tag{A-23}$$

We use a reference length, L, equal to the length of the "Z" axis and a constant reference permeability, k_0, equal to an equivalent crack permeability, discussed later, to make the following definitions

$$\overline{X} = \frac{X}{L} \tag{A-24a}$$

$$\overline{Y} = \frac{Y}{L} \tag{A-24b}$$

$$\overline{Z} = \frac{Z}{L} \tag{A-24c}$$

$$\overline{k}_x = \frac{k_x}{k_0} \tag{A-25a}$$

$$\overline{k}_y = \frac{k_y}{k_0} \tag{A-25b}$$

$$\bar{k}_z = \frac{k_z}{k_0} \tag{A-25c}$$

$$\tau = \frac{k_0 (P_1 - P_0)t}{\varepsilon \mu L^2} . \tag{A-26}$$

The variables with bars then are normalized and τ is a dimensionless time. Combining these definitions with the constant

$$N = \frac{P_1}{P_0} \tag{A-27}$$

in Eq. (A-23) gives

$$\frac{\partial}{\partial \bar{X}} \left[\bar{k}_x \left(\bar{P} + \frac{1}{N-1} \right) \frac{\partial}{\partial \bar{X}} \left(\bar{P} + \frac{1}{N-1} \right) \right]$$

$$+ \frac{\partial}{\partial \bar{Y}} \left[\bar{k}_y \left(\bar{P} + \frac{1}{N-1} \right) \frac{\partial}{\partial \bar{Y}} \left(\bar{P} + \frac{1}{N-1} \right) \right]$$

$$+ \frac{\partial}{\partial \bar{Z}} \left[\bar{k}_z \left(\bar{P} + \frac{1}{N-1} \right) \frac{\partial}{\partial \bar{Z}} \left(\bar{P} + \frac{1}{N-1} \right) \right]$$

$$= \frac{\partial \left[\bar{P} + \frac{1}{N-1} \right]}{\partial \tau} . \tag{A-28}$$

If $\bar{k}_x$, $\bar{k}_y$, and $\bar{k}_z$ are considered independent of their associated spatial coordinate, then Eq. (A-28) may be simplified to

$$\frac{\bar{k}_x}{2} \frac{\partial^2}{\partial \bar{X}^2} \left[\left(\bar{P} + \frac{1}{N-1} \right)^2 \right] + \frac{\bar{k}_y}{2} \frac{\partial^2}{\partial \bar{Y}^2} \left[\left(\bar{P} + \frac{1}{N-1} \right)^2 \right]$$

$$+ \frac{\bar{k}_z}{2} \frac{\partial^2}{\partial \bar{Z}^2} \left[\left(\bar{P} + \frac{1}{N-1} \right)^2 \right] = \frac{\partial}{\partial \tau} \left[\bar{P} + \frac{1}{N-1} \right] . \tag{A-29}$$

This development follows the arguments of Morrison[9] who reasoned that we could reduce the error involved in approximating the derivatives by finite differences if we take the function

$$F = \left(\bar{P} + \frac{1}{N-1} \right)^2 \tag{A-30}$$

as the dependent variables for differentiation. Realizing that N is a constant and using the definition for F, Eq. (A-29) becomes

$$\frac{\bar{k}_x}{2} \frac{\partial^2 F}{\partial \bar{X}^2} + \frac{\bar{k}_y}{2} \frac{\partial^2 F}{\partial \bar{Y}^2} + \frac{\bar{k}_z}{2} \frac{\partial^2 F}{\partial \bar{Z}^2} = \frac{\partial \bar{P}}{\partial \tau} \quad . \tag{A-31}$$

Eq. (A-31) is the governing equation for flow in the solid if the normalized permeabilities are constant. If the normalized permeabilities vary spatially, then the governing equation is

$$\frac{\partial}{\partial \bar{X}} \left(\frac{\bar{k}_x}{2} \frac{\partial F}{\partial \bar{X}} \right) + \frac{\partial}{\partial \bar{Y}} \left(\frac{\bar{k}_y}{2} \frac{\partial F}{\partial \bar{Y}} \right) + \frac{\partial}{\partial \bar{Z}} \left(\frac{\bar{k}_z}{2} \frac{\partial F}{\partial \bar{Z}} \right) = \frac{\partial \bar{P}}{\partial \tau} \tag{A-32}$$

FLOW IN THE CRACK

Flow in the crack is similar to flow within a pipe with porous walls. Consider a control volume which extends from the centerline of the crack to the boundary of the porous solid as shown in Fig. A-4. The total dimensions of the crack in the "Y" and "Z" directions are considerably larger than those of the control volume. A continuity equation is written by equating the net influx of mass to the time change of mass within the control volume and becomes

$$\left[\rho u_x + \frac{\partial}{\partial X} (\rho u_x)\, dX \right] dY dZ - \rho u_x dY dZ + \left[\rho u_y + \frac{\partial}{\partial Y} (\rho u_y) dY \right] dX dZ - \rho u_y dX dZ$$

$$+ \left[\rho u_z + \frac{\partial}{\partial Z} (\rho u_z) dZ \right] dX dY - \rho u_z\, dX dY + \frac{\partial \rho}{\partial t} dX dY dZ = 0 \tag{A-33}$$

or

$$\frac{\partial}{\partial X}(\rho u_x) + \frac{\partial}{\partial Y}(\rho u_y) + \frac{\partial}{\partial Z}(\rho u_z) + \frac{\partial \rho}{\partial t} = 0 \quad . \tag{A-34}$$

The porosity does not enter the crack flow equation as was the case in the porous solid because it is unity. The centerline of the crack is a line of symmetry and as such, no flow crosses the left hand boundary. Flow across the right hand boundary is dependent on the pressure gradient in the porous solid to the right. Since the distance, dX, is equal to one-half the crack thickness and since the velocity is zero across the left face we rewrite Eq. (A-34) as

$$\frac{\rho u_x}{d_c/2} + \frac{\partial}{\partial Y}(\rho u_y) + \frac{\partial}{\partial Z}(\rho u_z) + \frac{\partial \rho}{\partial t} = 0 \quad . \tag{A-35}$$

The velocity u_x is identical to the apparent velocity defined when deriving the equations for flow in the porous solid. This velocity may be equated, using Darcy's law, to the pressure in the porous solid.

$$u_x = -\frac{k_x}{\mu}\frac{\partial P}{\partial X} \tag{A-36}$$

We use the fully developed internal flow momentum equation (Ref. 10, Chapter 20) in the "Y" and "Z" directions. The shear forces along the sides of the channel are equated to the difference of normal pressure forces between the ends of the control volume as shown in Fig. A-5. The value d_h is the hydraulic diameter with dN equal to an elemental length in the direction of the total velocity vector. That is, the velocity in the crack normally has components in both the "Y" and "Z" directions. The total velocity vector is the sum of these two components. Using a frictional coefficient, λ, defined with a total velocity vector, V, and wall shear stress, τ_ω, as

$$\lambda = \frac{\tau_\omega}{\frac{\rho V}{2g}} \tag{A-37}$$

then a force balance gives

$$\left[P - \left(P + \frac{dP}{dN}\,dN\right)\right] d_h = \tau_\omega\, dN = \frac{\lambda \rho V^2}{2g}\, dN \tag{A-38}$$

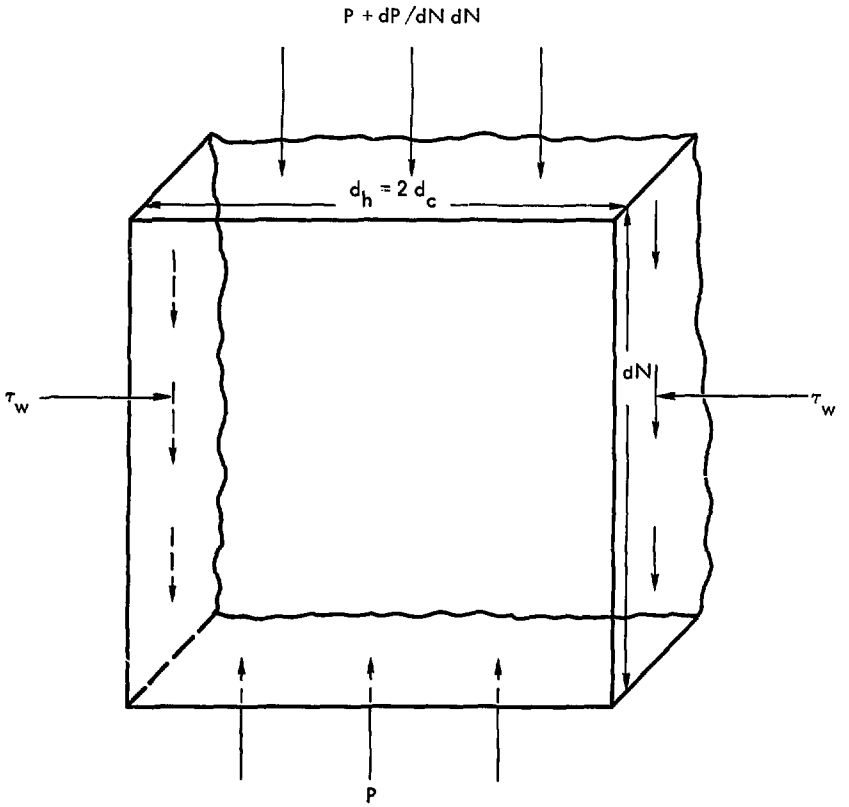

Fig. A-5. Equivalent control volume for determining a force balance in the crack.

or

$$\frac{dP}{dN} = -\frac{\lambda}{d_h}\frac{\rho V^2}{2g} \quad . \tag{A-39}$$

The crack geometry approximates two parallel plates separated by a small distance. The hydraulic diameter* for this geometry is twice the separation or twice the crack width. That is

$$d_h = 2d_c \quad . \tag{A-40}$$

Eq. (A-39) is broken into the following two component equations using velocities parallel to the "Y" and "Z" directions.

$$\frac{\partial P}{\partial Y} = -\frac{\lambda}{2d_c}\frac{\rho u_y^2}{2g} \tag{A-41}$$

$$\frac{\partial P}{\partial Z} = -\frac{\lambda}{2d_c}\frac{\rho u_z^2}{2g} \tag{A-42}$$

Combining the continuity and momentum equations for flow within the crack with the ideal gas equation of state, (Eq. A-18) gives

$$-\frac{2}{d_c}\frac{P}{R\,T}\frac{k_x}{\mu}\frac{\partial P}{\partial X} \pm \frac{\partial}{\partial Y}\left(\frac{P}{R\,T}\left(\left|\frac{4gd_c}{\lambda}\frac{R\,T}{P}\frac{\partial P}{\partial Y}\right|\right)^{1/2}\right)$$

$$\pm \frac{\partial}{\partial Z}\left(\frac{P}{R\,T}\left(\left|\frac{4gd_c}{\lambda}\frac{R\,T}{P}\frac{\partial P}{\partial Z}\right|\right)^{1/2}\right) + \frac{\partial}{\partial t}\frac{P}{R\,T} = 0 \quad . \tag{A-43}$$

*The hydraulic diameter used is equal to four times the flow area divided by the wetted perimeter. Different definitions are used by different authors.

The plus sign on the "Y" and "Z" terms is used if the pressure gradient is <0 and the minus sign if the pressure gradient is >0. As before we take the flow to be isothermal which gives

$$- \frac{k_x}{\mu d_c} \frac{\partial(P^2)}{\partial X} \pm \frac{\partial}{\partial Y} \left(\left| \frac{2gd_c}{\lambda} R T \frac{\partial(P^2)}{\partial Y} \right| \right)^{\frac{1}{2}}$$

$$\pm \frac{\partial}{\partial Z} \left(\left| \frac{2gd_c}{\lambda} R T \frac{\partial(P^2)}{\partial Z} \right| \right)^{\frac{1}{2}} + \frac{\partial P}{\partial t} = 0 \quad . \tag{A-44}$$

If we use the definition of the normalized variables for $\overline{P}$, $\overline{X}$, $\overline{Y}$, $\overline{Z}$, τ, and F we find

$$\frac{\partial(P^2)}{\partial X} = \frac{(P_1-P_0)^2}{L} \frac{\partial F}{\partial \overline{X}} \tag{A-45a}$$

$$\frac{\partial(P^2)}{\partial Y} = \frac{(P_1-P_0)^2}{L} \frac{\partial F}{\partial \overline{Y}} \tag{A-45b}$$

$$\frac{\partial(P^2)}{\partial \overline{Z}} = \frac{(P_1-P_0)^2}{L} \frac{\partial F}{\partial \overline{Z}} \tag{A-45c}$$

$$\frac{\partial P}{\partial t} = \frac{k_0(P_1-P_c)^2}{\epsilon \mu L^2} \frac{\partial \overline{P}}{\partial \tau} \tag{A-46}$$

so that Eq. (A-44) becomes

$$-\frac{k_x(P_1-P_0)}{\mu\, d_c}\frac{\partial \bar{F}}{\partial \bar{X}} \pm \frac{1}{L}\frac{\partial}{\partial \bar{Y}}\left(\left|\frac{2g\, d_c\, L\, R\, T}{\lambda}\frac{\partial \bar{F}}{\partial \bar{Y}}\right|\right)^{\frac{1}{2}}$$

$$\pm \frac{1}{L}\frac{\partial}{\partial \bar{Z}}\left(\left|\frac{2g\, d_c\, L\, R\, T}{\lambda}\frac{\partial \bar{F}}{\partial \bar{Z}}\right|\right)^{\frac{1}{2}} + \frac{k_0(P_1-P_0)}{\varepsilon\, \mu\, L}\frac{\partial \bar{P}}{\partial \tau} = 0 \,. \qquad \text{(A-47)}$$

Finally we simplify Eq. (A-47) by defining effective crack permeabilities in the "X" direction and the "Y" or "Z" direction as

$$\bar{k}_{cx} = \frac{\varepsilon\, L\, k_x}{d_c k_0} \qquad \text{(A-48)}$$

$$k_{cyz} = \frac{\varepsilon\, \mu}{(P_1-P_0)k_0}\left(\frac{2g\, d_c\, L\, R\, T}{\lambda}\right)^{\frac{1}{2}} \qquad \text{(A-49)}$$

to give the governing equation for flow inside the crack as

$$-\bar{k}_{cx}\frac{\partial \bar{F}}{\partial \bar{X}} \pm \frac{\partial}{\partial \bar{Y}}\left(\bar{k}_{cyz}\left(\left|\frac{\partial \bar{F}}{\partial \bar{Y}}\right|\right)^{\frac{1}{2}}\right) \pm \frac{\partial}{\partial \bar{Z}}\left(\bar{k}_{cyz}\left(\left|\frac{\partial \bar{F}}{\partial \bar{Z}}\right|\right)^{\frac{1}{2}}\right) + \frac{\partial \bar{P}}{\partial \tau} = 0 \,. \qquad \text{(A-50)}$$

The value of reference permeability, k_0, may be taken as any representative quantity. We set k_0 so that all values of k_{cyz} are initially less than or equal to unity. That is

$$k_0 = \frac{\varepsilon\, \mu}{(P_1-P_0)}\left(\frac{2g\, d_{c_{max}}\, L\, R\, T}{\lambda}\right)^{\frac{1}{2}} \,. \qquad \text{(A-51)}$$

where $d_{c_{max}}$ is evaluated as its maximum initial value. This reference permeability is a constant for each problem.

The value of frictional coefficient, λ, depends on Reynolds number and relative roughness. Both laminar and turbulent frictional coefficients are calculated at each node within the crack based on the Reynolds number and relative roughness present. The larger of the frictional coefficient values is used since in accordance with reported data (Ref. 10, Fig. 20.18) the laminar frictional coefficient will be greater only if the flow is laminar. This is explained graphically in Fig. (A-6).

The frictional coefficient for turbulent flow is based on the completely rough regime with one of the turbulent curves selected based on relative roughness. Even though the crack wall is considered to have a uniform absolute roughness, the relative roughness will be different for each node in the crack because of a varying crack thickness. The transition flow regime is omitted with the completely rough turbulent frictional coefficient used for all Reynolds numbers unless the flow is laminar.

CALCULATION OF THE FRICTIONAL COEFFICIENTS

In calculating the laminar frictional coefficient, we find that the shape of the flow channel is important. For the case of parallel plates (or an annular region with small separation between the walls), the experimental data correlates with (Ref. 10, Fig. 20.12)

$$\lambda_{\ell} = \frac{96}{Re} \tag{A-52}$$

where the subscript ℓ represents laminar. The value of Reynolds number is based on the total velocity vector, V, and the hydraulic diameter, d_h, which for the case of parallel plates is twice the crack thickness, d_c. The Reynolds number then is

$$Re = \frac{V\, d_h\, \rho}{\mu\, g}$$

$$= \frac{2V\, d_c\, \rho}{\mu\, g} \quad . \tag{A-53}$$

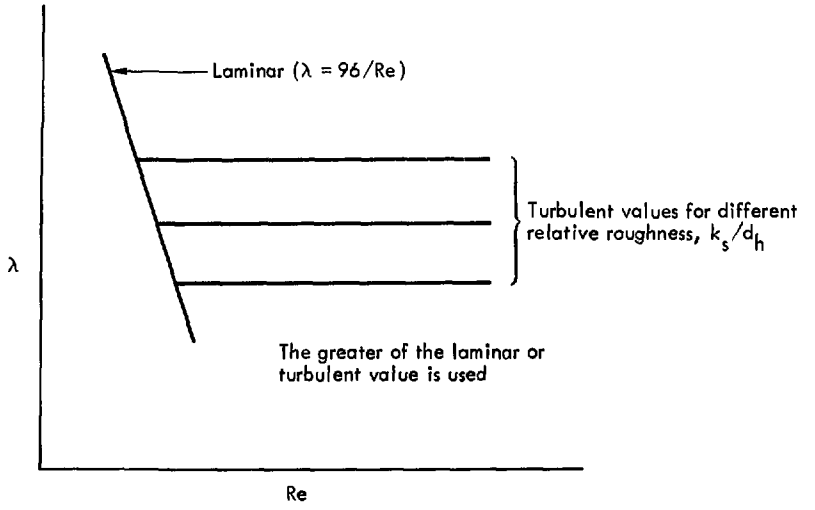

Fig. A-6. Variation of frictional coefficient with Reynolds number and relative roughness.

A comparison may be made between the experimental values which yield Eq. (A-52) and the theory of steady laminar flow through a straight channel (Ref. 10, p 77). Referring to Fig. A-7 the velocity distribution and volumetric flow rate, Q, are

$$u = -\frac{1}{2\mu}\frac{dP}{dX}\ (b^2-Y^2) \qquad \text{(A-54)}$$

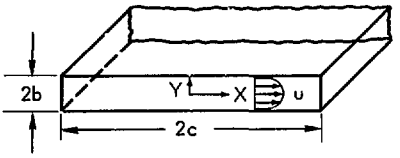

Fig. A-7. Parallel-flow channel used to develop a theoretical laminar flow frictional coefficient.

where $\frac{dP}{dX}$ is a constant and

$$Q = 4 \int_0^c \int_0^b u \, dY \, dX$$

$$= - \frac{2}{\mu} \frac{dP}{dX} \int_0^c \left[b^2 Y - \frac{Y^3}{3} \right]_0^b dX$$

$$= - \frac{4b^3}{3\mu} \frac{dP}{dX} \; X \Big|_0^c$$

$$= - \frac{4}{3} \frac{b^3 c}{\mu} \frac{dP}{dX} \; . \qquad \text{(A-55)}$$

Q is also related to an average velocity across the channel which is set equal to the total velocity vector, V, which is the sum of the "Y" and "Z" direction components of velocity

$$Q = 4 \, bc \, V \; . \qquad \text{(A-56)}$$

Equating Eqs. (A-55) and A-56)

$$- \frac{dP}{dX} = \frac{3\mu V}{b^2} = \frac{3\mu V}{(d_h/4)^2} = \frac{48\mu V}{d_h^2} \qquad \text{(A-57)}$$

The pressure gradient is related by Ref. 10, p 561ff:

$$-\frac{dP}{dX} = \frac{\lambda_\ell}{d_h}\frac{\rho V^2}{2g} \quad . \tag{A-58}$$

Combining Eqs. (A-57) and A-58)

$$\lambda_\ell = \frac{96\ g\mu}{\rho\ d_h\ V} = \frac{96}{Re} \tag{A-59}$$

which gives an identical result to experimental data of Eq. (A-52). We note that for Hagen-Poiseuille flow through a circular pipe the value of the constant would be 64 rather than 96.

The hydrodynamic theory of lubrication (Ref. 10, p 108 ff) is an extension to the above analysis for the case when the plates are not parallel. If the angle between the two plates is significant, then the acceleration term in the Navier Stokes equation, $u\frac{\partial u}{\partial X}$, becomes important and must be compared to the viscous term, $\mu\partial^2 u/\partial y^2$, even though the velocity is small. In our case, this angle is negligible throughout the entire crack and the case of parallel plates applies.

For the turbulent frictional coefficient, λ_t, we utilize the extensive experimental results for fully developed turbulent flow (Ref. 10, Eq. 20.35) which relates λ_t with relative roughness as

$$\lambda_t = \frac{1}{\left(2\ \log\frac{d_h}{k_s} + 1.74\right)^2} \quad . \tag{A-60}$$

The value of relative roughness, k_s/d_h, is the average grain size of particles composing the crack boundary divided by the hydraulic diameter.

ALTERNATE MEANS OF CALCULATING THE "Y" AND "Z" DIRECTION MOMENTUM EQUATIONS IN THE CRACK

The momentum equations utilized for the "Y" and "Z" direction within the crack should include acceleration and transient terms to be complete. The method outlined below adds substantial complication to the analysis but

does include these additional terms which were neglected earlier. Use of steady flow momentum equations in the "Y" and "Z" directions appears intuitively justified since the transit time in the crack is much less than for gas permeation in the solid.

Let us consider that the total velocity in the crack is nearly parallel to the "Z" axis. This will simplify the analysis since $u_y \approx 0$. Extension to the more general case would follow the same outline. Neglecting body forces, the "Z" direction momentum equation is (Ref. 10, Chapter 3)

$$\rho u_z \frac{\partial u_z}{\partial Z} + \rho \frac{\partial u_z}{\partial t} = - \frac{\partial P}{\partial Z} + \mu \frac{\partial^2 u_z}{\partial X^2} . \qquad \text{(A-61)}$$

The terms $\partial^2 u_z/\partial Y^2$ and $\partial^2 u_z/\partial Z^2$ are omitted since they are negligible when compared to $\partial^2 u_z/\partial X^2$.

There is some question as to the form in which the last term of Eq. (A-61) may be written for transient flow. This term relates to the viscous forces present and for steady flows is equated to a frictional coefficient, λ, (Ref. 10, Chapters 19 and 20) as follows.

$$\begin{aligned} \mu \frac{\partial^2 u_z}{\partial X^2} &= \frac{\partial}{\partial X}\left[(\mu + \rho\varepsilon_t) \frac{\partial u_z}{\partial X}\right] \\ &= \frac{\partial}{\partial X} [\tau_\ell + \tau_t] \\ &= \frac{\lambda \rho u_z^2}{4g\, d_c} \end{aligned} \qquad \text{(A-62)}$$

Here τ_ℓ and τ_t are the laminar and turbulent shear stresses and ε_t is the turbulent eddy viscosity.

As explained in the main body of the report, Ginzberg[28] and Petrova[29] both assume that the resistance properties established for steady flow apply for transient conditions. Yeremenko and Markov[30] develop a relationship between increases in frictional coefficient for accelerating flow and an unsteady flow parameter, δ_0, but do not indicate how to obtain δ_0 without knowing the velocity distribution. Although this velocity distribution has been analyzed for laminar flow by Doughty[31], it is unknown in general. Therefore we have used the frictional coefficient based on steady flow.

Combining Eqs. (A-61) and (A-62) with the gas equation of state (Eq. A-18) gives

$$P\,u_z\frac{\partial u_z}{\partial Z} + P\frac{\partial u_z}{\partial t} = -\,R\,T\frac{\partial P}{\partial Z} + \frac{\lambda P u_z^2}{4g\,d_c}\,. \qquad \text{(A-63)}$$

We cannot use Eq. (A-63) to eliminate u_z in the continuity equation for flow in the crack (Eq. A-28) as we had done previously. Instead, Eq. (A-63) is used as one equation in a set of coupled equations which could be solved numerically to obtain values of u_z and P.

The second of the coupled equations is developed for the case when $u_y \approx 0$ by combining the continuity equation, Eq. (A-35), with the "X" direction momentum equation, Eq. (A-36), and the ideal gas equation of state, Eq. (A-18). This gives

$$-\frac{2P\,k_x}{d_c\mu}\frac{\partial P}{\partial X} + \frac{\partial(Pu_z)}{\partial Z} + \frac{\partial P}{\partial t} = 0\,. \qquad \text{(A-64)}$$

It is needless to say that the coupling between Eqs. (A-63) and (A-64) results in substantial complication in obtaining a solution. Rather than attempt this form of solution we choose to use the simpler formulation that includes the momentum equations for fully developed flow in the "Y" and "Z" directions. We then checked the magnitude of the neglected transient and acceleration terms using results of the calculations with the momentum equations for fully developed flow. Fortunately we found that the transient and acceleration terms were less than 10% of the included terms in the momentum equations except at times less than one eighth the total problem time.

does include these additional terms which were neglected earlier. Use of steady flow momentum equations in the "Y" and "Z" directions appears intuitively justified since the transit time in the crack is much less than for gas permeation in the solid.

Let us consider that the total velocity in the crack is nearly parallel to the "Z" axis. This will simplify the analysis since $u_y \approx 0$. Extension to the more general case would follow the same outline. Neglecting body forces, the "Z" direction momentum equation is (Ref. 10, Chapter 3)

$$\rho u_z \frac{\partial u_z}{\partial Z} + \rho \frac{\partial u_z}{\partial t} = - \frac{\partial P}{\partial Z} + \mu \frac{\partial^2 u_z}{\partial X^2} . \qquad \text{(A-61)}$$

The terms $\partial^2 u_z/\partial Y^2$ and $\partial^2 u_z/\partial Z^2$ are omitted since they are negligible when compared to $\partial^2 u_z/\partial X^2$.

There is some question as to the form in which the last term of Eq. (A-61) may be written for transient flow. This term relates to the viscous forces present and for steady flows is equated to a frictional coefficient, λ, (Ref. 10, Chapters 19 and 20) as follows.

$$\mu \frac{\partial^2 u_z}{\partial X^2} = \frac{\partial}{\partial X}\left[(\mu + \rho\varepsilon_t) \frac{\partial u_z}{\partial X}\right]$$

$$= \frac{\partial}{\partial X} [\tau_\ell + \tau_t]$$

$$= \frac{\lambda \rho u_z^2}{4g\, d_c} \qquad \text{(A-62)}$$

Here τ_ℓ and τ_t are the laminar and turbulent shear stresses and ε_t is the turbulent eddy viscosity.

As explained in the main body of the report, Ginzberg[28] and Petrova[29] both assume that the resistance properties established for steady flow apply for transient conditions. Yeremenko and Markov[30] develop a relationship between increases in frictional coefficient for accelerating flow and an unsteady flow parameter, δ_0, but do not indicate how to obtain δ_0 without knowing the velocity distribution. Although this velocity distribution has been analyzed for laminar flow by Doughty[31], it is unknown in general. Therefore we have used the frictional coefficient based on steady flow.

Combining Eqs. (A-61) and (A-62) with the gas equation of state (Eq. A-18) gives

$$P\, u_z \frac{\partial u_z}{\partial Z} + P \frac{\partial u_z}{\partial t} = - R\, T \frac{\partial P}{\partial Z} + \frac{\lambda P u_z^2}{4g\, d_c} . \qquad \text{(A-63)}$$

We cannot use Eq. (A-63) to eliminate u_z in the continuity equation for flow in the crack (Eq. A-28) as we had done previously. Instead, Eq. (A-63) is used as one equation in a set of coupled equations which could be solved numerically to obtain values of u_z and P.

The second of the coupled equations is developed for the case when $u_y \approx 0$ by combining the continuity equation, Eq. (A-35), with the "X" direction momentum equation, Eq. (A-36), and the ideal gas equation of state, Eq. (A-18). This gives

$$- \frac{2P\, k_x}{d_c \mu} \frac{\partial P}{\partial X} + \frac{\partial (P u_z)}{\partial Z} + \frac{\partial P}{\partial t} = 0 . \qquad \text{(A-64)}$$

It is needless to say that the coupling between Eqs. (A-63) and (A-64) results in substantial complication in obtaining a solution. Rather than attempt this form of solution we choose to use the simpler formulation that includes the momentum equations for fully developed flow in the "Y" and "Z" directions. We then checked the magnitude of the neglected transient and acceleration terms using results of the calculations with the momentum equations for fully developed flow. Fortunately we found that the transient and acceleration terms were less than 10% of the included terms in the momentum equations except at times less than one eighth the total problem time.

Even at these early times we felt the transient and acceleration terms could be neglected for two reasons. First, the actual application of applied pressure appears over a short period of time rather than the mathematical step change we had used in the analysis. Second, the effect of any error included by neglecting the transient and acceleration terms at early times has little effect on the overall solution since most changes in gas pressure occurred after the time when the transient and acceleration terms were important.

References for Appendix A

A-1 J. Boussinesq, "Application des Potentials a l'Etude de l'Equilibre et du Mouvement des Solides Elastiques," (Gauthier-Villars, Paris, 1885).

A-2 J. C. Holden, Stresses and Strains in a Sand Mass Subjected to a Uniform Circular Load, Ph.D. Thesis, University of Melbourne, 1967.

A-3 Waterways Experiment Station, Investigation of Pressures and Deflections for Flexible Pavements, Report No. 4, Homogeneous Sand Test Section, Technical Memorandum No. 3-323 (1954).

A-4 M. K. Hubbert, "Darcy's Law and the Field Equations of the Flow of Underground Fluids," Trans. Soc. Petrol. Eng. AIME, Vol. 207 (1956), pp 222-239.

A-5 P. Forcheimer, "Wasserbewegung durch Boden," Zeitschrift des Vereines Deutscher Ingenieure, Vol. 45 (1901), pp 1781-1788.

A-6 F. A. Morrison Jr., Transient Compressible Flows in Porous Media, Final Report (UILU Eng-75 4004) Dept. of Mechanical and Industrial Engineering, University of Illinois at Urbana-Champaign (1975).

Appendix B - Development of the Equations Used for Computation

This appendix converts the governing equations into the difference equations used for numerical computation in the computer code CHASM. If feasible, the difference equations also are written in terms of the variables used in the computer code.

The arrangement of this appendix follows the logic of the computations which is shown on the flow chart of Fig. B-1. After input, calculation of constants, and initialization, we iterate with time through a main computational loop. Within the main computational loop we first calculate the crack wall deflection based on the known values of pressure at time, n. We next calculate the frictional coefficient and values of the coefficients used in the crack-flow equations. Lastly we simultaneously calculate the pressures at a new time, n+1, throughout the solid and crack. If desired, we print out results before repeating the calculations in the main computational loop for the next time step.

The problem is considered complete if the tip of the crack reaches the maximum node in the "Z" direction which normally represents the surface of the earth or if it reaches the maximum node in the "Y" direction which indicates additional nodes need to be added to obtain a proper solution.

Superscripts are used for time variations and subscripts are used for spatial variations as indicated in Table B-1.

Table B-1 - Subscripts and Superscripts used in the Difference Equations

Subscript or superscript	Meaning
n	old time value when conditions are known
n+1	new time value when conditions are unknown
*,**	intermediate time values
...,i-1,i,i+1,...	"X" direction spatial nodes with node i located where values are being calculated
...,j-1,j,...k,k+1,...	"Y" and "Z" direction spatial nodes

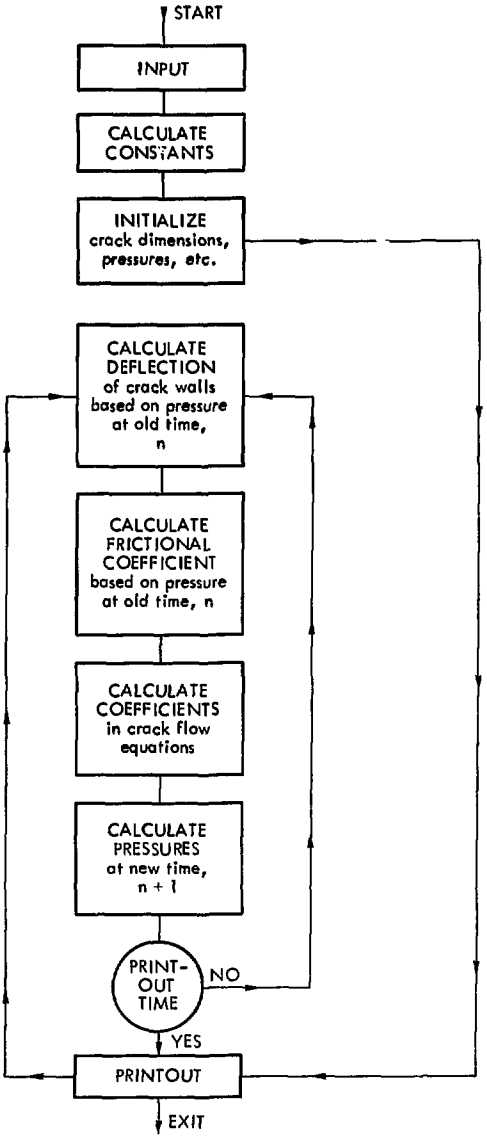

Fig. B-1. Flow chart of computations in the CHASM computer code.

CRACK WALL DEFLECTIONS

Deflections are calculated in dimensional form using Eq. (A-7) multiplied by the reference length, L.

$$\bar{D}\ (\bar{Y},\bar{Z}) = \sum C_G \frac{(1-\nu^2)}{\bar{E}} (\bar{P}-\bar{P}_r)\ (\Delta\bar{Y}'\Delta\bar{Z}')^{\frac{1}{2}} \qquad \text{(A-7)}$$

$$D\ (\bar{Y},\bar{Z}) = \sum C_G \frac{(1-\nu^2)L}{\bar{E}} (\bar{P}-\bar{P}_r)\ (\Delta\bar{Y}'\Delta\bar{Z}')^{\frac{1}{2}} \qquad \text{(B-1)}$$

Values of C_G are established as input in the main computer program from Gerrard and Morgan's[8] and Campen and Smith's[13] deflection data. These coefficients account for the effect of distance between the point the deflection is being calculated and the area subjected to uniform pressure loading as shown in Table A-1. We sum the component deflections only over those areas where C_G is non zero which in our analysis comprises the region within three nodes of the area subjected to uniform pressure loading. In the main computer program we define a term, CDEF, which contains all the constants in Eq. (B-1) and an array, CSUBG(j,k), of the Gerrard and Morgan deflection coefficients as

$$\text{CDEF} = \frac{(1-\nu^2)L}{\bar{E}} \qquad \text{(B-2)}$$

$$\begin{aligned} \text{CSUBG}(j,k) &= C_G\ (\Delta\bar{Y}'\Delta\bar{Z}')^{\frac{1}{2}} \\ &= C_G\ /\ \text{NM1}\ . \end{aligned} \qquad \text{(B-3)}$$

Here, NM1 is the computer term for the number of "Z" direction nodes minus one. Our mesh spacing over the X=0 plane is composed of uniform squares and the values of C_G are calculated for uniform square areas. If a difference mesh spacing such as a rectangle is incorporated, a new set of C_G values in Table A-1 would need to be developed.

The summation in Eq. (B-1) is accomplished in three parts in the computer program. First we sum over all areas which are at the same elevation as the point where deflection is being calculated. If the point is near a boundary

and the circle of influence, where C_G is greater than zero, extends beyond the plane $\bar{Y} = 0$, we utilize a symmetry condition to account for $\bar{Y}<0$. If the circle of influence extends beyond the maximum "$\bar{Y}$" plane we set those gas pressures equal to the value at the maximum "$\bar{Y}$". This is consistent with the boundary condition that the pressure gradient perpendicular to and at the maximum "$\bar{Y}$" plane is zero.

Second we calculate the contribution due to nodes below the $\bar{Z}=0$ plane if the circle of influence extends that far. If the $\bar{Y}$ node is within the region of applied pressure at $\bar{Z}=0$ we utilize the applied pressure less the appropriate earth formation resistive pressure due to overburden as the net force tending to open the crack. If the $\bar{Y}$ node is outside the region of applied pressure we take the pore pressure to be a symmetric image of that above the $\bar{Z}=0$ plane.

Finally, we calculate the contribution of all nodes above the $\bar{Z}=0$ plane which have a non-zero C_G and which have not been calculated previously. In all calculations, the appropriate Gerrard and Morgan deflection coefficient is chosen based on the number of nodes away from the point at which deflection is being calculated. We then multiply by the difference between the gas pressure in excess of the atmospheric pressure present at the node and the earth-formation resistive pressure.

FRICTIONAL COEFFICIENT

The governing equation for a laminar flow frictional coefficient with a geometry of closely spaced parallel walls is

$$\lambda_\ell = 96/Re \qquad \text{(A-52)}$$

where

$$Re = \frac{2V\, d_c\, \rho}{\mu g} \quad . \qquad \text{(A-53)}$$

We first determine a relationship between the total velocity vector, V, and the pressure gradients in the "Y" and "Z" direction. Recalling that in the crack

$$\frac{\partial P}{\partial Y} = - \frac{\lambda}{2d_c} \frac{\rho u_y^2}{2g} \tag{A-41}$$

$$\frac{\partial P}{\partial Z} = - \frac{\lambda}{2d_c} \frac{\rho u_z^2}{2g} \tag{A-42}$$

we may establish the velocity vector relationship as

$$V^2 = u_y^2 + u_z^2$$

$$= \frac{4gd_c}{\rho \lambda_\ell} \left(\left| \frac{\partial P}{\partial Y} \right| + \left| \frac{\partial P}{\partial Z} \right| \right) . \tag{B-4}$$

The absolute value signs are necessary to assure that u_y^2 and u_z^2 are positive for all values of pressure gradient as they must be. We take the values of λ in Eqs. (A-41) and (A-42) to be for laminar flow since we are calculating λ_ℓ. If the flow is actually turbulent, then the calculated value of λ_ℓ will be discarded since the corresponding value calculated for λ_t will be greater.

Combining equations we have

$$\lambda_\ell^2 = \frac{96^2 \mu^2 g^2}{4V^2 d_c^2 \rho^2}$$

$$= \frac{96^2 \mu^2 g \lambda_\ell}{16 d_c^3 \rho \left(\left| \frac{\partial P}{\partial Y} \right| + \left| \frac{\partial P}{\partial Z} \right| \right)} . \tag{B-5}$$

Eliminating the density by using the equation of state (Eq. A-18) yields

$$\lambda_\ell = \frac{96^2\ \mu\ g\ R\ T}{16\ d_c^{\,3}\ P\left(\left|\frac{\partial P}{\partial Z}\right| + \left|\frac{\partial P}{\partial Z}\right|\right)}$$

$$= \frac{96^2\ \mu^2\ g\ R\ T}{8\ d_c^{\,3}\left(\left|\frac{\partial P^2}{\partial Y}\right| + \left|\frac{\partial P^2}{\partial Z}\right|\right)} . \qquad \text{(B-6)}$$

We wish to write Eq. (B-6) in terms of the pressure function, F. From the definitions

$$\bar{P} = \frac{P - P_0}{P_1 - P_0} \qquad \text{(B-7)}$$

$$F = \left(\bar{P} + \frac{1}{N-1}\right)^2 \qquad \text{(A-30)}$$

we obtain

$$P^2 = (P_1-P_0)^2\ \bar{P}^2 + 2P_0\ (P_1-P_0)\ \bar{P} + P_0^{\,2}$$

$$= (P_1-P_0)^2\left(\bar{P}^2 + \frac{2P_0}{P_1-P_0}\bar{P} + \frac{P_0^2}{(P_1-P_0)^2}\right)$$

$$= (P_1-P_0)^2\ F \qquad \text{(B-8)}$$

and

$$\frac{\partial P^2}{\partial Y} = \frac{\partial P^2}{L\partial \bar{Y}}$$

$$= \frac{(P_1-P_0)^2}{L}\ \frac{\partial F}{\partial \bar{Y}} . \qquad \text{(B-9)}$$

Similarly

$$\frac{\partial P^2}{\partial Z} = \frac{(P_1-P_0)^2}{L} \frac{\partial F}{\partial \bar{Z}} . \tag{B-10}$$

Combining Eq. (B-6), (B-9), and (B-10)

$$\lambda_\ell = \frac{96^2 \mu^2 g L R T}{8(P_1-P_0)^2 d_c^3 \left(\left|\frac{\partial F}{\partial \bar{Y}}\right| + \left|\frac{\partial F}{\partial \bar{Z}}\right|\right)} . \tag{B-11}$$

The equation used for computation is written in terms of the crack half thickness rather than the crack thickness so that

$$\lambda_\ell = \frac{144 \mu^2 g L R T}{(P_1-P_0)^2 (d_c/2)^3 \left(\left|\frac{\partial F}{\partial \bar{Y}}\right| + \left|\frac{\partial F}{\partial \bar{Z}}\right|\right)} . \tag{B-12}$$

Care must be exercised to assure compatibility of units. We calculate all constants once in the first part of the main program as

$$\text{CFRICT1} = \frac{144 \mu^2 g L R T}{(P_1-P_0)^2} . \tag{B-13}$$

The difference equations used along with Eqs. (B-12) and (B-13) are

$$\left|\frac{\partial F}{\partial \bar{Y}}\right| = \left|F^n_{j+1,k} - F^n_{j-1,k}\right| \Big/ 2\,\Delta\bar{Y} \tag{B-14}$$

$$\left|\frac{\partial F}{\partial \bar{Z}}\right| = \left|F^n_{j,k+1} - F^n_{j,k-1}\right| \Big/ 2\,\Delta\bar{Z} \tag{B-15}$$

and

$$d_c/2 = d^n_{c_{j,k}} \Big/ 2 . \tag{B-16}$$

If the location at which the frictional coefficient is being calculated is on a boundary then the gradients of the pressure function, F, are evaluated with either forward or backward differences rather than central differences.

The value of the turbulent frictional coefficient is calculated directly as

$$\lambda_t = \frac{1}{\left(2 \log \frac{d_h}{k_s} + 1.74\right)^2} \qquad \text{(A-60)}$$

where k_s/d_h is the relative roughness equal to the average diameter of the solid grains composing the crack wall divided by the hydraulic diameter, $d_h = 2\, d_c = 4(d_c/2)$.

We choose the greater of the laminar or turbulent frictional coefficient for actual use. Because insignificant crack thicknesses can be obtained mathematically, upper limits to the frictional coefficients are imposed to assure that reasonable values are not exceeded.

In the computer program, Reynolds number is calculated after the frictional coefficients. For laminar flow

$$Re = \frac{96}{\lambda_\ell} \, . \qquad \text{(B-17)}$$

For turbulent flow we use Eq. (A-53), (B-4), (B-9) and (B-10). If we recall that the actual equation used for computation is written in terms of the crack half thickness, then

$$Re = \frac{|V|\, d_h\, \rho}{\mu\, g}$$

$$= \frac{2\, d_c}{\mu} \left(\frac{4\, d_c\, \rho}{\lambda_t\, g} \left(\left|\frac{\partial P}{\partial Y}\right| + \left|\frac{\partial P}{\partial Z}\right| \right) \right)^{\frac{1}{2}}$$

$$= \frac{2\, d_c\, (P_1 - P_0)}{\mu} \left(\frac{2\, d_c}{\lambda_t\, g\, L\, R\, T} \left(\left|\frac{\partial F}{\partial \bar{Y}}\right| + \left|\frac{\partial F}{\partial \bar{Z}}\right| \right) \right)^{\frac{1}{2}}$$

$$= \frac{8\, (d_c/2)\, (P_1 - P_0)}{\mu} \left(\frac{(d_c/2)}{\lambda_t\, g\, L\, R\, T} \left(\left|\frac{\partial F}{\partial \bar{Y}}\right| + \left|\frac{\partial F}{\partial \bar{Z}}\right| \right) \right)^{\frac{1}{2}}. \qquad \text{(B-18)}$$

Again the constant values are combined into a single coefficient calculated in the main program which is

$$CFRIC2 = \frac{8(P_1 - P_0)}{\mu} \left(\frac{1}{g\, L\, R\, T} \right)^{\frac{1}{2}} \qquad \text{(B-19}$$

IMPLICIT DIFFERENCING OF THE POROUS-SOLID FLOW EQUATIONS

Above the crack tip but in the plane of the crack as well as throughout the rest of the porous solid, the permeabilities in the spatial coordinates are considered as constants so that the governing equation is

$$\frac{\bar{k}_x}{2} \frac{\partial^2 F}{\partial \bar{X}^2} + \frac{\bar{k}_y}{2} \frac{\partial^2 F}{\partial \bar{Y}^2} + \frac{\bar{k}_z}{2} \frac{\partial^2 F}{\partial \bar{Z}^2} = \frac{\partial \bar{P}}{\partial \bar{T}} \qquad \text{(A-31)}$$

where

$$F = \left(\bar{P} + \frac{1}{N-1} \right)^2 \qquad \text{(B-20)}$$

We wish to difference Eq. (A-31) in terms of the pressure function, F. Using Eq. (B-20) we solve for $\overline{P}$ and $\partial\overline{P}/\partial\tau$ as

$$\overline{P} = F^{\frac{1}{2}} - \frac{1}{N-1} \tag{B-21}$$

$$\frac{\partial\overline{P}}{\partial\tau} = \frac{\partial\overline{P}}{\partial F}\frac{\partial F}{\partial\tau}$$

$$= \frac{1}{2} F^{-\frac{1}{2}} \frac{\partial F}{\partial\tau} \tag{B-22}$$

Substituting into (A-31) we obtain

$$k_x \frac{\partial^2 F}{\partial\overline{X}^2} + k_y \frac{\partial^2 F}{\partial\overline{Y}^2} + k_z \frac{\partial^2 F}{\partial\overline{Z}^2} = F^{-\frac{1}{2}} \frac{\partial F}{\partial\tau} \tag{B-23}$$

The coefficient of the time derivative is always finite since F is bounded by $0 \leq F \leq N^2/(N-1)^2$. Each spatial term taken separately with the time derivative forms a parabolic equation. We follow the procedure described by Carnahan, Luther, and Wilkes[23] which was originally developed by Brian[25] since this reduces to the alternating direction implicit method in two dimensions used in differencing the crack flow equations. Use of Douglas'[B-1] method described by Carnahan is an extension of the Crank-Nicolson method and as such would not be as compatible with the differencing chosen for the implicit solution of gas flow inside the crack in the "Y" and "Z" directions.

The major advantage of the solution method chosen is the tri-diagonal form of the matrix which results. That is, the matrix has non-zero elements only along the diagonal and immediately adjacent elements as shown in Fig. (B-2). A particularly efficient method to solve the matrix is available. Following Brian's[23] method, the solution is broken into three parts as

$$\bar{k}_x \delta_x^2 F^* + \bar{k}_y \delta_y^2 F^n + \bar{k}_z \delta_z^2 F^n = (F^{n,*})^{-\frac{1}{2}} \frac{F^* - F^n}{\Delta\tau/2} \tag{B-24}$$

$$\bar{k}_x \delta_x^2 F^* + \bar{k}_y \delta_y^2 F^{**} + \bar{k}_z \delta_z^2 F^n = (F^{n,**})^{-\frac{1}{2}} \frac{F^{**} - F^n}{\Delta\tau/2} \tag{B-25}$$

$$\bar{k}_x \delta_x^2 F^* + \bar{k}_y \delta_y^2 F^{**} + \bar{k}_z \delta_z^2 F^{n+1} = (F^{**,n+1})^{-\frac{1}{2}} \frac{F^{n+1} - F^{**}}{\Delta\tau/2} \tag{B-26}$$

Here δ_x^2, δ_y^2, and δ_z^2 are finite difference forms of the second derivative acting on the pressure function at the time shown. The double superscripts indicate a value of F between the times denoted by the superscripts.

The actual equations used for computations are developed following the solution method for tridiagonal matricies outlined by Roache.[24] We let

$$\alpha = \bar{k}_x \tag{B-27}$$

$$\gamma = \bar{k}_y \tag{B-28}$$

$$\xi = \bar{k}_z \tag{B-29}$$

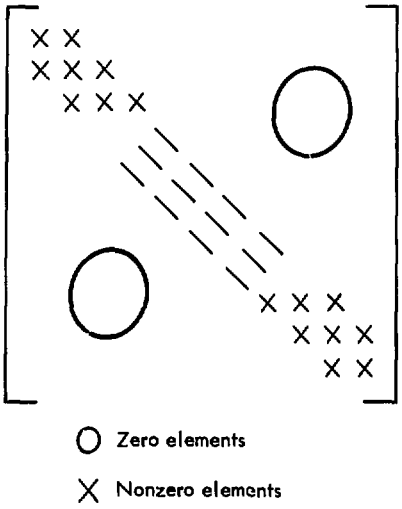

Fig. B-2. Form of a tri-diagonal matrix.

and

$$\eta^{n,*}_{i,j,k} = \theta(F^{*}_{i,j,k})^{-\frac{1}{2}} + (1-\theta)\ (F^{n}_{i,j,k})^{-\frac{1}{2}} \qquad \text{(B-30)}$$

The coefficients α, γ, and ξ are taken to be independent of time and space. Time superscripts and spatial subscripts could also be included for generality if desired. The correct time value to use when calculating the value of $F_{i,j,k}$ in the $\eta_{i,j,k}$ coefficient is a matter at some debate. We include a weighting coefficient θ in the calculation of $\eta^{n,*}_{i,j,k}$ which may be varied depending on the specific problem. The superscript contains the two time values used in calculating the η coefficient.

We use Blottner's grid stretching method[26] in the "X" direction to increase the effectiveness of the number of grid points used. This makes the grid size variable in the "X" direction. Substituting Eqs. (B-27) through (B-30) into (B-24) with the derivatives expanded into differences gives

$$\frac{2\,\alpha}{\left(\Delta\bar{X}_{i+1/2} + \Delta\bar{X}_{i-1/2}\right)}\left[\frac{\left(F^{*}_{i+1,j,k} - F^{*}_{i,j,k}\right)}{\Delta\bar{X}_{i+1/2}} - \frac{\left(F^{*}_{i,j,k} - F^{*}_{i-1,j,k}\right)}{\Delta\bar{X}_{i-1/2}}\right]$$

$$+ \gamma\,\frac{\left(F^{n}_{i,j+1,k} - 2F^{n}_{i,j,k} + F^{n}_{i,j-1,k}\right)}{(\Delta\bar{Y})^{2}}$$

$$+ \zeta\,\frac{\left(F^{n}_{i,j,k+1} - 2F^{n}_{i,j,k} + F^{n}_{i,j,k-1}\right)}{(\Delta\bar{Z})^{2}} = \eta^{n,*}_{i,j,k}\,\frac{\left(F^{*}_{i,j,k} - F^{n}_{i,j,k}\right)}{\Delta\tau/2} \qquad \text{(B-31)}$$

where

$$\Delta\bar{X}_{i+1/2} = \bar{X}_{i+1} - \bar{X}_{i} \qquad \text{(B-32)}$$

$$\Delta\bar{X}_{i-1/2} = \bar{X}_{i} - \bar{X}_{i-1}\,. \qquad \text{(B-33)}$$

Values of the spatial derivatives at the boundaries would use either the Dirichlet condition where the boundary value is specified or the Neumann condition where the spatial derivative is equal to zero. Within the crack, over the portion of the lower surface where the pressure is specified as input, and over the total upper surface where the normalized pressure is zero, we use the Dirichlet condition. On all other portions of the boundary we use the Neumann condition.

"$\bar{X}$" Direction Implicit Differencing

Equation (B-31) is written in the following form for use in the computer program when considering the "$\bar{X}$" direction implicit with the "$\bar{Y}$" and "$\bar{Z}$" directions explicit.

$$- A_{i,j,k} F^{*}_{i+1,j,k} + B_{i,j,k} F^{*}_{i,j,k} - C_{i,j,k} F^{*}_{i-1,j,k} = D_{i,j,k} \qquad \text{(B-34)}$$

where

$$A_{i,j,k} = \frac{2\,\alpha}{\Delta X_{i+1/2}(\Delta X_{i+1/2} + \Delta X_{i-1/2})} \qquad \text{(B-35)}$$

$$B_{i,j,k} = \frac{2\,\alpha}{(\Delta X_{i+1/2} + \Delta X_{i-1/2})}\left[\frac{1}{\Delta X_{i+1/2}} + \frac{1}{\Delta X_{i-1/2}}\right] + \frac{\eta^{n,*}_{i,j,k}}{\Delta\tau/2}$$

$$= \frac{2\,\alpha}{\Delta X_{i+1/2}\Delta X_{i-1/2}} + \frac{\eta^{n,*}_{i,j,k}}{\Delta\tau/2} \qquad \text{(B-36)}$$

$$C_{i,j,k} = \frac{2\,\alpha}{\Delta X_{i-1/2}(\Delta X_{i+1/2} + \Delta X_{i-1/2})} \qquad \text{(B-37)}$$

$$D_{i,j,k} = \gamma \frac{(F^{n}_{i,j+1,k} - 2F^{n}_{i,j,k} + F^{n}_{i,j-1,k})}{(\Delta\bar{Y})^2}$$

$$+ \xi \frac{(F^{n}_{i,j,k+1} - 2F^{n}_{i,j,k} + F^{n}_{i,j,k-1})}{(\Delta\bar{Z})^2} + \frac{\eta^{n,*}_{i,j,k} F^{n}_{i,j,k}}{\Delta\tau/2} . \qquad \text{(B-38)}$$

In turn we have

$$F^{*}_{i,j,k} = E_{i,j,k} F^{*}_{i+1,j,k} + \tilde{F}_{i,j,k} \qquad \text{(B-39)}$$

where

$$E_{i,j,k} = \frac{A_{i,j,k}}{B_{i,j,k} - C_{i,j,k} E_{i-1,j,k}} \tag{B-40}$$

$$\tilde{F}_{i,j,k} = \frac{D_{i,j,k} + C_{i,j,k} \tilde{F}_{i-1,j,k}}{B_{i,j,k} - C_{i,j,k} E_{i-1,j,k}} \quad . \tag{B-41}$$

At the left boundary, the subscript i=1, and from Eq. (B-39)

$$F^*_{1,j,k} = E_{1,j,k} F^*_{2,j,k} + \tilde{F}_{1,j,k} \quad . \tag{B-42}$$

For a Dirichlet boundary condition where the value of $F^*_{1,j,k}$ is specified

$$\left.\begin{aligned} E_{1,j,k} &= 0 \\ \tilde{F}_{1,j,k} &= \text{specified value} \end{aligned}\right\} \text{Dirichlet condition} \quad . \tag{B-43}$$

For a Newmann boundary condition where the derivative is zero

$$\left.\begin{aligned} E_{1,j,k} &= 1 \\ \tilde{F}_{1,j,k} &= 0 \end{aligned}\right\} \text{Neumann condition} \quad . \tag{B-44}$$

Using the boundary conditions above and the recursion relationship of Eqs. (B-40) and (B-41) we may calculate all the values of $E_{i,j,k}$ and $\tilde{F}_{i,j,k}$. At the right hand boundary, where the subscript, i, has its maximum value we use either the Dirichlet condition to specify the value of $F^*_{L,j,k}$ or the Neumann condition which gives from Eq. (B-39) that

$$F^*_{L,j,k} = \frac{\tilde{F}_{L-1,j,k}}{1-E_{L-1,j,k}} \tag{B-45}$$

where the subscript, L, indicates the maximum "$\bar{X}$" direction node. We may then use the recursion relation, Eq. (B-39) to calculate all other values of $F^{*}_{i,j,k}$ starting with the maximum "$\bar{X}$" direction node.

"$\bar{Y}$" Direction Implicit Differencing

Working with the "$\bar{Y}$" direction implicit portion of the calculation, we have from Eq. (B-25)

$$\frac{2\,\alpha}{(\Delta\bar{X}_{i+1/2} + \Delta\bar{X}_{i-1/2})}\left[\frac{F^{*}_{i+1,j,k} - F^{*}_{i,j,k})}{\Delta\bar{X}_{i+1/2}} - \frac{(F^{*}_{i,j,k} - F^{*}_{i-1,j,k})}{\Delta\bar{X}_{i-1/2}}\right]$$

$$+ \gamma\,\frac{(F^{**}_{i,j+1,k} - 2F^{**}_{i,j,k} + F^{**}_{i,j-1,k})}{(\Delta\bar{Y})^{2}}$$

$$+ \xi\,\frac{(F^{n}_{i,j,k+1} - 2F^{n}_{i,j,k} + F^{n}_{i,j,k-1})}{(\Delta\bar{Z})^{2}}$$

$$= \eta^{n,**}_{i,j,k}\,\frac{(F^{**}_{i,j,k} - F^{n}_{i,j,k})}{\Delta\tau/2} \qquad \text{(B-46)}$$

or

$$-A_{i,j,k}\,F^{**}_{i,j+1,k} + B_{i,j,k}\,F^{**}_{i,j,k} - C_{i,j,k}\,F^{**}_{i,j-1,k} = D_{i,j,k} \qquad \text{(B-47)}$$

with

$$A_{i,j,k} = \gamma \qquad \text{(B-48)}$$

$$B_{i,j,k} = 2\gamma + \frac{(\Delta\bar{Y})^{2}}{\Delta\tau/2}\,\eta^{n,**}_{i,j,k} \qquad \text{(B-49)}$$

$$C_{i,j,k} = \gamma \qquad \text{(B-50)}$$

and

$$D_{i,j,k} = \left[\frac{2\,\alpha}{(\Delta\bar{X}_{i+1/2} + \Delta\bar{X}_{i-1/2})} \left(\frac{(F^{*}_{i+1,j,k} - F^{*}_{i,j,k})}{\Delta\bar{X}_{i+1/2}} - \frac{(F^{*}_{i,j,k} - F^{*}_{i-1,j,k})}{\Delta\bar{X}_{i-1/2}} \right) \right.$$

$$+ \xi \frac{(F^{n}_{i,j,k+1} - 2F^{n}_{i,j,k} + F^{n}_{i,j,k-1})}{(\Delta\bar{Z})^{2}}$$

$$\left. + \frac{\eta^{n,**}_{i,j,k} F^{n}_{i,j,k}}{\Delta\tau/2} \right] (\Delta\bar{Y})^{2} \,. \qquad \text{(B-51)}$$

Rewriting Eq. (B-46)

$$F^{**}_{i,j,k} = E_{i,j,k} F^{**}_{i,j+1,k} + \tilde{F}_{i,j,k} \qquad \text{(B-52)}$$

with

$$E_{i,j,k} = \frac{A_{i,j,k}}{B_{i,j,k} - C_{i,j,k} E_{i,j-1,k}} \qquad \text{(B-53)}$$

$$\tilde{F}_{i,j,k} = \frac{D_{i,j,k} + C_{i,j,k} \tilde{F}_{i,j-1,k}}{B_{i,j,k} - C_{i,j,k} E_{i,j-1,k}} \,. \qquad \text{(B-54)}$$

As before we use both Dirichlet and Neumann boundary conditions as appropriate for calculating first the values of $E_{i,j,k}$ and $\tilde{F}_{i,j,k}$, and then the values of $F^{**}_{i,j,k}$.

"$\bar{Z}$" Direction Implicit Differencing

For the "$\bar{Z}$" direction implicit portion, the difference equations used are developed from Eq. (B-26) as

$$\frac{2\,\alpha}{(\Delta\bar{X}_{i+1/2} + \Delta\bar{X}_{i-1/2})}\left[\frac{(F^{*}_{i+1,j,k} - F^{*}_{i,j,k})}{\Delta\bar{X}_{i+1/2}} - \frac{(F^{*}_{i,j,k} - F^{*}_{k-1,j,k})}{\Delta\bar{X}_{i-1/2}}\right]$$

$$+ \gamma\,\frac{(F^{**}_{i,j+1,k} - 2F^{**}_{i,j,k} + F^{**}_{i,j-1,k})}{(\Delta\bar{Y})^{2}}$$

$$+ \xi\,\frac{(F^{n+1}_{i,j,k+1} - 2F^{n+1}_{i,j,k} + F^{n+1}_{i,j,k-1})}{(\Delta\bar{Z})^{2}}$$

$$= \eta^{**,n+1}_{i,j,k}\,\frac{(F^{n+1}_{i,j,k} - F^{**}_{i,j,k})}{\Delta\tau/2} \qquad \text{(B-55)}$$

or

$$-A_{i,j,k}\,F^{n+1}_{i,j,k+1} + B_{i,j,k}\,F^{n+1}_{i,j,k} - C_{i,j,k}\,F^{n+1}_{i,j,k-1} = D_{i,j,k} \qquad \text{(B-56)}$$

with

$$A_{i,j,k} = \xi \qquad \text{(B-57)}$$

$$B_{i,j,k} = 2\xi + \frac{(\Delta\bar{Z})^{2}}{\Delta\tau/2}\,\eta^{**,n+1}_{i,j,k} \qquad \text{(B-58)}$$

$$C_{i,j,k} = \xi \qquad \text{(B-59)}$$

$$D_{i,j,k} = \left[\frac{2\,\alpha}{(\Delta\bar{X}_{i+1/2} + \Delta\bar{X}_{i-1/2})} \left(\frac{(F^{*}_{i+1,j,k} - F^{*}_{i,j,k})}{\Delta\bar{X}_{i+1/2}} - \frac{(F^{*}_{i,j,k} - F^{*}_{i-1,j,k})}{\Delta\bar{X}_{i-1/2}} \right) \right.$$

$$\left. + \gamma \frac{(F^{**}_{i,j+1,k} - 2F^{**}_{i,j,k} + F^{**}_{i,j-1,k})}{(\Delta\bar{Y})^2} + \frac{\eta^{**,n+1}_{i,j,k} F^{**}_{i,j,k}}{\Delta\tau/2} \right] (\Delta\bar{Z})^2 \quad . \qquad \text{(B-60)}$$

In turn,

$$F^{n+1}_{i,j,k} = E_{i,j,k} F^{n+1}_{i,j,k+1} + \tilde{F}_{i,j,k} \qquad \text{(B-61)}$$

with

$$E_{i,j,k} = \frac{A_{i,j,k}}{B_{i,j,k} - C_{i,j,k} E_{i,j,k-1}} \qquad \text{(B-62)}$$

$$\tilde{F}_{i,j,k} = \frac{D_{i,j,k} + C_{i,j,k} \tilde{F}_{i,j,k-1}}{B_{i,j,k} - C_{i,j,k} E_{i,j,k-1}} \qquad \text{(B-63)}$$

Maps outlining the calculations for all the spatial locations in each step are shown in Figs. B-3 through B-5 since there are a number of regions with different boundary conditions. The circled numbers outline the sequence of steps in the computer program.

IMPLICIT DIFFERENCING OF THE CRACK-FLOW EQUATIONS

We explored two ways of differencing the crack flow equations both of which are related here. Each method of differencing is satisfactory and result in nearly identical answers when compared in a sample problem. The method described first was used for all the calculations documented because there appears to be an advantage in stability. The alternate method has the possible advantage of being more accurate for the same spatial grid size.

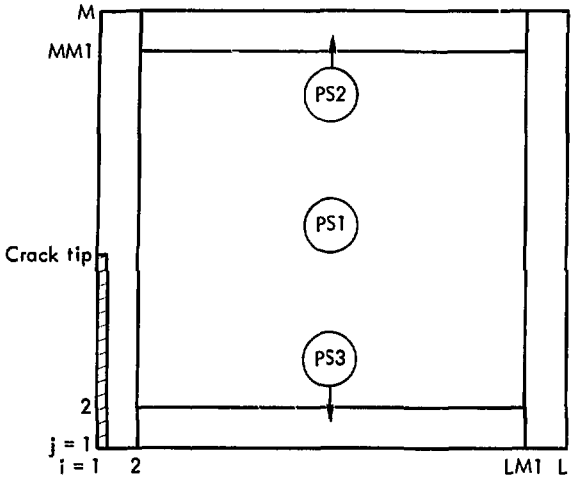

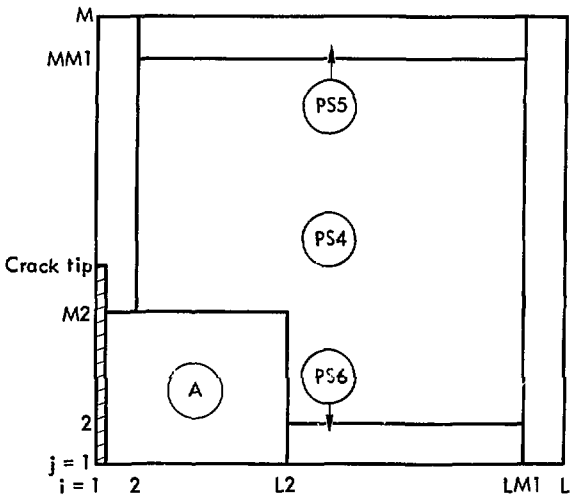

Fig. B-3. Calculational steps for the $\bar{X}$-direction implicit calculations for the porous solid.

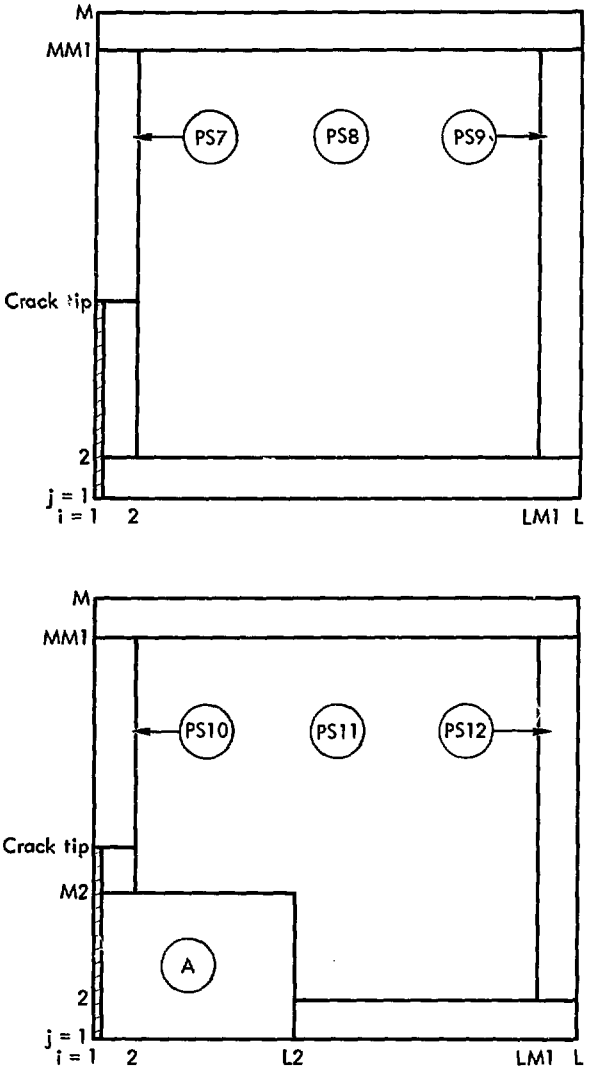

Fig. B-4. Calculational steps for the $\bar{Y}$-direction implicit calculations for the porous solid.

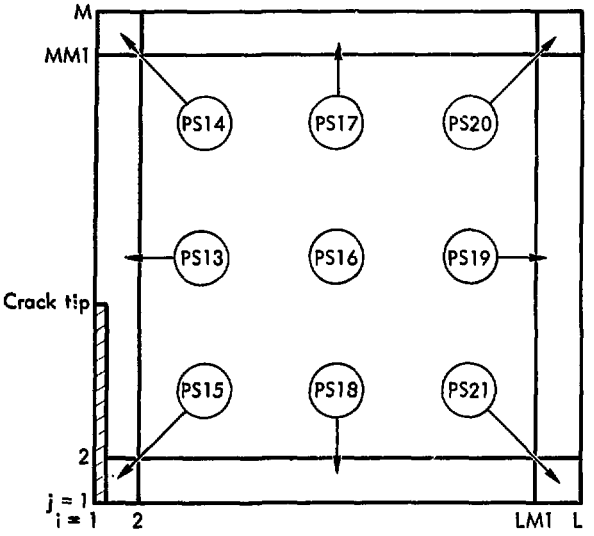

Fig. B-5. Calculational steps for the $\bar{Z}$-direction implicit calculations for the porous solid.

The governing equation for flow within the crack is

$$- \bar{k}_{cx} \frac{\partial F}{\partial \bar{X}} \pm \frac{\partial}{\partial \bar{Y}} \left(\bar{k}_{cyz} \left(\left| \frac{\partial F}{\partial \bar{Y}} \right| \right)^{\frac{1}{2}} \right) \pm \frac{\partial}{\partial \bar{Z}} \left(\bar{k}_{cyz} \left(\left| \frac{\partial F}{\partial \bar{Z}} \right| \right)^{\frac{1}{2}} \right) + \frac{\partial \bar{P}}{\partial \bar{\tau}} = 0. \qquad \text{(A-50)}$$

We replace the temporal derivative of pressure with a derivative of the pressure function using Eq. (B-22) which results in

$$- \bar{k}_{cx} \frac{\partial F}{\partial \bar{X}} \pm \frac{\partial}{\partial \bar{Y}} \left(\bar{k}_{cyz} \left(\left| \frac{\partial F}{\partial \bar{Y}} \right| \right)^{\frac{1}{2}} \right) \pm \frac{\partial}{\partial \bar{Z}} \left(\bar{k}_{cyz} \left(\left| \frac{\partial F}{\partial \bar{Z}} \right| \right)^{\frac{1}{2}} \right)$$

$$+ \frac{1}{2} F^{-\frac{1}{2}} \frac{\partial F}{\partial \bar{\tau}} = 0 . \qquad \text{(B-64)}$$

In the first method of differencing, we differentiate the second and third terms from the left in closed form to obtain

$$- \bar{k}_{cx} \frac{\partial F}{\partial \bar{X}} \pm \left(\left| \frac{\partial F}{\partial \bar{Y}} \right| \right)^{\frac{1}{2}} \frac{\partial \bar{k}_{cyz}}{\partial \bar{Y}} \pm \frac{\bar{k}_{cyz}}{2 \left(\left| \frac{\partial F}{\partial \bar{Y}} \right| \right)^{\frac{1}{2}}} \frac{\partial}{\partial \bar{Y}} \left| \frac{\partial F}{\partial \bar{Y}} \right|$$

$$\pm \left(\left| \frac{\partial F}{\partial \bar{Z}} \right| \right)^{\frac{1}{2}} \frac{\partial \bar{k}_{cyz}}{\partial \bar{Z}} \pm \frac{\bar{k}_{cyz}}{2 \left(\left| \frac{\partial F}{\partial \bar{Z}} \right| \right)^{\frac{1}{2}}} \frac{\partial}{\partial \bar{Z}} \left| \frac{\partial F}{\partial \bar{Z}} \right| + \frac{1}{2} F^{-\frac{1}{2}} \frac{\partial F}{\partial \tau} = 0 \qquad \text{(B-65)}$$

The value of F is bounded by $0 \leq F \leq N^2/(N-1)^2$ so that the coefficient of the right hand term is always finite. On the other hand, it is possible for singularities to occur numerically in the third or fifth term from the left if $\partial F/\partial \bar{Y}$ or $\partial F/\partial \bar{Z}$ approach zero. One means of avoiding such difficulties is to multiply through by these values. However, this yields an equation which in the limit does not conform to the physics of the problem. For example, if $\partial F/\partial \bar{Y} \to 0$, only the second and third terms from the left in Eq. (B-65) should approach zero. Yet if we multiply Eq. (B-65) by $(\partial F/\partial \bar{Y})^{\frac{1}{2}}$ we find that all terms approach zero as $\partial F/\partial \bar{Y} \to 0$ leaving us with a trivial result. A better way of eliminating the possible singularity is to set the second and third terms from the right equal to zero if $|\partial F/\partial \bar{Y}|$ is less than some small value. Similarly, we would set the fourth and fifth terms from the right equal to zero if $|\partial F/\partial \bar{Z}|$ is less than some small value.

The plus signs in the second and third terms from the left in Eq. (B-65) are used if $\partial F/\partial \bar{Y} < 0$ and the minus signs are used if $\partial F/\partial \bar{Y} > 0$. If we multiply the numerator and denominator of the second term by $(|\partial F/\partial \bar{Y}|)^{\frac{1}{2}}$ and remove the absolute value signs in the numerator, then the minus sign should be used regardless of the magnitude of $\partial F/\partial \bar{Y}$. In the third term we may

eliminate the absolute value signs in the numerator if the minus sign is used. Similar arguments may be made for the fourth and fifth terms from the left. This gives, after rearranging,

$$\bar{k}_{cx}\frac{\partial F}{\partial \bar{X}} + \left(\frac{\partial F}{\partial \bar{Y}} \Big/ \left(\left|\frac{\partial F}{\partial \bar{Y}}\right|\right)^{1/2}\right) \frac{\partial\, \bar{k}_{cyz}}{\partial \bar{Y}} + \left(\bar{k}_{cyz} \Big/ 2\left(\left|\frac{\partial F}{\partial \bar{Y}}\right|\right)^{1/2}\right) \frac{\partial^2 F}{\partial \bar{Y}^2}$$

$$+ \left(\frac{\partial F}{\partial \bar{Z}} \Big/ \left(\left|\frac{\partial F}{\partial \bar{Z}}\right|\right)^{1/2}\right) \frac{\partial\, \bar{k}_{cyz}}{\partial \bar{Z}} + \left(\bar{k}_{cyz} \Big/ 2\left(\left|\frac{\partial F}{\partial \bar{Z}}\right|\right)^{1/2}\right) \frac{\partial^2 F}{\partial \bar{Z}^2}$$

$$= \frac{1}{2} F^{-1/2} \frac{\partial F}{\partial \tau} \qquad \text{(B-66)}$$

In Eq. (B-66), the terms containing $\partial F/\partial \bar{Y}$ are set equal to zero in the computer program, CHASM, if $|\partial F/\partial \bar{Y}|$ is less than 10^{-25}. Similarly, terms containing $\partial F/\partial \bar{Z}$ are set equal to zero if $|\partial F/\partial \bar{Z}| < 10^{-25}$.

The "$\bar{X}$" direction term taken separately with the temporal term forms a hyperbolic equation whereas either the "$\bar{Y}$" or "$\bar{Z}$" direction second derivative terms taken individually with the temporal term form parabolic equations. Accordingly, we retain an explicit differencing scheme in the "$\bar{X}$" direction to prevent artificial numerical damping. In the "$\bar{Y}$" and "$\bar{Z}$" directions we retain an implicit differencing scheme because of its inherently better stability. We use an operator splitting technique (Ref. 33 and B-2) where Eq. (B-66) is broken into two parts which are

$$\bar{k}_{cx}\frac{\partial F}{\partial \bar{X}} = \frac{1}{2} F^{-1/2} \frac{\partial F}{\partial \tau} \qquad \text{(B-67)}$$

and

$$\left(\frac{\partial F}{\partial \bar{Y}} \Big/ \left(\left|\frac{\partial F}{\partial \bar{Y}}\right|\right)^{\frac{1}{2}}\right)\frac{\partial \bar{k}_{cyz}}{\partial \bar{Y}} + \left(\bar{k}_{cyz} \Big/ 2 \left(\left|\frac{\partial F}{\partial \bar{Y}}\right|\right)^{\frac{1}{2}}\right)\frac{\partial^2 F}{\partial \bar{Y}^2}$$

$$+\left(\frac{\partial F}{\partial \bar{Z}} \Big/ \left(\left|\frac{\partial F}{\partial \bar{Z}}\right|\right)^{\frac{1}{2}}\right)\frac{\partial \bar{k}_{cyz}}{\partial \bar{Z}} + \left(\bar{k}_{cyz} \Big/ 2 \left(\left|\frac{\partial F}{\partial \bar{Z}}\right|\right)^{\frac{1}{2}}\right)\frac{\partial^2 F}{\partial \bar{Z}^2}$$

$$= \frac{1}{2} F^{-\frac{1}{2}} \frac{\partial F}{\partial \tau} . \qquad \text{(B-68)}$$

In using Eqs. (B-67) and (B-68) as an alternate to Eq. (B-66) we are determining first the effect of the "$\bar{X}$" direction spatial component throughout a given time to find a hypothetical value of the pressure function from Eq. (B-67). Then we use this hypothetical pressure function over the same time period to calculate the actual pressure function at the new time using Eq. (B-68).

Since we explicitly difference Eq. (B-67), the value of the time step must be less than the "$\bar{X}$" direction spatial step size divided by the equivalent velocity if stability is to exist. This time step would be

$$\Delta\tau \leq \frac{\Delta \bar{X}}{2\, \bar{k}_{cx}\, F^{\frac{1}{2}}} \qquad \text{(B-69)}$$

We repeat the explicit "$\bar{X}$" direction calculation using Eq. (B-67) a number of times until we have advanced from time τ^n to time τ^*. The time τ^* is a hypothetical time value which occurs after completion of the "$\bar{X}$" direction calculations.

Next we use an alternating direction implicit scheme[23,24] for the "$\bar{Y}$" and "$\bar{Z}$" directions in two time steps from time τ^n to time τ^{n+1}. In the first step

the "$\bar{Y}$" direction spatial second derivative is differenced implicitly and in the second time step the "$\bar{Z}$" direction spatial second derivative is differenced implicitly. In the alternating direction implicit calculations, all coefficients are evaluated using some average value of the pressure function, F, between the hypothetical time, τ^*, and the new time t^{n+1}. The total time difference in the explicit calculation, $\tau^*-\tau^n$, must be identical to the total time difference in the implicit calculations, $\tau^{n+1}-\tau^n$, if the solution we obtain from Eqs. (B-67 and B-68) is to be equivalent to a solution to Eq. (B-66).

Use of an alternating direction implicit scheme is unconditionally stable for any time step if Eq. (B-68) is linear. Because Eq. (B-68) is nonlinear, stability must still be considered in selecting a time step. We approached the time step selection on a trial basis. We found the results were independent of variations in time step by over a factor of 100 as long as stability was maintained.

The best means of differencing the coefficients of Eqs. (B-67) and (B-68) depend on the problem and it is not clear which values of time should be used in evaluating the pressure function, F. We use a weighting factor, θ, for all implicit calculations which may be varied and which is a fraction used to multiply the new time value of F. The following coefficients are defined for use in the "$\bar{Y}$" direction implicit portion of the calculation:

$$\alpha_{1,j,k} = \bar{k}_{cx_{j,k}} \tag{B-70}$$

$$\beta^{*,**}_{1,j,k} = \theta\left(F^{**}_{1,j+1,k} - F^{**}_{1,j-1,k}\right) \Big/ \left(2\,\Delta\bar{Y}\left(\left|F^{**}_{1,j+1,k} - F^{**}_{1,j-1,k}\right|\right)\right)^{\frac{1}{2}}$$

$$+ (1-\theta)\left(F^{*}_{1,j+1,k} - F^{*}_{1,j-1,k}\right) \Big/ \left(2\,\Delta\bar{Y}\left(\left|F^{*}_{1,j+1,k} - F^{*}_{1,j-1,k}\right|\right)\right)^{\frac{1}{2}} \tag{B-71}$$

$$\gamma^{*,**}_{1,j,k} = \bar{k}_{cyz_{j,k}} \left[\theta \Big/ \left(2 \left(\left| F^{**}_{1,j+1,k} - F^{**}_{1,j-1,k} \right| \right) / \Delta\bar{Y} \right)^{\frac{1}{2}} \right.$$

$$\left. + (1-\theta) \Big/ \left(2 \left(\left| F^{*}_{1,j+1,k} - F^{*}_{1,j-1,k} \right| \right) / \Delta\bar{Y} \right)^{\frac{1}{2}} \right] \qquad \text{(B-72)}$$

$$\delta^{*,**}_{1,j,k} = \theta \left(F^{**}_{1,j,k+1} - F^{**}_{1,j,k-1} \right) \Big/ \left(2\,\Delta\bar{Z} \left(\left| F^{**}_{1,j,k+1} - F^{**}_{1,j,k-1} \right| \right) \right)^{\frac{1}{2}}$$

$$+ (1-\theta) \left(F^{*}_{1,j,k+1} - F^{*}_{1,j,k-1} \right) \Big/ \left(2\,\Delta\bar{Z} \left(\left| F^{*}_{1,j,k+1} - F^{*}_{1,j,k-1} \right| \right) \right)^{\frac{1}{2}} \qquad \text{(B-73)}$$

$$\xi^{*,**}_{1,j,k} = k_{cyz_{j,k}} \left[\theta \Big/ \left(2 \left(\left| F^{**}_{1,j,k+1} - F^{**}_{1,j,k-1} \right| \right) / \Delta\bar{Z} \right)^{\frac{1}{2}} \right.$$

$$\left. + (1-\theta) \left(2 \left(\left| F^{*}_{1,j,k+1} - F^{*}_{1,j,k-1} \right| \right) / \Delta\bar{Z} \right)^{\frac{1}{2}} \right] \qquad \text{(B-74)}$$

$$\eta^{*,**}_{1,j,k} = 0.5 \left[\theta \Big/ \left(F^{**}_{1,j,k} \right)^{\frac{1}{2}} + (1-\theta) \Big/ \left(F^{*}_{1,j,k} \right)^{\frac{1}{2}} \right] \qquad \text{(B-75)}$$

with

$$\beta^{*,**}_{1,j,k} = \gamma^{*,**}_{1,j,k} = 0 \text{ if } F^{*}_{i,j+1,k} \approx F^{*}_{1,j-1,k} \qquad \text{(B-76)}$$

$$\delta^{*,**}_{1,j,k} = \xi^{*,**}_{1,j,k} = 0 \text{ if } F^{*}_{1,j,k-1} \approx F^{*}_{1,j,k-1} \qquad \text{(B-77)}$$

Similar values of the coefficients are defined between the times, τ^{**} and τ^{n+1} for use during the "$\bar{Z}$"-direction-implcit portion of the calculations. The values of $\bar{k}_{cx_{j,k}}$ are considered to be time independent.

In the first step of the operator splitting scheme the difference equation for the "$\bar{X}$" direction is utilized.

$$\alpha_{1,j,k} \frac{\left(F^{n}_{2,j,k} - F^{n}_{1,j,k}\right)}{\Delta\bar{X}} = \eta^{n,*}_{1,j,k} \frac{\left(F^{*}_{1,j,k} - F^{n}_{1,j,k}\right)}{\Delta\tau} \qquad \text{(B-78)}$$

The difference equations for the second step uses an alternating direction implicit scheme for the "$\bar{Y}$" and "$\bar{Z}$" directions.

$$\beta^{*,**}_{1,j,k} \frac{\left(\bar{k}_{cyz_{j+1,k}} - \bar{k}_{cyz_{j-1,k}}\right)}{2\,\Delta\bar{Y}} + \gamma^{*,**}_{1,j,k} \frac{\left(F^{**}_{1,j+1,k} - 2F^{**}_{1,j,k} + F^{**}_{1,j-1,k}\right)}{(\Delta Y)^2}$$

$$+ \delta^{*,**}_{1,j,k} \frac{\left(\bar{k}_{cyz_{j,k+1}} - \bar{k}_{cyz_{j,k-1}}\right)}{2\,\Delta\bar{Z}} + \xi^{*,**}_{1,j,k} \frac{\left(F^{*}_{1,j,k+1} - 2F^{*}_{1,j,k} + F^{*}_{1,j,k-1}\right)}{(\Delta\bar{Z})^2}$$

$$= \eta^{*,**}_{1,j,k} \frac{\left(F^{**}_{1,j,k} - F^{*}_{1,j,k}\right)}{\Delta\tau/2} \qquad \text{(B-79)}$$

$$\beta^{**,n+1}_{1,j,k} \frac{\left(\bar{k}_{cyz_{j+1,k}} - \bar{k}_{cyz_{j-1,k}}\right)}{2\Delta\bar{Y}} + \gamma^{**,n+1}_{1,j,k} \frac{\left(F^{**}_{1,j+1,k} - 2F^{**}_{1,j,k} + F^{**}_{1,j-1,k}\right)}{(\Delta\bar{Y})^2}$$

$$+ \delta^{**,n+1}_{1,j,k} \frac{\left(\bar{k}_{cyz_{j,k+1}} - \bar{k}_{cyz_{j,k-1}}\right)}{2\Delta\bar{Z}} + \xi^{**,n+1}_{1,j,k} \frac{\left(F^{n+1}_{1,j,k+1} - 2F^{n+1}_{1,j,k} + F^{n+1}_{1,j,k-1}\right)}{(\Delta\bar{Z})^2}$$

$$= \eta^{**,n+1}_{1,j,k} \frac{\left(F^{n+1}_{1,j,k} - F^{**}_{1,j,k}\right)}{\Delta\tau/2} \qquad \text{(B-80)}$$

Eq. (B-78) is solved for each new value of pressure function directly without iteration and the process is repeated until the total time difference equal to $\tau^{n+1} - \tau^{n}$ is reached. We rewrite Eq. (B-79) to obtain a standard algorithm form for solving a tri-diagonal matrix as follows:

$$- A_{1,j,k} F^{**}_{i,j+1,k} + B_{1,j,k} F^{**}_{1,j,k} - C_{1,j,k} F^{**}_{1,j-1,k} = D_{1,j,k} \qquad \text{(B-81)}$$

where

$$A_{1,j,k} = \gamma^{*,**}_{1,j,k} \tag{B-82}$$

$$B_{1,j,k} = 2\gamma^{*,**}_{1,j,k} + \frac{(\Delta\bar{Y})^2}{\Delta\tau/2}\,\gamma^{*,**}_{1,j,k} \tag{B-83}$$

$$C_{1,j,k} = \gamma^{*,**}_{1,j,k} \tag{B-84}$$

and

$$D_{1,j,k} = \left[\beta^{*,**}_{1,j,k} \frac{\left(\bar{k}_{cyz_{j+1,k}} - \bar{k}_{cyz_{j-1,k}}\right)}{2\,\Delta\bar{Y}} + \xi^{*,**}_{1,j,k} \frac{\left(k_{cyz_{j,k+1}} - k_{cyz_{j,k-1}}\right)}{2\,\Delta\bar{Z}} \right.$$

$$\left. + \xi^{*,**}_{1,j,k} \frac{\left(F^{*}_{1,j,k+1} - 2F^{*}_{1,j,k} + F^{*}_{1,j,k-1}\right)}{(\Delta\bar{Z})^2} + \frac{\gamma^{*,**}_{1,j,k} F^{*}_{1,j,k}}{\Delta\tau/2} \right] (\Delta\bar{Y})^2 \tag{B-85}$$

in turn, for the "$\bar{Y}$" direction we write

$$F^{**}_{1,j,k} = E_{1,j,k} F^{**}_{1,j+1,k} + \tilde{F}_{1,j,k} \tag{B-86}$$

with

$$E_{1,j,k} = \frac{A_{1,j,k}}{B_{1,j,k} - C_{1,j,k} E_{1,j-1,k}} \tag{B-87}$$

$$\tilde{F}_{1,j,k} = \frac{D_{1,j,k} + C_{1,j,k} \tilde{F}_{1,j-1,k}}{B_{1,j,k} - C_{1,j,k} E_{1,j-1,k}} \tag{B-88}$$

At the boundaries we use conditions identical with those mentioned previously for flow in the porous solid. That is

Dirichlet Condition: (boundary value specified) $E_{1,j,k} = 0$ and $\tilde{F}_{1,j,k} = F_{1,j,k}$

Neumann Condition: $E_{1,j,k} = 1$ and $\tilde{F}_{1,j,k} = 0$
(boundary derivative
equal to zero)

for the "$\bar{Z}$" direction we write Eq. (B-80) as

$$- A_{1,j,k} F^{n+1}_{1,j,k+1} + B_{1,j,k} F^{n+1}_{1,j,k} - C_{1,j,k} F^{n+1}_{1,j,k-1} + D_{1,j,k} \tag{B-89}$$

where

$$A_{1,j,k} = \beta^{**,n+1}_{1,j,k} \tag{B-90}$$

$$B_{1,j,k} = 2\beta^{**,n+1}_{1,j,k} + \frac{(\Delta\bar{Z})^2}{\Delta\tau/2} \alpha^{**,n+1}_{1,j,k} \tag{B-91}$$

$$C_{1,j,k} = \beta^{**,n+1}_{1,j,k} \tag{B-92}$$

and

$$\begin{aligned} D_{1,j,k} = \Bigg[& \beta^{**,n+1}_{1,j,k} \frac{\left(\bar{k}_{cyz_{j+1,k}} - \bar{k}_{cyz_{j-1,k}}\right)}{2\,\Delta\bar{Y}} \\ & + \gamma^{**,n+1}_{1,j,k} \frac{\left(F^{**}_{1,j+1,k} - 2F^{**}_{1,j,k} \pm F^{**}_{1,j-1,k}\right)}{(\Delta\bar{Y})^2} \\ & + \delta^{**,n+1}_{1,j,k} \frac{\left(\bar{k}_{cyz_{j,k+1}} - \bar{k}_{cyz_{j,k-1}}\right)}{2\,\Delta\bar{Z}} + \frac{\left(\eta^{**,n+1}_{1,j,k} F^{**}_{1,j,k}\right)}{\Delta\tau/2} \Bigg] (\Delta\bar{Z})^2. \end{aligned} \tag{B-93}$$

In turn, for the "$\bar{Z}$" direction

$$F^{n+1}_{1,j,k} = E_{1,j,k} F^{n+1}_{1,j,k+1} + \tilde{F}_{1,j,k} \tag{B-94}$$

where

$$E_{l,j,k} = \frac{A_{l,j,k}}{B_{l,j,k} - C_{l,j,k} E_{l,j,k-1}} \tag{B-95}$$

$$F_{l,j,k} = \frac{D_{l,j,k} + C_{l,j,k} \tilde{F}_{l,j,k-1}}{B_{l,j,k} - C_{l,j,k} E_{l,j,k-1}} \quad . \tag{B-96}$$

In all implicit calculations we iterate to update those coefficients which vary with time. The equations for the flow inside the crack are coupled with the equations for the porous solid in the $\bar{Y}$ and $\bar{Z}$ directions so that a single matrix is formed that covers all nodes in the problem. That is we calculate changes in the $\bar{X}$ direction for all nodes either within the crack or in the solid iterating as necessary for the implicit calculations. Then we calculate changes and iterate in the $\bar{Y}$ direction for all nodes. The $\bar{Z}$ direction calculations and iterations for all nodes are performed next. A final iteration loop over the total implicit calculations in the $\bar{X}$, $\bar{Y}$, plus $\bar{Z}$ directions is included to assure convergence.

ALTERNATE METHOD FOR DIFFERENCING THE CRACK-FLOW EQUATIONS

We again start with the governing equation for flow inside the crack, which is

$$-\bar{k}_{cx} \frac{\partial F}{\partial \bar{X}} \pm \frac{\partial}{\partial \bar{Y}} \left(\bar{k}_{cyz} \left(\left| \frac{\partial F}{\partial \bar{Y}} \right| \right)^{\frac{1}{2}} \right) \pm \frac{\partial}{\partial \bar{Z}} \left(\bar{k}_{cyz} \left(\left| \frac{\partial F}{\partial \bar{Z}} \right| \right)^{\frac{1}{2}} \right) + \frac{1}{2} F^{-\frac{1}{2}} \frac{\partial F}{\partial \tau} = 0 \tag{B-64}$$

Rather than differentiating in closed form, Winslow[B-3] has suggested incorporating into the coefficient $\bar{k}_{cyz}$ the necessary multiple of $\partial F/\partial \bar{Y}$ or $\partial F/\partial \bar{Z}$ to eliminate the square roots. That is, since the coefficients $\bar{k}_{cyz}$ are variable we could add such a multiple to the coefficients without appreciable complication and obtain a form of Eq. (B-64) that may be directly applied to the tri-diagonal matrix solution algorithm. We obtain the following form of the equation:

$$\bar{k}_{cx}\frac{\partial F}{\partial \bar{X}}+\frac{\partial}{\partial \bar{Y}}\left(\frac{\bar{k}_{cyz}}{\left(\left|\frac{\partial F}{\partial \bar{Y}}\right|\right)^{\frac{1}{2}}}\frac{\partial F}{\partial \bar{Y}}\right)+\frac{\partial}{\partial \bar{Z}}\left(\frac{\bar{k}_{cyz}}{\left(\left|\frac{\partial F}{\partial \bar{Z}}\right|\right)^{\frac{1}{2}}}\frac{\partial F}{\partial \bar{Z}}\right)=\frac{1}{2}F^{-\frac{1}{2}}\frac{\partial F}{\partial \tau}\ . \tag{B-97}$$

In differencing Eq. (B-97) we define the following.

$$\alpha_{1,j,k}=\bar{k}_{cx_{j,k}} \tag{B-98}$$

$$\gamma^{*,**}_{1,j+1/2,k}=\bar{k}_{cyz_{j+1/2,k}}\left[\theta\Big/\left(\left(\left|F^{**}_{1,j+1,k}-F^{**}_{1,j,k}\right|\right)/\Delta\bar{Y}\right)^{\frac{1}{2}}\right.$$

$$\left.+(1-\theta)\Big/\left(\left(\left|F^{*}_{1,j+1,k}-F^{*}_{1,j,k}\right|\right)/\Delta\bar{Y}\right)^{\frac{1}{2}}\right] \tag{B-99}$$

$$\xi^{*,**}_{1,j,k+1/2}=\bar{k}_{cyz_{j+1/2,k}}\left[\theta\Big/\left(\left(\left|F^{**}_{1,j,k+1}-F^{**}_{1,j,k}\right|\right)/\Delta\bar{Z}\right)^{\frac{1}{2}}\right.$$

$$\left.+(1-\theta)\Big/\left(\left(\left|F^{*}_{1,j,k+1}-F^{*}_{1,j,k}\right|\right)/\Delta\bar{Z}\right)^{\frac{1}{2}}\right] \tag{B-100}$$

$$\eta^{*,**}_{1,j,k}=0.5\left[\theta\Big/\left(F^{**}_{1,j,k}\right)^{\frac{1}{2}}+(1-\theta)\Big/\left(F^{*}_{1,j,k}\right)^{\frac{1}{2}}\right] \tag{B-101}$$

where

$$\bar{k}_{cyz_{j+1/2,k}}=\left(\bar{k}_{cyz_{j,k}}+\bar{k}_{cyz_{j+1,k}}\right)\Big/2\ . \tag{B-102}$$

We retain the operator splitting technique using the "$\bar{X}$" direction as explicit and an alternating direction implicit scheme in the "$\bar{Y}$" and "$\bar{Z}$" directions.

In the "$\bar{X}$" direction the difference equation is

$$\alpha_{1,j,k}\left(\frac{F^{n}_{2,j,k}-F^{n}_{1,j,k}}{\Delta\bar{X}}\right)=\eta^{n,*}_{1,j,k}\left(\frac{F^{*}_{1,j,k}-F^{n}_{1,j,k}}{\Delta\tau}\right). \tag{B-103}$$

In the "$\bar{Y}$" and "$\bar{Z}$" directions the difference equations are

$$\frac{1}{(\Delta\bar{Y})^2}\left[\gamma^{*,**}_{1,j+1/2,k}\left(F^{**}_{1,j+1,k}-F^{**}_{1,j,k}\right)-\gamma^{*,**}_{1,j-1/2,k}\left(F^{**}_{1,j,k}-F^{**}_{1,j-1,k}\right)\right]$$

$$+\frac{1}{(\Delta\bar{Z})^2}\left[\xi^{*,**}_{1,j,k+1/2}\left(F^{*}_{1,j,k+1}-F^{*}_{1,j,k}\right)-\xi^{*,**}_{1,j,k-1/2}\left(F^{*}_{1,j,k}-F^{*}_{1,j,k-1}\right)\right]$$

$$=\eta^{*,**}_{1,j,k}\left(\frac{F^{**}_{1,j,k}-F^{*}_{1,j,k}}{\Delta\tau/2}\right) \tag{B-104}$$

and

$$\frac{1}{(\Delta\bar{Y})^2}\left[\gamma^{**,n+1}_{1,j+1/2,k}\left(F^{**}_{1,j+1,k}-F^{**}_{1,j,k}\right)-\gamma^{**,n+1}_{1,j-1/2,k}\left(F^{**}_{1,j,k}-F^{**}_{1,j-1,k}\right)\right]$$

$$+\frac{1}{(\Delta\bar{Z})^2}\left[\xi^{**,n+1}_{1,j,k+1/2}\left(F^{n+1}_{1,j,k+1}-F^{n+1}_{1,j,k}\right)-\xi^{**,n+1}_{1,j,k-1/2}\left(F^{n+1}_{1,j,k}-F^{n+1}_{1,j,k-1}\right)\right]$$

$$=\eta^{**,n+1}_{1,j,k}\left(\frac{F^{n+1}_{1,j,k}-F^{**}_{1,j,k}}{\Delta\tau/2}\right). \tag{B-105}$$

This alternate formulation of the difference equations contains less terms and conservation of the pressure function flux across an elemental control volume is more apparent than in the method we used to obtain results. However, the alternate formulation was discarded because we found the stability limits to be more severe. Both formulations gave the same results on sample problems.

If the alternate method were to be utilized we would write Eq. (B-104) for the "$\bar{Y}$" direction as

$$- A_{i,j,k} F^{**}_{1,j+1,k} + B_{i,j,k} F^{**}_{1,j,k} - C_{1,j,k} F^{**}_{1,j-1,k} = D_{1,j,k} \tag{B-106}$$

where

$$A_{1,j,k} = \gamma^{*,**}_{1,j+1/2,k} \tag{B-107}$$

$$B_{1,j,k} = \left(\gamma^{*,**}_{1,j+1/2,k} + \gamma^{*,**}_{1,j-1/2,k}\right) + \eta^{*,**}_{1,j,k} \frac{(\Delta\bar{Y})^2}{\Delta\tau/2}$$

$$C_{1,j,k} = \gamma^{*,**}_{1,j-1/2,k} \tag{B-109}$$

$$D_{1,j,k} = \left[\frac{1}{(\Delta\bar{Z})^2}\left|\xi^{*,**}_{1,j,k+1/2}\left(F^{*}_{1,j,k+1} - F^{*}_{1,j,k}\right) - \xi^{*,**}_{1,j,k-1/2}\left(F^{*}_{1,j,k} - F_{1,j,k-1}\right)\right| + \frac{\eta^{*,**}_{1,j,k}}{\Delta\tau/2} F^{*}_{1,j,k}\right] \left(\Delta\bar{Y}\right)^2 \tag{B-110}$$

This gives

$$F^{**}_{1,j,k} = E_{1,j,k} F^{**}_{1,j+1,k} + \tilde{F}_{1,j,k} \tag{B-111}$$

where $E_{1,j,k}$ and $\tilde{F}_{1,j,k}$ are defined by Eqs. (B-87) and (B-88). We write Eq. (B-105) for the "Z" direction as

$$- A_{1,j,k} F^{n+1}_{1,j,k+1} + B_{1,j,k} F^{n+1}_{1,j,k} - C_{1,j,k} F^{n+1}_{1,j,k-1} = D_{1,j,k} \tag{B-112}$$

where

$$A_{1,k,j} = \xi^{**,n+1}_{1,j,k+1/2} \tag{B-113}$$

$$B_{1,j,k} = \left(\xi^{**,n+1}_{1,j,k+1/2} + \xi^{**,n+1}_{1,j,k-1/2}\right) + \frac{\eta^{**,n+1}_{1,j,k}}{\Delta\tau/2} \frac{(\Delta\bar{Z})^2}{\Delta\tau/2} \tag{B-114}$$

$$C_{1,j,k} = \xi^{**,n+1}_{1,j,k-1/2} \tag{B-115}$$

$$D_{1,j,k} = \left[\frac{1}{(\Delta\bar{Y})^2}\left\{\gamma^{**,n+1}_{1,j+1/2,k}\left(F^{**}_{1,j+1,k} - F^{**}_{1,j,k}\right) - \gamma^{**,n+1}_{1,j-1/2,k}\left(F^{**}_{1,j,k} - F^{**}_{1,j-1,k}\right)\right\} + \frac{\eta^{**,n+1}_{1,j,k}}{\Delta\tau/2} F^{**}_{1,j,k}\right] (\Delta\bar{Z})^2 \tag{B-106}$$

which in turn we write as

$$F^{n+1}_{1,j,k} = E_{1,j,k}\, F^{n+1}_{1,j,k+1} + \tilde{F}_{1,j,k} \quad . \tag{B-107}$$

We use the definition of $E_{1,j,k}$ and $\tilde{F}_{1,j,k}$ in Eqs. (B-95) and (B-96) for use "Z" direction. Boundary conditions are identical to those described earlier.

EVALUATION OF AN EFFECTIVE CRACK THICKNESS AT THE TIP OF THE CRACK

At the crack tip there is a control volume which is represented half as a crack and half as a porous solid as shown in Fig. B-6. The crack thickness diminishes to zero at the central node location so that flow in the lower half of the control volume is governed by the crack-flow equations. In the upper half the porous solid flow equations apply. Our calculations consider that the control volume has a single gas pressure and a single effective crack thickness.

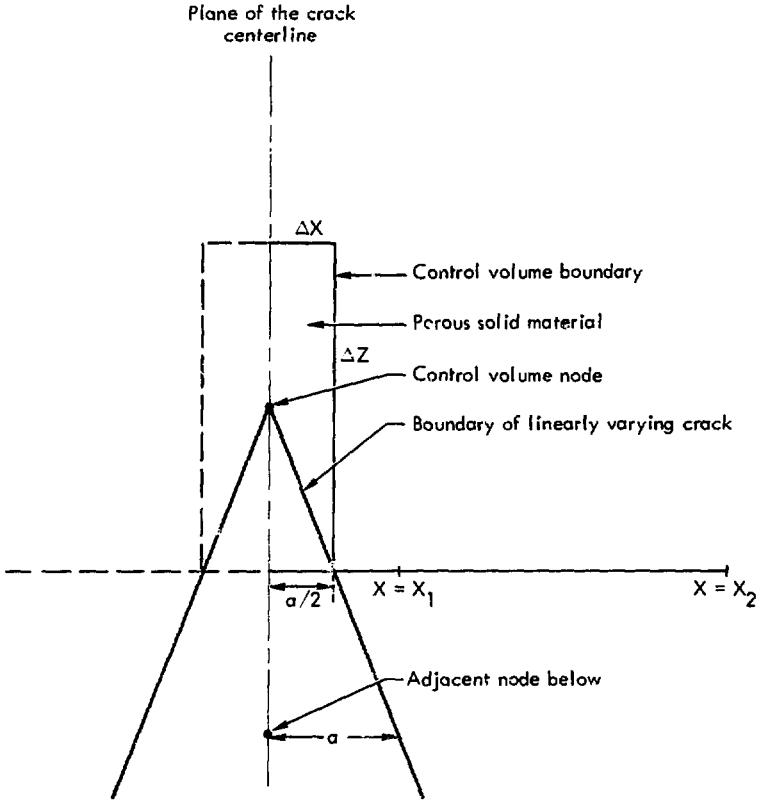

Fig. B-6. Crack-tip control volume at a region on top of the crack where no Y-direction variation exists.

If the crack boundary varies in a linear fashion over the localized region, then the crack thickness at the lower surface of the control volume would be one half the value at the adjacent node below. The average thickness of the crack in the lower half of control volume would be one fourth that of the adjacent node below.

Since the resistance to flow in the porous solid is generally much greater than that the resistance to flow inside the crack, the pressure at the node of interest would be approximately equal to that determined by the gas flow in the crack portion of the control volume. It could be argued that the average crack thickness represents an effective value to be used for calculating the average pressure over the control volume.

Normally the shape of the crack wall is convex outward so that the thickness remains large over most of its length and diminishes rapidly near the tip. This characteristic suggests that the effective crack thickness would be more than 1/4 that of the adjacent node below. On the other hand, any pressures calculated using the crack-flow equations apply only to the lower portion of the control volume so that the average pressure over the entire control volume would be less. We have varied the effective thickness between 1/4 and 1/2 that of the adjacent node below and find less than 5% difference in the results of sample problems. This effective thickness is left as an input variable with the recommendation that a value equal to about 1/4 that of the adjacent node below be utilized.

References for Appendix B

B-1 J., Douglas, "Alternating Direction Methods for Three Space Variables", Numerische Mathematik, Vol. 4, (1962), pp 41-63.

B-2 R. D., Richtmyer, and K. W., Morton, Difference Methods for Initial-Value Problems (Interscience Publishers, New York, 2nd Edition, 1967), pp 216-217.

B-3 A., Winslow, Lawrence Livermore Laboratory, Private Communication, (1974-1975).

Appendix C - The Computer Code CHASM

Included in this appendix is a listing of the computer code, CHASM, which was used to generate all results of this research on a CDC 7600 computer, a sample input for one of the problems, and a portion of the output.

The computer code consists of a main program and three subroutines. The main program is used to calculate constants, initialize variables, call the subroutines during each time iteration, and printout the results. The first subroutine, DEFL, determines the deflection of the crack walls due to gas pressure inside the crack. The second subroutine, FRICT, calculates frictional coefficients for use in the last subroutine, FLOW. All calculations for gas flow in the crack and in the porous solid are performed within subroutine FLOW. Comment cards are included to describe each set of calculations. Also included is a listing of the nomenclature. The definition of the pressure function, F, in this report is revised from that used in the computer program. This revision results in simplification of some equations in the report. The definition in the computer program differs by a constant factor $(1/N-1)^2$ and is consistent with all calculations performed.

The sample input shows the format for those variables called for on lines 198 to 200 and line 423 of the computer code. Although results are presented in metric units in the body of this report, English units were used for the computer input and output.

The output shown includes only the first portion and a representative portion toward the end of the problem. The first portion lists the input variables and some calculated constants. The representative portion gives the output at one specific time in the problem. Similar portions for all other printout times are found in a complete output.

```
      PROGRAM CHASM(TAPE59,INPUT,TAPE2=INPUT,ANSWER,TAPE3=ANSWER)
C
C     GAS-INITIATED CRACK PROPAGATION IN A POROUS SOLID--A COMPUTER CODE
C     IN THREE DIMENSIONS WHICH USES AN IDEAL GAS AS A FLUID.  THE
C     PROGRAM CALCULATES THE CRACK WALL DEFLECTION, FRICTIONAL
C     COEFFICIENTS, AND GAS FLOW BOTH IN THE CRACK AND IN THE POROUS
C     SOLID.  THE FORTRAN PROGRAMMING USES MIXED MODE ARITHMETIC.
C     INITIALIZATION OF ALL VARIABLES TO ZERO BY THE COMPILER IS
C     REQUIRED.
C
      COMMON /CRACK/ AF(10,15,20),AFF(10,15,20),BB(10,15,20),BETA(1,15,2
     10),CDEF,CFRIC1,CFRIC2,CKX(15,20),CKYZ(15,20),CSUBG(3,3),D(15,20),D
     2D(10,15,20),DELTA(1,15,20),DT,DTOT(15,20),DT2,DX(10),DY,DY2,DZ,DZ2
     3,EE(10,15,20),EFFTIP,ETA(10,15,20),F(10,15,20),FF(10,15,20),FMAX,F
     4STAR(10,15,20),FSSTAR(10,15,20),GAMMA(1,15,20),IO,JSTOP(20),L,LM1,
     5LM2,L2,M,MM1,MM2,M2,N,NM1,NM2,NTTOT,NYTIP(15),P(10,15,20),PR,PRFUN
     6,PS(60),REYNC(15,20),SIZE,SPACE(15,20),THETA,THETA1,X(10),XKX,XLAM
     7B(20,30),YKY,ZETA(1,15,20),ZKZ
      CALL DEVICE (6HCREATE,6HANSWER,110000)
C
C     NOMENCLATURE
C
C     AAF--PREVIOUS VALUE OF THE PRESSURE FUNCTION AF(I,J,K) USED IN "Z"
C          DIRECTION FLOW CALCULATION ITERATION
C     AF(I,J,K)--VALUE OF THE PRESSURE FUNCTION F(I,J,K) AT ADVANCED
C          TIME AFTER COMPLETION OF "Z" DIRECTION FLOW CALCULATIONS
C     AFF(I,J,K)--VALUE OF THE PRESSURE FUNCTION F(I,J,K) AFTER "X",
C          AND "Z" DIRECTION FLOW CALCULATION ITERATIONS
C     AJ,AK--VARIABLES USED IN CALCULATING THE INITIAL CRACK THICKNESS
C     ARG--ARGUMENT IN LOG BASE 10 FUNCTION FOR CALCULATING TURBULENT
C          FRICTION FACTOR, SUBROUTINE FRICT
C     BB(I,J,K)--VARIABLE USED FOR INVERSION OF THE TRI-DIAGONAL MATRIX,
C          SUBROUTINE FLOW
C     BETA(I,J,K)--VARIABLE COEFFICIENT IN THE CRACK FLOW CALCULATIONS
C     BLOTK--VALUE OF KAPPA IN BLOTTNER'S GRID STRETCHING METHOD
C     BLOTN--VARIABLE IN THE EXPONENT OF BLOTTNER'S GRID STRETCHING
C          METHOD (EQUATION 13)
C     B1,B2--VARIABLES USED IN CALCULATING BETA(I,J,K) WITHIN
C          SUBROUTINE FLOW
C     CDEF--CONSTANT USED IN SUBROUTINE DEFL (EQUATION B-2)
C     CFRIC1--CONSTANT USED TO CALCULATE XLLAM IN SUBROUTINE FRICT
C          (EQUATION B-13)
C     CFRIC2--CONSTANT USED TO CALCULATE TURBULENT REYNC(J,K) IN
C          SUBROUTINE FRICT (EQUATION B-19)
C     CKX(J,K)--NORMALIZED "X" DIRECTION PERMEABILITY THROUGH THE CRACK
C          WALL
C     CKYZ(J,K)--NORMALIZED EFFECTIVE PERMEABILITY IN THE "Y" & "Z"
C          DIRECTIONS WITHIN THE CRACK
C     COMPARE--DIFFERENCE BETWEEN OLD AND NEW VALUES OF FSTAR(I,J,K),
C          FSSTAR(I,J,K), AF(I,J,K), OR AFF(I,J,K) USED TO CHECK
C          CONVERGENCE IN SUBROUTINE FLOW
C     CONCKX--CONSTANT USED IN CALCULATING CKX(J,K)
C     CSUBG(J,K)--GERRARD AND MORGAN DEFLECTION COEFFICIENT ACCOUNTING
C          FOR THE DISTANCE AWAY FROM THE POINT OF PRESSURE APPLICATION
C          DURING THE CALCULATION OF THE DEFLECTION OF THE CRACK WALL
C     D(J,K)--DEFLECTION OF THE CRACK WALL IN "X" DIRECTION (FEET)
C     DBLOTN--DIFFERENTIAL SPACING IN BLOTTNER'S GRID STRETCHING METHOD
C          (EQUATION 13)
C     DD(I,J,K)--VARIABLE USED FOR INVERSION OF THE TRI-DIAGONAL MATRIX,
C          SUBROUTINE FLOW
```

```
C     DEFLCT- TEMPORARY VALUE OF D(J,K)
C     DEFTOT--TEMPORARY VALUE OF DTOT(J,K)
C     DELTA(I,J,K)--VARIABLE COEFFICIENT USED IN CRACK FLOW CALCULATIONS
C     DEN--VALUE OF THE DENOMINATOR USED IN CALCULATING EE(I,J,K) AND
C          FF(I,J,K) IN SUBROUTINE FLOW
C     DF--TOTAL DERIVATIVE OF THE FUNCTION, F(I,J,K)
C     DFY--¤Y¤ DIRECTION DERIVATIVE OF THE PRESSURE FUNCTION, F(I,J,K)
C     DFZ--¤Z¤ DIRECTION DERIVATIVE OF THE PRESSURE FUNCTION, F(I,J,K)
C     DT--DIMENSIONLESS TIME STEP
C     DTDX--VALUE EQUAL TO DT/DX USED IN SUBROUTINE FLOW FOR THE ¤X¤
C          DIRECTION EXPLICIT CALCULATIONS
C     DTOT(J,K)--CRACK HALF THICKNESS IN ¤X¤ DIRECTION (FEET)
C     DT2--HALF OF DT
C     DX(I)--NORMALIZED ¤X¤ DIRECTION SPATIAL MESH SIZE
C     DY--NORMALIZED ¤Y¤ DIRECTION SPATIAL MESH SIZE
C     DY2--DY SQUARED
C     DZ--NORMALIZED ¤Z¤ DIRECTION SPATIAL MESH SIZE
C     DZ2--DZ SQUARED
C     D1,D2--VARIABLES USED IN CALCULATING DELTA(I,J,K) WITHIN
C          SUBROUTINE FLOW
C     E--MODULUS OF ELASTICITY OF SOLID NORMALIZED TO P1MP0
C     EE(I,J,K)--VARIABLE USED FOR INVERSION OF THE TRI-DIAGONAL MATRIX,
C          SUBROUTINE FLOW
C     EFFTIP--EFFECTIVE CRACK TIP THICKNESS FRACTION
C     EMOD--MODULUS OF ELASTICITY OF THE SOLID (PSI)
C     ENU--POISSONS RATIO IN THE SOLID
C     EPS--POROSITY OF THE SOLID
C     ETA(I,J,K)--VARIABLE COEFFICIENT IN THE CRACK FLOW AND POROUS SOLID
C          CALCULATIONS (NOTE THERE IS A DIFFERENT DEFINITION IN EACH)
C     F(I,J,K)--PRESSURE FUNCTION IN THE SOLID AND CRACK EQUAL TO
C          P*P+2.*P/(N-1.).
C     FF(I,J,K)--VARIABLE USED FOR INVERSION OF THE TRI-DIAGONAL MATRIX,
C          SUBROUTINE FLOW
C     FMAX--MAXIMUM POSSIBLE VALUE OF THE PRESSURE FUNCTION, F(I,J,K)
C          EQUAL TO (PR+1.)/(PR-1.)
C     FRACT--VALUE USED IN DEFLECTION CRITERION EQUAL TO THE LITHOSTATIC
C          PRESSURE AT THE LOWER BOUNDARY OF THE PROBLEM DIVIDED BY THE
C          INITIAL GAS PRESSURE APPLIED TO THE LOWER BOUNDARY
C     FSIZE--MULTIPLIER OF THE AVERAGE GRAIN SIZE USED IN CALCULATING
C          THE CRACK HALF THICKNESS
C     FSSTAR(I,J,K)--INTERMEDIATE VALUE OF PRESSURE FUNCTION F(I,J,K)
C          AFTER ¤Y¤ DIRECTION CALCULATIONS
C     FSTAR(I,J,K)--INTERMEDIATE VALUE OF PRESSURE FUNCTION F(I,J,K)
C          AFTER ¤X¤ DIRECTION CALCULATIONS
C     GAMMA(I,J,K)--VARIABLE COEFFICIENT USED IN CRACK FLOW CALCULATIONS
C     G1,G2--VARIABLES USED IN CALCULATING GAMMA(I,J,K) WITHIN
C          SUBROUTINE FLOW
C     I--INDEX FOR ¤X¤ DIRECTION
C     IK,IKK,IKKK,& IKS--INDICIES USED TO CALCULATE DEFLECTION IN
C          SUBROUTINE DEFL
C     IO--INPUT-OUTPUT FLAG FOR PRINTOUTS
C     IX,IY,IZ,& IT--NUMBER OF NODES EXCEEDING THE CONVERGENCE CRITERION
C          IN SUBROUTINE FLOW FOR THE ¤X¤,¤Y¤,¤Z¤ DIRECTION AND TOTAL
C          SPACE LOOPS
C     ITERX,ITERXX,ITERY,ITERZ, & ITERT--NUMBER OF ITERATIONS THROUGH
C          ¤X¤,¤Y¤,¤Z¤ DIRECTION AND TOTAL SPACE LOOPS, SUBROUTINE FLOW
C     J,JJ,JJJ--INDICIES FOR ¤Y¤ DIRECTION
C     JDEF--INDEX FOR CSUBG(JDEF,KDEF) IN SUBROUTINE DEFL
C     JKMAX--INDEX USED FOR CALCULATING CRACK DEFLECTION.
C     JSTOP(K)--ARRAY DEFINING APPROXIMATE CIRCLE OF INFLUENCE IN
```

```
C          SUBROUTINE DEFL (NUMBER OF NON-ZERO ELEMENTS MUST EQUAL
C          JSTOP(K)+1.  ALSO, KMINUS MUST BE GREATER THAN OR EQUAL TO
C          JSTOP(1))
C     K,KK,KKK,--INDICIES FOR ¤Z¤ DIRECTION
C     KDEF--INDEX FOR CSUBG(JDEF,KDEF) IN SUBROUTINE DEFL
C     KMINUS--NUMBER OF NODES BELOW THE LOWER BOUNDARY USED IN
C          SUBROUTINE DEFL FOR CALCULATING DEFLECTIONS.  MUST BE
C          GREATER THAN OR EQUAL TO JSTOP(1).
C     L--NUMBER OF ¤X¤ DIRECTION NODES
C     LB--BACKWARD INDEX OF ¤X¤ DIRECTION NODES
C     LM1--NUMBER EQUAL TO L-1
C     LM2--NUMBER EQUAL TO L-2
C     L2--MAXIMUM ¤X¤ DIRECTION NODE OVER WHICH THE DRIVING PRESSURE IS
C          APPLIED ON THE LOWER BOUNDARY (¤Z¤ NODE EQUAL TO ONE)
C     M--NUMBER OF ¤Y¤ DIRECTION NODES
C     MB--BACKWARD INDEX OF ¤Y¤ DIRECTION NODES
C     MM1--NUMBER EQUAL TO M-1
C     MM2--NUMBER EQUAL TO M-2
C     M2--MAXIMUM ¤Y¤ DIRECTION NODE OVER WHICH THE DRIVING PRESSURE IS
C          APPLIED ON THE LOWER BOUNDARY (¤Z¤ NODE EQUAL TO ONE)
C     N--NUMBER OF ¤Z¤ DIRECTION NODES
C     NB--BACKWARD INDEX OF ¤Z¤ DIRECTION NODES
C     NMTIP--INTEGER VALUE EQUAL TO NYTIP(J)-1
C     NM1--NUMBER EQUAL TO N-1
C     NM2--NUMBER EQUAL TO N-2.
C     NNTIP--PAST VALUE OF NYTIP(1) USED AS FLAG FOR WRITE STATEMENT
C     NTIP--INTEGER VALUE OF NYTIP(J)
C     NTTOT--NUMBER OF ITERATIONS OF EXPLICIT ¤X¤ DIRECTION PRESSURE
C          CALCULATIONS IN THE CRACK FOR EACH IMPLICIT PRESSURE
C          CALCULATION IN THE SOLID OR IN THE CRACK
C     NYTIP(J)--CRACK TIP ¤Z¤ NODE LOCATION WHICH IS A FUNCTION OF ¤Y¤
C     NYTIPI--INITIAL VALUE OF CRACK TIP ¤Y¤ DIRECTION NODE LOCATION
C     NYTIPM--VALUE OF NYTIPI MINUS ONE
C     NZTIPI--INITIAL VALUE OF CRACK TIP ¤Z¤ DIRECTION NODE LOCATION
C     NZTIPM--VALUE OF NZTIPI MINUS ONE
C     P(I,J,K)--PRESSURE IN SOLID AND CRACK NORMALIZED TO THE INITIAL
C          DRIVING PRESSURE
C     PDOWNH--INITIAL PORE PRESSURE IN THE SOLID (PSI)
C     PERM--PERMEABILITY OF THE SOLID (DARCYS)
C     PFSSTAR,PFSTAR--PAST VALUES OF FSSTAR(I,J,K) AND FSTAR(I,J,K) USED
C          FOR CHECKING CONVERGENCE IN SUBROUTINE FLOW
C     PR--RATIO OF THE INITIAL DRIVING PRESSURE TO AMBIENT PRESSURE
C     PRFUN--FUNCTION OF PRESSURE RATIO USED IN SUBROUTINE FLOW
C     PRINT--PRINTOUT INTERVAL
C     PS(K)--RESISTIVE PRESSURE IN THE SOLID NORMALIZED TO THE INITIAL
C          DRIVING PRESSURE AND USED IN DETERMINING CRACK PROPAGATION
C     PIMPQ--INITIAL ¤Z¤ DIRECTION PRESSURE DIFFERENCE ACROSS THE POROUS
C          SOLID (PSI)
C     R--GAS CONSTANT IN UNITS OF FEET/DEGREE RANKINE
C     REYNC(J,K)--REYNOLDS NUMBER IN CRACK
C     SIZE--AVERAGE GRAIN SIZE (DIAMETER) OF SOLID MATERIAL (FEET)
C     SPACE(J,K)--INITIAL CRACK HALF THICKNESS IN ¤X¤ DIRECTION (FEET)
C     TEMP--TEMPERATURE IN DEGREES RANKINE
C     TERM1--CONTRIBUTION TO THE CRACK WALL DEFLECTION BY NODES AT THE
C          SAME ELEVATION AS THE POINT DEFLECTION IS BEING CALCULATED.
C     TERM2--CONTRIBUTION BY NODES BELOW ¤Z¤=0.
C     TERM3--CONTRIBUTION BY NODES ABOVE THE PLANE ¤Z¤=0.
C     TFIN--MAXIMUM DIMENSIONLESS TIME BEFORE PROBLEM STOPS
C     THETA,THETA1--WEIGHTING FACTORS ON NONLINEAR COEFFICIENTS
C          EVALUATED AT THE NEW AND OLD TIMES IN SUBROUTINE FLOW
```

```
C      TIME--DIMENSIONLESS TIME
C      TPRINT--TIME FOR NEXT PRINTOUT
C      X(I)--¤X¤ DIRECTION SPATIAL GRID LOCATION (FEET)
C      XKX--NORMALIZED ¤X¤ DIRECTION PERMEABILITY IN THE POROUS SOLID
C      XKZERO--NORMALIZING VALUE FOR PERMEABILITY (DARCYS)
C      XLAMB(J,K)--FRICTIONAL COEFFICIENT OF GAS FLOW IN THE CRACK
C      XLLAM--LAMINAR FRICTIONAL COEFFICIENT OF GAS FLOW IN THE CRACK
C      XLTURB--TURBULENT FRICTIONAL COEFFICIENT OF GAS FLOW IN THE CRACK
C      XMAX--LENGTH OF SOLID IN ¤X¤ DIRECTION (FEET)
C      XMU--GAS VISCOSITY (LB-SEC/SQ.FT.)
C      YKY--NORMALIZED ¤Y¤ DIRECTION PERMEABILITY IN SOLID
C      ZETA(I,J,K)--VARIABLE COEFFICIENT IN CRACK FLOW CALCULATIONS
C      ZKZ--NORMALIZED ¤Z¤ DIRECTION PERMEABILITY IN SOLID
C      ZLENG--LENGTH OF SOLID ALONG CRACK AXIS OR ¤Z¤ DIRECTION (FEET)
C
C      INPUT
C
       READ (2,19) BLOTK,DT,EFFTIP,EMOD,ENU,EPS,FRACT,FSIZE,L2,M2,NTTOT,N
      1YTIPI,NZTIPI,PDOWNH,PERM,PRINT,PIMPO,R,SIZE,TEMP,TFIN,XMAX,XMU,ZLE
      2NG
       DATA IO,(JSTOP(I),I=1,3),KMINUS,L,M,N/3,2,2,2,2.10,15,20/
       DATA THETA,TPRINT/0.5,-1.E-10/
C
C      CALCULATED CONSTANTS
C
       E=EMOD/PIMPO
       CDEF=(1.-ENU*ENU)*ZLENG/E
       CFRIC1=(12.*XMU/(144.*PIMPO))**2*32.2*ZLENG*R*TEMP
       CFRIC2=8.*144.*PIMPO/(XMU*SQRT(32.2*ZLENG*R*TEMP))
       DT2=DT/2.
C
C      IF DY IS NOT EQUAL TO DZ, CHANGES IN SUBROUTINE DEFL ARE REQUIRED.
C
       DY=1./(N-1)
       DY2=DY*DY
       DZ=1./(N-1)
       DZ2=DZ*DZ
       LM1=L-1
       LM2=L-2
       MM1=M-1
       MM2=M-2
       NM1=N-1
       NM2=N-2
       NYTIPM=NYTIPI-1
       NZTIPM=NZTIPI-1
       PR=(PIMPO+PDOWNH)/PDOWNH
       PRFUN=1./(PR-1.)**2
       THETA1=1.-THETA
       CSUBG(1,1)=0.950/NM1
       CSUBG(2,1)=0.300/NM1
       CSUBG(3,1)=0.050/NM1
       CSUBG(1,2)=0.300/NM1
       CSUBG(2,2)=0.100/NM1
       CSUBG(3,2)=0.020/NM1
       CSUBG(1,3)=0.050/NM1
       CSUBG(2,3)=0.020/NM1
       CSUBG(3,3)=0.002/NM1
       FMAX=(PR+1.)/(PR-1.)
C
C      CALCULATE X(I) AND DX(I) USING BLOTTNER'S EQUATION NUMBER 9, COMP.
```

```
241 C      METHODS IN APP. MECH. & ENGR. (1974).  SEE EQUATION 13 OF THE
242 C      PRESENT REPORT.
243 C
244        X(1)=0.
245        BLOTN=0.
246        DBLOTN=1./LM1
247        X(1)=0.
248        DO 1 I=2,L
249        BLOTN=BLOTN+DBLOTN
250        X(I)=XMAX*(BLOTK**(BLOTN/DBLOTN)-1.)/(BLOTK**(1./DBLOTN)-1.)
251   1    CONTINUE
252        DO 2 I=2,L
253        DX(I)=(X(I)-X(I-1))/ZLENG
254   2    CONTINUE
255 C
256 C      CALCULATE OVERBURDEN PRESSURE, PS(K)
257 C
258        DO 3 K=1,NM1
259        KK=N-K
260        PS(K)=FRACT*KK/NM1
261   3    CONTINUE
262        DO 4 K=1,KMINUS
263        KK=N-K
264        KKK=N+K
265        PS(KKK)=PS(1)+PS(KK)
266   4    CONTINUE
267 C
268 C      SET UP INITIAL CRACK DIMENSIONS
269 C
270        DO 5 J=1,NYTIPM
271        NYTIP(J)=NZTIPI
272   5    CONTINUE
273        NNTIP=NYTIP(1)
274 C
275 C      SET UP INITIAL CRACK HALF THICKNESS.  THE PRESENT ANALYSIS USES A
276 C      LINEAR RELATIONSHIP.
277 C
278        DO 7 J=1,NYTIPM
279        AJ=J-1
280        NMTIP=NYTIP(J)-1
281        NTIP=NYTIP(J)
282        DO 6 K=1,NTIP
283        AK=K-1
284        IF (NMTIP.EQ.0.OR.NYTIPM.EQ.0) GO TO 7
285        SPACE(J,K)=(1.-AK/NMTIP)*(1.-AJ/NYTIPM)*FSIZE*SIZE
286        DTOT(J,K)=SPACE(J,K)
287   6    CONTINUE
288        DTOT(J,NTIP)=DTOT(J,NMTIP)/EFFTIP
289   7    CONTINUE
290        DO 8 K=1,NZTIPM
291        DTOT(NYTIPI,K)=DTOT(NYTIPM,K)/EFFTIP
292   8    CONTINUE
293 C
294 C      XKZERO IS CALCULATED USING EQUATION 21 FOR K BAR SUB CYZ.
295 C      K BAR SUB CYZ IS TAKEN TO BE UNITY AT TIME ZERO WHEN BOTH ¤Y¤ AND
296 C      ¤Z¤ NODES EQUAL ONE.  XKZERO IS IN DARCYS.  THE VALUE OF A
297 C      REPRESENTATIVE LAMBDA IS TAKEN AS 0.0454, WHICH CORRESPONDS TO A
298 C      REYNOLDS NUMBER OF 2100.  1.06E-11 SQ FT=1 DARCY, IS USED AS A
299 C      CONVERSION CONSTANT.
300 C
```

```
      XKZERO=EPS*XMU*SQRT(64.4*2.*SPACE(I,1)*R*TEMP*ZLENG/0.0454)/(1.0E-
     1)*P1MP0*144.)
C
C     SET DIRECTIONAL PERMEABILITIES IN THE S'LID
C
      XKX=PERM/XKZERO
      YKY=PERM/XKZERO
      ZKZ=PERM/XKZERO
      CONCKX=XKX*EPS*ZLENG/2.
C
C     INITIALIZE THE DRIVING PRESSURE OVER THE APPROPRIATE PART OF THE
C     PLANE WHERE THE ¤Z¤ NODE EQUALS ONE.
C
      DO 9 I=1,L2
      DO 9 J=1,M2
      P(I,J,1)=1.
      F(I,J,1)=FMAX
    9 CONTINUE
C
C     WRITE OUT INPUT VALUES
C
      WRITE (10,20) BLOTK,DT,EFFTIP,EMOD,ENU,EPS,FRACT,FSIZE,IO,KMINUS,L
     1,M,N,L2,M2,NTTOT,NYTIPI,NZTIPI,PDOWNH,PERM,PRINT,P1MP0,R,SIZE,TEMP
     2,TFIN,XMAX,XMU,ZLENG,E,XKX,XKZERO,(X(I),I=1,10)
      GO TO 18
C
C     MAIN CALCULATIONAL LOOPS
C
C     UPDATE CRACK HALF THICKNESS AND EFFECTIVE PERMEABILITY IN THE ¤Z¤
C     DIRECTION DUE TO CRACK DIMENSION CHANGES.
C
   10 CALL DEFL
      DO 13 J=1,M
      DO 11 K=1,N
C
C     CALCULATE FRICTION COEFFICIENTS
C
      IF (DTOT(J,K).LE.0.) GO TO 12
      CALL FRICT (J,K)
C
C     CALCULATE CRACK EFFECTIVE PERMEABILITIES FROM EQUATIONS 20 AND 21.
C     NOTE THAT INITIALLY CKYZ(I,1)=1.0
C
      CKX(J,K)=CONCKX/DTOT(J,K)
      IF (XLAMB(J,K).LE.0.) GO TO 12
      CKYZ(J,K)=SQRT(DTOT(J,K)*0.0454/(SPACE(I,1)*XLAMB(J,K)))
   11 CONTINUE
   12 IF (DTOT(J,1).LE.0.) J=M
   13 CONTINUE
      CALL FLOW
      TIME=TIME+DT
      IF (DTOT(1,N).GT.0..OR.DTOT(M,1).GT.0.) GO TO 16
C
C     REDUCE THE DRIVING PRESSURE WITH TIME.  INCLUDE A MATHEMATICAL
C     RELATIONSHIP HERE OR DELETE THE LOOP IF THE DRIVING PRESSURE IS
C     CONSTANT.
C
      DO 14 I=1,L2
      DO 14 J=1,M2
      P(I,J,1)=(1472./EXP(0.034422*TIME)+29.)/1501.
```

```
      F(I,J,1)=P(I,J,1)*(P(I,J,1)+2./(PR-1.))
14    CONTINUE
      IF (NNTIP.EQ.NYTIP(1)) GO TO 15
      WRITE (10,21) TIME,(NYTIP(J),J=1,15)
      NNTIP=NYTIP(1)
15    IF (TIME.GE.TPRINT.OR.TIME.GE.TFIN) GO TO 16
      GO TO 10
16    DO 17 I=1,L
      DO 17 J=1,M
      DO 17 K=1,NM1
      P(I,J,K)=SQRT(F(I,J,K)+PRFUN)-1./(PR-1.)
17    CONTINUE
C
C     PRINTOUTS
C
18    WRITE (10,25)
      WRITE (10,22) ((P(I,J,1),I=1,10),J=1,15)
      WRITE (10,26)
      WRITE (10,22) ((P(I,J,2),I=1,10),J=1,15)
      WRITE (10,27)
      WRITE (10,22) ((P(I,J,3),I=1,10),J=1,15)
      WRITE (10,28)
      WRITE (10,22) ((P(I,J,4),I=1,10),J=1,15)
      WRITE (10,29)
      WRITE (10,22) ((P(I,J,5),I=1,10),J=1,15)
      WRITE (10,30)
      WRITE (10,22) ((P(I,J,6),I=1,10),J=1,15)
      WRITE (10,31)
      WRITE (10,22) ((P(I,J,7),I=1,10),J=1,15)
      WRITE (10,32)
      WRITE (10,22) ((P(I,J,8),I=1,10),J=1,15)
      WRITE (10,33)
      WRITE (10,22) ((P(I,J,9),I=1,10),J=1,15)
      WRITE (10,34)
      WRITE (10,22) ((P(I,J,10),I=1,10),J=1,15)
      WRITE (10,35)
      WRITE (10,22) ((P(I,J,15),I=1,10),J=1,15)
      WRITE (10,36)
      WRITE (10,22) ((P(I,J,19),I=1,10),J=1,15)
      WRITE (10,37)
      WRITE (10,23) ((D(J,K),J=1,15),K=1,19)
      WRITE (10,38)
      WRITE (10,23) ((DTOT(J,K),J=1,15),K=1,19)
      WRITE (10,39)
      WRITE (10,23) ((CKX(J,K),J=1,15),K=1,19)
      WRITE (10,40)
      WRITE (10,23) ((CKYZ(J,K),J=1,15),K=1,19)
      WRITE (10,41)
      WRITE (10,23) ((XLAMB(J,K),J=1,15),K=1,19)
      WRITE (10,42)
      WRITE (10,23) ((REYNC(J,K),J=1,15),K=1,19)
      WRITE (10,43)
      WRITE (10,44) ((NYTIP(J),J=1,15))
      WRITE (10,24) TIME,DT
      TPRINT=TPRINT+PRINT
      CALL EMPTY (3)
      IF (TIME.GE.TFIN) CALL EXIT (1)
      IF (DTOT(1,N).GT.0..OR.DTOT(M,1).GT.0.) CALL EXIT (1)
      GO TO 10
C
```

```
421 C
422 C
423   19    FORMAT (8F10.5,/,5I5,/,7F10.5,/,4F10.5)
424   20    FORMAT (41HBLOTK,DT,EFFTIP,EMOD,ENU,EPS,FRACT,FSIZE=,/,8E15.5,//,4
425          12HIO,KMINUS,L,M,N,L2,M2,NTTOT,NYTIPI,NZTIPI=,/,10I10,//,36HPDOWNH,
426          2PERM,PRINT,P1MP0,R,SIZE,TEMP=,/,7E15.5,//,33HTFIN,XMAX,XMU,ZLENG,E
427          3,XKX,XKZERO=,/,7E15.5,//,5HX(I)=,/,5E15.5,/,5E15.5,////)
428   21    FORMAT (14HTIME,NYTIP(J)=,E15.5,15I5,//)
429   22    FORMAT (10(F8.5,2X))
430   23    FORMAT (8E14.4,/,5X,7E14.4)
431   24    FORMAT (9H TIME,DT=,E14.3,2X,E14.3,///)
432   25    FORMAT (9HP(I,J,1)=)
433   26    FORMAT (9HP(I,J,2)=)
434   27    FORMAT (9HP(I,J,3)=)
435   28    FORMAT (9HP(I,J,4)=)
436   29    FORMAT (9HP(I,J,5)=)
437   30    FORMAT (9HP(I,J,6)=)
438   31    FORMAT (9HP(I,J,7)=)
439   32    FORMAT (9HP(I,J,8)=)
440   33    FORMAT (9HP(I,J,9)=)
441   34    FORMAT (10HP(I,J,10)=)
442   35    FORMAT (10HP(I,J,15)=)
443   36    FORMAT (10HP(I,J,19)=)
444   37    FORMAT (7HD(J,K)=)
445   38    FORMAT (10HDTOT(J,K)=)
446   39    FORMAT (9HCKX(J,K)=)
447   40    FORMAT (10HCKYZ(J,K)=)
448   41    FORMAT (11HXLAMB(J,K)=)
449   42    FORMAT (11HREYNC(J,K)=)
450   43    FORMAT (9HNYTIP(J)=)
451   44    FORMAT (10(5X,I5))
452         END
453 C       CCCCCCCCCCCCCCCCCCCCCCCCCCCCCCCCCCCCCCCCCCCCCCCCCCCCCCCCCCCCCCCCCCC
454 C
455         SUBROUTINE DEFL
456 C
457 C       CCCCCCCCCCCCCCCCCCCCCCCCCCCCCCCCCCCCCCCCCCCCCCCCCCCCCCCCCCCCCCCCCCC
458 C
459 C       A SUBROUTINE TO CALCULATE THE ¤X¤ DIRECTION DEFLECTION OF THE
460 C       CRACK WALL CAUSED BY PRESSURE WITHIN THE CRACK.  THE ANALYSIS
461 C       FOLLOWS THAT OF TIMOSHENKO AND GOODIER ¤THEORY OF ELASTICITY¤,
462 C       SECTION 139, AND OF GERRARD AND MORGAN, GEOTECHNIQUE, VOLUME 22,
463 C       1972.  A CIRCLE OF INFLUENCE IS DEFINED BY THE ARRAY JSTOP(K) WITH
464 C       NO EFFECT ON DEFLECTION PRODUCED BY PRESSURES BEYOND THIS CIRCLE.
465 C       THE CENTER OF THE CIRCLE IS THE POINT WHERE THE DEFLECTION IS
466 C       BEING CALCULATED.  A COEFFICIENT, CSUBG(J,K), IS USED TO ACCOUNT
467 C       FOR THE EFFECT OF DISTANCE AWAY FROM THE POINT OF PRESSURE
468 C       APPLICATION ON THE DEFLECTION.
469 C
470         COMMON /CRACK/ AF(10,15,20),AFF(10,15,20),BB(10,15,20),BETA(1,15,2
471        10),CDEF,CFRIC1,CFRIC2,CKX(15,20),CKYZ(15,20),CSUBG(3,3),D(15,20),D
472        2D(10,15,20),DELTA(1,15,20),DT,DTOT(15,20),DT2,DX(10),DY,DY2,DZ,DZ2
473        3,EE(10,15,20),EFFTIP,ETA(10,15,20),F(10,15,20),FF(10,15,20),FMAX,F
474        4STAR(10,15,20),FSSTAR(10,15,20),GAMMA(1,15,20),IO,JSTOP(20),L,LM1,
475        5LM2,L2,M,MM1,MM2,M2,N,NM1,NM2,NTTOT,NYTIP(15),P(10,15,20),PR,PRFUN
476        6,PS(60),REYNC(15,20),SIZE,SPACE(15,20),THETA,THETA1,X(10),XKX,XLAM
477        7B(20,30),YKY,ZETA(1,15,20),ZKZ
478 C
479 C       CALCULATE VALUES OF PRESSURE FROM THE PRESSURE FUNCTION.
480 C
```

```
      DO 1 K=1,N
      DO 1 J=1,M
      P(I,J,K)=SQRT(F(I,J,K)+PRFUN)-1./(PR-1.)
    1 CONTINUE
C
C     CALCULATE CRACK DEFLECTIONS OVER THE ¤X¤=0 PLANE USING EQUATIONS
C     B-1,B-2, AND B-3.
C
      DO 12 K=1,N
      DO 11 J=1,M
      TERM1=0.
      JKMAX=2*JSTOP(I)+1
      DO 3 JJ=1,JKMAX
      JJJ=J-1-JSTOP(I)+JJ
      JDEF=IABS(JSTOP(I)-JJ+1)+1
      IF (JJJ.GE.1) GO TO 2
      JJJ=2-JJJ
C
C     NODES BEYOND J=M ARE CONSIDERED IDENTICAL TO NODE J=M
C
    2 IF (JJJ.GT.M) JJJ=M
      TERM1=TERM1+CSUBG(JDEF,I)*(P(I,JJJ,K)-PS(K))
    3 CONTINUE
      TERM2=0.
      TERM3=0.
      DO 10 KKK=1,JKMAX
      IKK=K-1-JSTOP(I)+KKK
      KDEF=IABS(JSTOP(I)-KKK+1)+1
C
C     NODE K=N HAS A ZERO PRESSURE BOUNDARY CONDITION
C
      IF (IKK.EQ.K.OR.IKK.GT.N-1) GO TO 10
      IK=IABS(IKK-K)+1
      JKMAX=2*JSTOP(IK)+1
      IF (IKK.GE.1) GO TO 7
C
C     CALCULATIONS BELOW NODE K=1
C
      IKS=N-IKK+1
      IKKK=2-IKK
      DO 6 JJ=1,JKMAX
      JJJ=J-1-JSTOP(IK)+JJ
      JDEF=IABS(JSTOP(IK)-JJ+1)+1
      IF (JJJ.GE.1) GO TO 4
      JJJ=2-JJJ
    4 IF (JJJ.GT.M2) GO TO 5
C
C     J NODE WITHIN THE CAVITY
C
      TERM2=TERM2+CSUBG(JDEF,KDEF)*(P(I,JJJ,1)-PS(IKS))
      GO TO 6
C
C     J NODE BEYOND THE CAVITY
C
    5 IF (JJJ.GT.M) JJJ=M
      TERM2=TERM2+CSUBG(JDEF,KDEF)*(P(I,JJJ,IKKK)-PS(IKS))
    6 CONTINUE
      GO TO 10
C
C     CALCULATIONS ABOVE NODE K=1
```

```
C
 7    DO 9 JJ=1,JKMAX
      JJJ=J-1-JSTOP(IK)+JJ
      JDEF=IABS(JSTOP(IK)-JJ+1)+1
      IF (JJJ.GE.1) GO TO 8
      JJJ=2-JJJ
 8    IF (JJJ.GT.M) JJJ=M
      TERM3=TERM3+CSUBG(JDEF,KDEF)*(P(1,JJJ,IKK)-PS(IKK))
 9    CONTINUE
 10   CONTINUE
      DEFLCT=CDEF*(TERM1+TERM2+TERM3)
      IF (DEFLCT.GT.D(J,K)) D(J,K)=DEFLCT
      DEFTOT=D(J,K)+SPACE(J,K)
      IF (DEFTOT.GT.DTOT(J,K)) DTOT(J,K)=DEFTOT
C
C     STOP □Y□ DIRECTION CALCULATION IF THE CRACK THICKNESS IS ZERO
C
      IF (DTOT(J,K).LE.0.) J=M
 11   CONTINUE
C
C     STOP □Z□ DIRECTION CALCULATION IF THE CRACK THICKNESS IS ZERO
C
      IF (DTOT(1,K).LE.0.) K=N
 12   CONTINUE
C
C     CALCULATE THE CRACK TIP BASED ON A POSITIVE CRACK THICKNESS
C
      DO 13 J=1,M
      K=NYTIP(J)
      IF (K.LT.1) K=1
      IF (D(J,K).GT.0.) NYTIP(J)=K+1
 13   CONTINUE
C
C     SET THE EFFECTIVE CRACK TIP THICKNESS
C
      DO 15 J=1,M
      IF (NYTIP(J).LE.1) GO TO 16
      K=NYTIP(J)
      DO 14 KK=2,K
      IF (DTOT(J,KK).LE.0.) DTOT(J,KK)=DTOT(J,KK-1)/EFFTIP
 14   CONTINUE
      DTOT(J,K)=DTOT(J,K-1)/EFFTIP
 15   CONTINUE
 16   DO 18 JJ=2,J
      IF (NYTIP(JJ-1).LE.NYTIP(JJ)) GO TO 18
      K=NYTIP(JJ)
      KK=NYTIP(JJ-1)-1
      DO 17 KKK=K,KK
      DTOT(JJ,KKK)=DTOT(JJ-1,KKK)/EFFTIP
 17   CONTINUE
 18   CONTINUE
      RETURN
      END
C     CCCCCCCCCCCCCCCCCCCCCCCCCCCCCCCCCCCCCCCCCCCCCCCCCCCCCCCCCCCCCCCCCC
C
      SUBROUTINE FRICT (J,K)
C
C     CCCCCCCCCCCCCCCCCCCCCCCCCCCCCCCCCCCCCCCCCCCCCCCCCCCCCCCCCCCCCCCCCC
C
C     CALCULATES FRICTION COEFFICIENTS FOR FLOW WITHIN THE CRACK USING
```

```
601 C      96/RE FOR LAMINAR FLOW OR EQUATION 20.35 IN SCHLICHTING'S
602 C      "BOUNDARY LAYER THEORY" FOR TURBULENT FLOW, WHICHEVER GIVES THE
603 C      LARGER VALUE.
604 C
605        COMMON /CRACK/ AF(10,15,20),AFF(10,15,20),BB(10,15,20),BETA(1,15,2
606       10),CDEF,CFRIC1,CFRIC2,CKX(15,20),CKYZ(15,20),CSUBG(3,3),D(15,20),D
607       2D(10,15,20),DELTA(1,15,20),DT,DTOT(15,20),DT2,DX(10),DY,DY2,DZ,DZ2
608       3,EE(10,15,20),EFFTIP,ETA(10,15,20),F(10,15,20),FF(10,15,20),FMAX,F
609       4STAR(10,15,20),FSSTAR(10,15,20),GAMMA(1,15,20,10,JSTOP(20),L,LM1,
610       5LM2,L2,M,MM1,MM2,M2,N,NM1,NM2,NTTOT,NYTIP(15),P(10,15,20),PR,PRFUN
611       6,PS(60  REYNC(15,20),SIZE,SPACE(15,20),THETA,THETA1,X(10),XKX,XLAM
612       7B(20,30),YKY,ZETA(1,15,20),ZKZ
613 C
614 C      CALCULATE COEFFICIENT ASSUMING LAMINAR FLOW USING EQUATION B-12.
615 C
616        IF (K.NE.1) GO TO 1
617        DFZ=ABS(F(1,J,1)-F(1,J,2))/DZ
618        GO TO 2
619   1    DFZ=0.5*ABS(F(1,J,K+1)-F(1,J,K-1))/DZ
620   2    IF (J.NE.1) GO TO 3
621        DFY=ABS(F(1,1,K)-F(1,2,K))/DY
622        GO TO 4
623   3    DFY=0.5*ABS(F(1,J+1,K)-F(1,J-1,K))/DY
624   4    DF=DFY+DFZ
625        IF (DF.EQ.0) GO TO 5
626        XLLAM=CFRIC1/(DTOT(J,K)**3*DF)
627 C
628 C      LIMIT XLLAM TO PREVENT INFINITE VALUES
629 C
630        IF (XLLAM.LT.10.) GO TO 6
631   5    XLLAM=10.
632 C
633 C      CALCULATE COEFFICIENT ASSUMING TURBULENT FLOW USING EQUATION A-60.
634 C
635   6    ARG=4.*DTOT(J,K)/SIZE
636 C
637 C      LIMIT XLTURB TO A MAXIMUM OF 0.0454.  THIS NUMBER EQUALS THE
638 C      LAMINAR FLOW COEFFICIENT FOR A REYNOLDS NUMBER OF 2100.
639 C
640        IF (ARG.LE.30.) GO TO 7
641        XLTURB=1./(2.*ALOG10(ARG)+1.74)**2
642        GO TO 8
643   7    XLTURB=0.0454
644 C
645 C      SELECT MAXIMUM OF XLLAM OR XLTURB
646 C
647   8    XLAMB(J,K)=AMAX1(XLLAM,XLTURB)
648 C
649 C      CALCULATE REYNOLDS NUMBER USING EQUATIONS (B-17) AND (B-18)
650 C
651        IF (XLLAM.LT.XLTURB) GO TO 9
652        REYNC(J,K)=96./XLLAM
653        GO TO 10
654   9    REYNC(J,K)=CFRIC2*DTOT(J,K)*SQRT(DTOT(J,K)*DF/XLTURB)
655   10   RETURN
656        END
657 C      CCCCCCCCCCCCCCCCCCCCCCCCCCCCCCCCCCCCCCCCCCCCCCCCCCCCCCCCCCCCCCCCCC
658 C
659        SUBROUTINE FLOW
660 C
```

```
C     CCCCCCCCCCCCCCCCCCCCCCCCCCCCCCCCCCCCCCCCCCCCCCCCCCCCCCCCCCCCCCCCCC
C
C     THIS SUBROUTINE DETERMINES THE PRESSURE AT EACH NODE IN THE POROUS
C     SOLID AND WITHIN THE CRACK DUE TO THE GAS FLOW.  FIRST FLOW IN
C     THE ¤X¤ DIRECTION IS CALCULATED EXPLICITLY WITHIN THE CRACK AND
C     IMPLICITLY OUTSIDE OF THE CRACK.  NEXT THE ¤Y¤ AND THEN THE ¤Z¤
C     DIRECTION FLOW IS FOUND IMPLICITLY.  WITHIN THE CRACK AN OPERATOR
C     SPLITTING METHOD IS USED BECAUSE THE GOVERNING EQUATION IS
C     HYPERBOLIC IN ¤X¤ AND PARABOLIC IN ¤Y¤ AND ¤Z¤.  AN ALTERNATING
C     DIRECTION IMPLICIT METHOD IS USED WHEN THE GOVERNING EQUATION
C     IS PARABOLIC.
C
      COMMON /CRACK/ AF(10,15,20),AFF(10,15,20),BB(10,15,20),BETA(1,15,2
     10),CDEF,CFRIC1,CFRIC2,CKX(15,20),CKYZ(15,20),CSUBG(3,3),D(15,20),D
     2D(10,15,20),DELTA(1,15,20),DT,DTOT(15,20),DT2,DX(10),DY,DY2,DZ,DZ2
     3,EE(10,15,20),EFFTIP,ETA(10,15,20),F(10,15,20),FF(10,15,20),FMAX,F
     4STAR(10,15,20),FSSTAR(10,15,20),GAMMA(1,15,20),IO,JSTOP(20),L,LM1,
     5LM2,L2,M,MM1,MM2,M2,N,NM1,NM2,NTTOT,NYTIP(15),P(10,15,20),PR,PRFUN
     6,PS(60),REYNC(15,20),SIZE,SPACE(15,20),THETA,THETA1,X(10),XKX,XLAM
     7B(20,30),YKY,ZETA(1,15,20),ZKZ
C
C     INITIALIZE VALUES
C
      ITERX=0
      ITERY=0
      ITERZ=0
      ITERT=0
      DO 1 K=1,N
      DO 1 J=1,M
      DO 1 I=1,L
      FSTAR(I,J,K)=F(I,J,K)
      AFF(I,J,K)=F(I,J,K)
    1 CONTINUE
C
C     ¤X¤ DIRECTION EXPLICIT -- USED FOR ¤X¤ NODE EQUAL TO ONE AND
C     INSIDE THE CRACK.  AN OPERATOR SPLITTING METHOD IS USED WHERE IN
C     THE ¤X¤ DIRECTION ONLY THE ¤X¤ COMPONENT EXPLICIT SPATIAL
C     DERIVATIVE AND THE TIME DERIVATIVE ARE CONSIDERED IN THE GOVERNING
C     EQUATION.  LATER IN THE ¤Y¤ AND ¤Z¤ DIRECTIONS AN ALTERNATING
C     DIRECTION IMPLICIT METHOD IS USED WHERE NO ¤X¤ DIRECTION SPATIAL
C     DERIVATIVES ARE PRESENT IN THE BASIC GOVERNING EQUATION.  THE
C     EXPLICIT TIME STEP IS SET EQUAL TO THE IMPLICIT TIME STEP DIVIDED
C     BY NTTOT.
C
      DTDX=DT/(DX(2)*NTTOT)
      DO 5 ITIME=1,NTTOT
      DO 4 K=1,NM1
      DO 3 J=1,M
      IF (DTOT(J,K).LE.0.) GO TO 3
      IF (J.LE.M2.AND.K.EQ.1) GO TO 3
      F(1,J,K)=FSTAR(1,J,K)
      ITERXX=0
    2 ETA(1,J,K)=0.5*(THETA/SQRT(FSTAR(1,J,K)+PRFUN)+THETA1/SQRT(F(1,J,K
     1)+PRFUN))
      FSTAR(1,J,K)=CKX(J,K)*DTDX*(F(2,J,K)-F(1,J,K))/ETA(1,J,K)+F(1,J,K)
      ITERXX=ITERXX+1
      IF (ITERXX.LT.1) GO TO 2
    3 CONTINUE
      IF (DTOT(1,K).LE.0.) K=N
    4 CONTINUE
```

```
721  5     CONTINUE
722 C
723 C      ITERATE THROUGH COMPLETE IMPLICIT CALCULATION (X,Y, AND Z
724 C      DIRECTIONS) UPDATING THE COEFFICIENTS UNTIL CONVERGENCE IS
725 C      REACHED.  ALSO ITERATE THROUGH EACH DIRECTION SEPARATELY.
726 C
727 C      ¤X¤ DIRECTION IMPLICIT -- USED FOR REGIONS OUTSIDE THE CRACK
728 C
729 C
730 C      CALCULATE COEFFICIENTS FOR ¤Z¤ NODE BETWEEN 2 AND NM1 UTILIZING A
731 C      WEIGHTED AVERAGE BETWEEN OLD AND NEW VALUES OF F(I,J,K).
732 C      CALCULATE FOR ¤X¤ NODES BETWEEN 2 AND LM1 WITH ¤Y¤ NODES BETWEEN 1
733 C      AND M.  IN CALCULATING ¤Y¤ BOUNDARY NODES, USE THE NEUMANN
734 C      CONDITION IN THE ¤Y¤ DIRECTION (DF(I,1,K)/DY=0. OR
735 C      DF(I,M,K)/DY=0.).
736 C
737  6     DO 9 K=2,NM1
738 C
739 C      INTERNAL NODES
740 C
741           DO 7 J=2,MM1
742           DO 7 I=2,LM1
743           ETA(I,J,K)=THETA/SQRT(FSTAR(I,J,K)+PRFUN)+THETA1/SQRT(F(I,J,K)+PRF
744          1UN)
745           BB(I,J,K)=2.*XKX/(DX(I+1)*DX(I))+ETA(I,J,K)/DT2
746           DD(I,J,K)=(YKY*(F(I,J+1,K)-2.*F(I,J,K)+F(I,J-1,K))/DY2+ZKZ*(F(I,J,
747          1K+1)-2.*F(I,J,K)+F(I,J,K-1))/DZ2+ETA(I,J,K)*F(I,J,K)/DT2)
748  7     CONTINUE
749 C
750 C      ¤Y¤ NODE EQUAL TO ¤M¤
751 C
752           DO 8 I=2,LM1
753           ETA(I,M,K)=THETA/SQRT(FSTAR(I,M,K)+PRFUN)+THETA1/SQRT(F(I,M,K)+PRF
754          1UN)
755           BB(I,M,K)=2.*XKX/(DX(I+1)*DX(I))+ETA(I,M,K)/DT2
756           DD(I,M,K)=(YKY*2.*(F(I,M-1,K)-F(I,M,K))/DY2+ZKZ*(F(I,M,K+1)-2.*F(I
757          1,M,K)+F(I,M,K-1))/DZ2+ETA(I,M,K)*F(I,M,K)/DT2)
758 C
759 C      ¤Y¤ NODE EQUAL TO 1
760 C
761           ETA(I,1,K)=THETA/SQRT(FSTAR(I,1,K)+PRFUN)+THETA1/SQRT(F(I,1,K)+PRF
762          1UN)
763           BB(I,1,K)=2.*XKX/(DX(I+1)*DX(I))+ETA(I,1,K)/DT2
764           DD(I,1,K)=(YKY*2.*(F(I,2,K)-F(I,1,K))/DY2+ZKZ*(F(I,1,K+1)-2.*F(I,1
765          1,K)+F(I,1,K-1))/DZ2+ETA(I,1,K)*F(I,1,K)/DT2)
766  8     CONTINUE
767  9     CONTINUE
768 C
769 C      CALCULATE COEFFICIENTS FOR ¤Z¤ DIRECTION NODE EQUAL TO ONE.  USE
770 C      THE NEUMANN CONDITION (DF(I,J,1)/DZ=0.) IN ¤Z¤ DIRECTION OUTSIDE
771 C      THE REGION WHERE F(I,J,1) IS SPECIFIED AS INPUT.  CALCULATE ONLY
772 C      WHERE F(I,J,1) IS NOT SPECIFIED AS INPUT.
773 C
774           IF (L.EQ.L2.AND.M.EQ.M2) GO TO 12
775 C
776 C      INTERNAL NODES
777 C
778           DO 10 J=2,MM1
779           DO 10 I=2,LM1
780           IF (I.LE.L2.AND.J.LE.M2) GO TO 10
```

```
781         ETA(I,J,1)=THETA/SQRT(FSTAR(I,J,1)+PRFUN)+THETA1/SQRT(F(I,J,1)+PRF
782        1UN)
783         BB(I,J,1)=2.*XKX/(DX(I+1)*DX(I))+ETA(I,J,1)/DT2
784         DD(I,J,1)=(YKY*(F(I,J+1,1)-2.*F(I,J,1)+F(I,J-1,1))/DY2+ZKZ*2.*(F(I
785        1,J,2)-F(I,J,1))/DZ2+ETA(I,J,1)*F(I,J,1)/DT2)
786   10    CONTINUE
787 C
788 C       ¤Y¤ NODE EQUAL TO ¤M¤
789 C
790         DO 11 I=2,LM1
791         IF (I.LE.L2.AND.M.EQ.M2) GO TO 11
792         ETA(I,M,1)=THETA/SQRT(FSTAR(I,M,1)+PRFUN)+THETA1/SQRT(F(I,M,1)+PRF
793        1UN)
794         BB(I,M,1)=2.*XKX/(DX(I+1)*DX(I))+ETA(I,M,1)/DT2
795         DD(I,M,1)=(YKY*2.*(F(I,M-1,1)-F(I,M,1))/DY2+ZKZ*2.*(F(I,M,2)-F(I,M
796        1,1))/DZ2+ETA(I,M,1)*F(I,M,1)/DT2)
797 C
798 C       ¤Y¤ NODE EQUAL TO 1
799 C
800         IF (I.LE.L2) GO TO 11
801         ETA(I,1,1)=THETA/SQRT(FSTAR(I,1,1)+PRFUN)+THETA1/SQRT(F(I,1,1)+PRF
802        1UN)
803         BB(I,1,1)=2.*XKX/(DX(I+1)*DX(I))+ETA(I,1,1)/DT2
804         DD(I,1,1)=(YKY*2.*(F(I,2,1)-F(I,1,1))/DY2+ZKZ*2.*(F(I,1,2)-F(I,1,1
805        1))/DZ2+ETA(I,1,1)*F(I,1,1)/DT2)
806   11    CONTINUE
807 C
808 C       CALCULATE EE(I,J,K) AND FF(I,J,K) FOR ¤X¤ NODES BETWEEN 1 AND LM1.
809 C       USE THE DIRICHLET CONDITION (FSTAR(I,J,K) IS OBTAINED FROM THE
810 C       EXPLICIT CALCULATIONS) FOR I=1 IF INSIDE THE CRACK.  USE THE
811 C       NEUMANN CONDITION FOR I=1 OUTSIDE THE CRACK (DF(1,J,K)/DX=0.).
812 C       USE THE RECURSION RELATIONSHIP FOR ALL OTHER ¤X¤ NODES.  IF THE
813 C       ¤Z¤ NODE EQUALS 1, VALUES ARE CALCULATED ONLY OUTSIDE THE REGION
814 C       WHERE F(I,J,1) IS SPECIFIED AS INPUT.
815 C
816 C       CALCULATIONS FOR ¤Z¤ NODE BETWEEN 2 AND NM1
817 C
818   12    DO 16 K=2,NM1
819         DO 16 J=1,M
820 C
821 C       INSIDE THE CRACK
822 C
823         IF (DTOT(J,K).LE.0.) GO TO 13
824         EE(1,J,K)=0.
825         FF(1,J,K)=FSTAR(1,J,K)
826         GO TO 14
827 C
828 C       OUTSIDE THE CRACK WITH I=1
829 C
830   13    EE(1,J,K)=1.
831         FF(1,J,K)=0.
832 C
833 C       ALL OTHER REGIONS
834 C
835   14    DO 15 I=2,LM1
836         DEN=BB(I,J,K)-2.*XKX*EE(I-1,J,K)/(DX(I)*(DX(I+1)+DX(I)))
837         EE(I,J,K)=2.*XKX/(DX(I+1)*(DX(I+1)+DX(I))*DEN)
838         FF(I,J,K)=(DD(I,J,K)+2.*XKX*FF(I-1,J,K)/(DX(I)*(DX(I+1)+DX(I))))/D
839        1EN
840   15    CONTINUE
```

```
 16   CONTINUE
C
C     CALCULATIONS FOR ¤Z¤ NODE EQUAL TO 1
C
      DO 21 J=1,M
      IF (J.LE.M2) GO TO 18
      IF (DTOT(J,1).LE.0.) GO TO 17
C
C     INSIDE THE CRACK
C
      EE(1,J,1)=0.
      FF(1,J,1)=FSTAR(1,J,1)
      GO TO 19
C
C     OUTSIDE THE CRACK WITH I=1
C
 17   EE(1,J,1)=1.
      FF(1,J,1)=0.
      GO TO 19
C
C     ALL OTHER REGIONS
C
 18   EE(L2,J,1)=0.
      FF(L2,J,1)=F(L2,J,1)
 19   DO 20 I=2,LM1
      IF (I.LE.L2.AND.J.LE.M2) GO TO 21
      DEN=BB(I,J,1)-2.*XKX*EE(I-1,J,1)/(DX(I)*(DX(I+1)+DX(I)))
      EE(I,J,1)=2.*XKX/(DX(I+1)*(DX(I+1)+DX(I))*DEN)
      FF(I,J,1)=(DD(I,J,1)+2.*XKX*FF(I-1,J,1)/(DX(I)*(DX(I+1)+DX(I))))/D
     1EN
 20   CONTINUE
 21   CONTINUE
C
C     CALCULATE FSTAR(I,J,K) -- AN INTERMEDIATE VALUE OF F(I,J,K) AFTER
C     COMPLETION OF THE ¤X¤ DIRECTION IMPLICIT CALCULATIONS.  AT ¤X¤
C     NODE EQUAL TO L USE A NEUMANN CONDITION (DFSTAR(L,J,K)/DX=0.) AND
C     THEN USE THE RECURSION RELATIONSHIP FOR VALUES TO ¤X¤ NODE EQUAL
C     TO 2.  FSTAR WAS SET PREVIOUSLY EQUAL TO THE VALUE CALCULATED
C     EXPLICITLY IF IN THE CRACK.  USE THE NEUMANN CONDITION FOR I=1 IF
C     OUTSIDE THE CRACK.  IF THE ¤Z¤ NODE IS EQUAL TO 1, SET FSTAR(I,J,1)
C     EQUAL TO F(I,J,1) IN THE REGION WHERE F(I,J,1) IS SPECIFIED AS
C     INPUT.  COMPARE VALUES OF FSTAR(I,J,K) WITH PREVIOUS VALUES AND
C     ITERATE THROUGH THE ¤X¤ DIRECTION IMPLICIT CALCULATIONS IF
C     CONVERGENCE IS NOT OBTAINED.
C
C     CALCULATIONS FOR ¤Z¤ NODE BETWEEN 2 AND NM1
C
      IX=0
      DO 24 K=2,NM1
      DO 24 J=1,M
      PFSTAR=FSTAR(L,J,K)
      FSTAR(L,J,K)=FF(LM1,J,K)/(1.-EE(LM1,J,K))
      COMPARE=ABS(FSTAR(L,J,K)-PFSTAR)/PFSTAR
      IF (COMPARE.LT.0.001.OR.FSTAR(L,J,K).EQ.PFSTAR) GO TO 22
      IX=IX+1
C
C     INTERNAL NODES
C
 22   DO 23 I=1,LM2
      LB=L-I
```

```
      PFSTAR=FSTAR(LB,J,K)
      FSTAR(LB,J,K)=EE(LB,J,K)*FSTAR(LB+1,J,K)+FF(LB,J,K)
      COMPARE=ABS(FSTAR(LB,J,K)-PFSTAR)/PFSTAR
      IF (COMPARE.LT.0.001.OR.FSTAR(LB,J,K).EQ.PFSTAR) GO TO 23
      IX=IX+1
 23   CONTINUE
C
C     OUTSIDE THE CRACK WITH I=1
C
      IF (DTOT(J,K).LE.0.) FSTAR(1,J,K)=FSTAR(2,J,K)
 24   CONTINUE
C
C     CALCULATIONS FOR ¤Z¤ NODE EQUAL TO 1
C
      DO 27 J=1,M
      IF (L.EQ.L2.AND.J.LE.M2) GO TO 25
      PFSTAR=FSTAR(L,J,1)
      FSTAR(L,J,1)=FF(LM1,J,1)/(1.-EE(LM1,J,1))
      COMPARE=ABS(FSTAR(L,J,1)-PFSTAR)/PFSTAR
      IF (COMPARE.LT.0.001.OR.FSTAR(L,J,1).EQ.PFSTAR) GO TO 25
      IX=IX+1
 25   DO 26 I=1,LM2
      LB=L-I
      IF (LB.LE.L2.AND.J.LE.M2) GO TO 26
      PFSTAR=FSTAR(LB,J,1)
      FSTAR(LB,J,1)=EE(LB,J,1)*FSTAR(LB+1,J,1)+FF(LB,J,1)
      COMPARE=ABS(FSTAR(LB,J,1)-PFSTAR)/PFSTAR
      IF (COMPARE.LT.0.001.OR.FSTAR(LB,J,1).EQ.PFSTAR) GO TO 26
      IX=IX+1
 26   CONTINUE
C
C     OUTSIDE THE CRACK WITH I=1
C
      IF (DTOT(J,1).LE.0.) FSTAR(1,J,1)=FSTAR(2,J,1)
 27   CONTINUE
      IF (IX.EQ.0) GO TO 28
      ITERX=ITERX+1
      IF (ITERX.LT.2) GO TO 6
C
C     ¤Y¤ DIRECTION IMPLICIT -- USED FOR ALL REGIONS
C
C
C     CALCULATE COEFFICIENTS FOR ¤Z¤ NODES BETWEEN 2 AND NM1 UTILIZING A
C     WEIGHTED AVERAGE BETWEEN OLD AND NEW VALUES OF F(I,J,K).  INSIDE
C     THE CRACK THE OLD VALUES ARE FSTAR(I,J,K) AND THE NEW VALUES ARE
C     FSSTAR(I,J,K).  OUTSIDE THE CRACK THE NEW VALUES ARE FSSTAR(I,J,K)
C     AND THE OLD VALUES ARE F(I,J,K).  CALCULATE FOR ¤Y¤ NODES BETWEEN
C     2 AND MM1 WITH ¤X¤ NODES BETWEEN 1 AND L.  IN CALCULATING THE ¤X¤
C     DIRECTION BOUNDARY NODES USE THE NEUMANN CONDITION OUTSIDE OF THE
C     CRACK IN THE ¤X¤ DIRECTION (DFSTAR(I,J,K)/DX=0. OR
C     DFSTAR(L,J,K)/DX=0.).  INSIDE THE CRACK THE OPERATOR SPLITTING
C     TECHNIQUE UTILIZED DOES NOT CONSIDER ANY ¤X¤ DIRECTION VARIATION.
C
 28   DO 29 I=1,L
      DO 29 J=1,M
      DO 29 K=1,NM1
      FSSTAR(I,J,K)=FSTAR(I,J,K)
 29   CONTINUE
 30   DO 38 K=2,NM1
      DO 38 J=2,MM1
```

```
C
C      ¤X¤ DIRECTION NODE EQUAL TO ONE
C
       IF (DTOT(J,K).GT.0.) GO TO 31
C
C      OUTSIDE THE CRACK
C
       ETA(I,J,K)=THETA/SQRT(FSSTAR(I,J,K)+PRFUN)+THETA1/SQRT(F(I,J,K)+PR
      1FUN)
       BB(I,J,K)=2.*YKY+DY2*ETA(I,J,K)/DT2
       DD(I,J,K)=(2.*XKX*(FSTAR(2,J,K)-FSTAR(1,J,K))/(DX(2)*DX(2))+ZKZ*(F
      1(I,J,K+1)-2.*F(I,J,K)+F(I,J,K-1))/DZ2+ETA(I,J,K)*F(I,J,K)/DT2)*DY2
       GO TO 36
C
C      INSIDE THE CRACK
C
   31  B1=0.
       B2=0.
       G1=0.
       G2=0.
       D1=0.
       D2=0.
       Z1=0.
       Z2=0.
       IF (ABS(FSSTAR(I,J+1,K)-FSSTAR(I,J-1,K)).LT.1.E-25) GO TO 32
       B1=THETA*(FSSTAR(I,J+1,K)-FSSTAR(I,J-1,K))/SQRT(2.*DY*ABS(FSSTAR(I
      1,J+1,K)-FSSTAR(I,J-1,K)))
       G1=THETA/SQRT(2.*ABS(FSSTAR(I,J+1,K)-FSSTAR(I,J-1,K))/DY)
   32  IF (ABS(FSTAR(I,J+1,K)-FSTAR(I,J-1,K)).LT.1.E-25) GO TO 33
       B2=THETA1*(FSTAR(I,J+1,K)-FSTAR(I,J-1,K))/SQRT(2.*DY*ABS(FSTAR(I,J
      1+1,K)-FSTAR(I,J-1,K)))
       G2=THETA1/SQRT(2.*ABS(FSTAR(I,J+1,K)-FSTAR(I,J-1,K))/DY)
   33  BETA(I,J,K)=B1+B2
       GAMMA(I,J,K)=CKYZ(J,K)*(G1+G2)
       IF (ABS(FSSTAR(I,J,K+1)-FSSTAR(I,J,K-1)).LT.1.E-25) GO TO 34
       D1=THETA*(FSSTAR(I,J,K+1)-FSSTAR(I,J,K-1))/SQRT(2.*DZ*ABS(FSSTAR(I
      1,J,K+1)-FSSTAR(I,J,K-1)))
       Z1=THETA/SQRT(2.*ABS(FSSTAR(I,J,K+1)-FSSTAR(I,J,K-1))/DZ)
   34  IF (ABS(FSTAR(I,J,K+1)-FSTAR(I,J,K-1)).LT.1.E-25) GO TO 35
       D2=THETA1*(FSTAR(I,J,K+1)-FSTAR(I,J,K-1))/SQRT(2.*DZ*ABS(FSTAR(I,J
      1,K+1)-FSTAR(I,J,K-1)))
       Z2=THETA1/SQRT(2.*ABS(FSTAR(I,J,K+1)-FSTAR(I,J,K-1))/DZ)
   35  DELTA(I,J,K)=D1+D2
       ZETA(I,J,K)=CKYZ(J,K)*(Z1+Z2)
       ETA(I,J,K)=0.5*(THETA/SQRT(FSSTAR(I,J,K)+PRFUN)+THETA1/SQRT(FSTAR(
      1I,J,K)+PRFUN))
       BB(I,J,K)=2.*GAMMA(I,J,K)+DY2*ETA(I,J,K)/DT2
       DD(I,J,K)=(0.5*BETA(I,J,K)*(CKYZ(J+1,K)-CKYZ(J-1,K))/DY+0.5*DELTA(
      1I,J,K)*(CKYZ(J,K+1)-CKYZ(J,K-1))/DZ+ZETA(I,J,K)*(FSTAR(I,J,K+1)-2.
      2*FSTAR(I,J,K)+FSTAR(I,J,K-1))/DZ2+ETA(I,J,K)*FSTAR(I,J,K)/DT2)*DY2
C
C      INTERNAL NODES
C
   36  DO 37 I=2,LM1
       ETA(I,J,K)=THETA/SQRT(FSSTAR(I,J,K)+PRFUN)+THETA1/SQRT(F(I,J,K)+PR
      1FUN)
       BB(I,J,K)=2.*YKY+DY2*ETA(I,J,K)/DT2
       DD(I,J,K)=(2.*XKX*((FSTAR(I+1,J,K)-FSTAR(I,J,K))/DX(I+1)-(FSTAR(I,
      1J,K)-FSTAR(I-1,J,K))/DX(I))/(DX(I+1)+DX(I))+ZKZ*(F(I,J,K+1)-2.*F(I
      2,J,K)+F(I,J,K-1))/DZ2+ETA(I,J,K)*F(I,J,K)/DT2)*DY2
```

```
 1021   37    CONTINUE
 1022 C
 1023 C       αxα NODE EQUAL TO αLα
 1024 C
 1025         ETA(L,J,K)=THETA/SQRT(FSSTAR(L,J,K)+PRFUN)*THETA1/SQRT(F(L,J,K)+PR
 1026        1FUN)
 1027         BB(L,J,K)=2.*YKY*DY2*ETA(L,J,K)/DT2
 1028         DD(L,J,K)=(XKX*2.*(FSTAR(LM1,J,K)-FSTAR(L,J,K)))/(DX(L)*DX(L))*ZKZ*
 1029        1(F(L,J,K+1)-2.*F(L,J,K)+F(L,J,K-1))/DZ2*ETA(L,J,K)*F(L,J,K)/DT2)*D
 1030        2Y2
 1031   38    CONTINUE
 1032 C
 1033 C       CALCULATE COEFFICIENTS FOR αZα DIRECTION NODE EQUAL TO ONE.  USE
 1034 C       THE NEUMANN CONDITION (DFSTAR(I,J,1)/DZ=0.) IN THE αZα DIRECTION
 1035 C       OUTSIDE THE REGION WHERE F(I,J,1) IS SPECIFIED AS INPUT.
 1036 C       CALCULATE ONLY WHERE F(I,J,1) IS NOT SPECIFIED AS INPUT.
 1037 C
 1038         IF (L.EQ.L2.AND.M.EQ.M2) GO TO 47
 1039         DO 46 J=2,MM1
 1040 C
 1041 C       αxα NODE EQUAL TO 1
 1042 C
 1043         IF (J.LE.M2) GO TO 44
 1044         IF (DTOT(J,1).GT.0.) GO TO 39
 1045 C
 1046 C       OUTSIDE THE CRACK
 1047 C
 1048         ETA(1,J,1)=THETA/SQRT(FSSTAR(1,J,1)+PRFUN)*THETA1/SQRT(F(1,J,1)+PR
 1049        1FUN)
 1050         BB(1,J,1)=2.*YKY*DY2*ETA(1,J,1)/DT2
 1051         DD(1,J,1)=(2.*XKX*(FSTAR(2,J,1)-FSTAR(1,J,1))/(DX(2)*DX(2))*ZKZ*2
 1052        1*(F(1,J,2)-F(1,J,1))/DZ2*ETA(1,J,1)*F(1,J,1)/DT2)*DY2
 1053         GO TO 44
 1054 C
 1055 C       INSIDE THE CRACK
 1056 C
 1057   39    B1=0.
 1058         B2=0.
 1059         G1=0.
 1060         G2=0.
 1061         D1=0.
 1062         D2=0.
 1063         Z1=0.
 1064         Z2=0.
 1065         IF (ABS(FSSTAR(1,J+1,1)-FSSTAR(1,J-1,1)).LT.1.E-25) GO TO 40
 1066         B1=THETA*(FSSTAR(1,J+1,1)-FSSTAR(1,J-1,1))/SQRT(2.*DY*ABS(FSSTAR(1
 1067        1,J+1,1)-FSSTAR(1,J-1,1)))
 1068         G1=THETA/SQRT(ABS(2.*FSSTAR(1,J+1,1)-FSSTAR(1,J-1,1))/DY)
 1069   40    IF (ABS(FSTAR(1,J+1,1)-FSTAR(1,J-1,1)).LT.1.E-25) GO TO 41
 1070         B2=THETA1*(FSTAR(1,J+1,1)-FSTAR(1,J-1,1))/SQRT(2.*DY*ABS(FSTAR(1,J
 1071        1+1,1)-FSTAR(1,J-1,1)))
 1072         G2=THETA1/SQRT(2.*ABS(FSTAR(1,J+1,1)-FSTAR(1,J-1,1))/DY)
 1073   41    BETA(1,J,1)=B1+B2
 1074         GAMMA(1,J,1)=CKYZ(J,1)*(G1+G2)
 1075         IF (ABS(FSSTAR(1,J,2)-FSSTAR(1,J,1)).LT.1.E-25) GO TO 42
 1076         D1=THETA*(FSSTAR(1,J,2)-FSSTAR(1,J,1))/SQRT(DZ*ABS(FSSTAR(1,J,2)-F
 1077        1SSTAR(1,J,1)))
 1078         Z1=THETA/SQRT(ABS(FSSTAR(1,J,2)-FSSTAR(1,J,1))/DZ)
 1079   42    IF (ABS(FSTAR(1,J,2)-FSTAR(1,J,1)).LT.1.E-25) GO TO 43
 1080         D2=THETA1*(FSTAR(1,J,2)-FSTAR(1,J,1))/SQRT(DZ*ABS(FSTAR(1,J,2)-FST
```

```
     1AR(I,J,1)))
      Z2=THETA1/SQRT(ABS(FSTAR(I,J,2)-FSTAR(I,J,1))/DZ)
 43   DELTA(I,J,1)=D1+D2
      ZETA(I,J,1)=0.5*CKYZ(J,1)*(Z1+Z2)
      ETA(I,J,1)=0.5*(THETA/SQRT(FSSTAR(I,J,1)+PRFUN)+THETA1/SQRT(FSTAR(
     11,J,1)+PRFUN))
      BB(I,J,1)=2.*GAMMA(I,J,1)+DY2*ETA(I,J,1)/DT2
      DD(I,J,1)=(0.5*BETA(I,J,1)*(CKYZ(J+1,1)-CKYZ(J-1,1))/DY+DELTA(I,J,
     11)*(CKYZ(J,2)-CKYZ(J,1))/DZ+ZETA(I,J,1)*2.*(FSTAR(I,J,2)-FSTAR(I,J
     2,1))/DZ2+ETA(I,J,1)*FSTAR(I,J,1)/DT2)*DY2
 44   DO 45 I=2,LM1
      IF (I.LE.L2.AND.J.LE.M2) GO TO 45
C
C     INTERNAL NODES
C
      ETA(I,J,1)=THETA/SQRT(FSSTAR(I,J,1)+PRFUN)+THETA1/SQRT(F(I,J,1)+PR
     1FUN)
      BB(I,J,1)=2.*YKY+DY2*ETA(I,J,1)/DT2
      DD(I,J,1)=(2.*XKX*((FSTAR(I+1,J,1)-FSTAR(I,J,1))/DX(I+1)-(FSTAR(I,
     1J,1)-FSTAR(I-1,J,1))/DX(I))/(DX(I+1)+DX(I))+ZKZ*2.*(F(I,J,2)-F(I,J
     2,1))/DZ2+ETA(I,J,1)*F(I,J,1)/DT2)*DY2
 45   CONTINUE
C
C     ¤X¤ NODE EQUAL TO ¤L¤
C
      IF (L.EQ.L2.AND.J.LE.M2) GO TO 46
      ETA(L,J,1)=THETA/SQRT(FSSTAR(L,J,1)+PRFUN)+THETA1/SQRT(F(L,J,1)+PR
     1FUN)
      BB(L,J,1)=2.*YKY+DY2*ETA(L,J,1)/DT2
      DD(L,J,1)=(XKX*2.*(FSTAR(LM1,J,1)-FSTAR(L,J,1))/(DX(L)*DX(L))+ZKZ*
     12.*(F(L,J,2)-F(L,J,1))/DZ2+ETA(L,J,1)*F(L,J,1)/DT2)*DY2
 46   CONTINUE
C
C     CALCULATE EE(I,J,K) AND FF(I,J,K) FOR ¤Y¤ NODES BETWEEN 1 AND MM1.
C     USE THE NEUMANN CONDITION FOR J=1 (DFSTAR(I,1,K)/DY=0.).  USE THE
C     RECURSION RELATIONSHIP FOR ALL OTHER ¤Y¤ NODES.  IF THE ¤Z¤ NODE
C     EQUALS 1, VALUES ARE CALCULATED ONLY OUTSIDE THE REGION WHERE
C     F(I,J,1) IS SPECIFIED AS INPUT.  THE DIRICHLET CONDITION IS USED
C     AT THE BOUNDARY OF THE REGION WHERE THE INPUT IS SPECIFIED
C     (FSSTAR(I,J,1)=F(I,J,1)).
C
 47   DO 49 K=2,NM1
      DO 49 I=1,L
      EE(I,1,K)=1.
      FF(I,1,K)=0.
      DO 49 J=2,MM1
      IF (DTOT(J,K).GT.0..AND.I.EQ.1) GO TO 48
C
C     OUTSIDE THE CRACK
C
      DEN=BB(I,J,K)-YKY*EE(I,J-1,K)
      EE(I,J,K)=YKY/DEN
      FF(I,J,K)=(DD(I,J,K)+YKY*FF(I,J-1,K))/DEN
      GO TO 49
C
C     INSIDE CRACK
C
 48   DEN=BB(I,J,K)-GAMMA(I,J,K)*EE(I,J-1,K)
      EE(I,J,K)=GAMMA(I,J,K)/DEN
      FF(I,J,K)=(DD(I,J,K)+GAMMA(I,J,K)*FF(I,J-1,K))/DEN
```

```
 49   CONTINUE
C
C     CALCULATIONS FOR ¤Z¤ NODE EQUAL TO 1
C
      DO 53 I=1,L
      IF (I.LE.L2) GO TO 50
      EE(I,1,1)=1.
      FF(I,1,1)=0.
      GO TO 51
 50   EE(I,M2,1)=0.
      FF(I,M2,1)=F(I,M2,1)
 51   DO 53 J=2,MM1
      IF (I.LE.L2.AND.J.LE.M2) GO TO 53
      IF (DTOT(J,1).GT.0..AND.I.EQ.1) GO TO 52
C
C     OUTSIDE CRACK
C
      DEN=BB(I,J,1)-YKY*EE(I,J-1,1)
      EE(I,J,1)=YKY/DEN
      FF(I,J,1)=(DD(I,J,1)+YKY*FF(I,J-1,1))/DEN
      GO TO 53
C
C     INSIDE CRACK
C
 52   DEN=BB(I,J,1)-GAMMA(I,J,1)*EE(I,J-1,1)
      EE(I,J,1)=GAMMA(I,J,1)/DEN
      FF(I,J,1)=(DD(I,J,1)+GAMMA(I,J,1)*FF(I,J-1,1))/DEN
 53   CONTINUE
C
C     CALCULATE FSSTAR(I,J,K) -- THE SECOND INTERMEDIATE VALUE OF
C     F(I,J,K) AFTER COMPLETION OF ¤Y¤ DIRECTION IMPLICIT CALCULATIONS.
C     USE A NEUMANN CONDITION IF THE ¤Y¤ NODE IS EQUAL TO M
C     (DFSSTAR(I,M,K)/DY=0.) AND THEN USE THE RECURSION RELATIONSHIP
C     FOR VALUES TO ¤Y¤ NODE EQUAL TO 2.  IF ¤Z¤ NODE EQUALS 1 SET
C     FSSTAR(I,J,1) EQUAL TO F(I,J,1) IN THE REGION WHERE F(I,J,1) IS
C     SPECIFIED AS INPUT.  COMPARE VALUES OF FSSTAR(I,J,K) WITH PREVIOUS
C     VALUES AND ITERATE THROUGH THE ¤Y¤ DIRECTION IMPLICIT CALCULATIONS
C     IF CONVERGENCE IS NOT OBTAINED.
C
C     CALCULATIONS FOR ¤Z¤ NODE BETWEEN 2 AND NM1
C
      IY=0
      DO 56 K=2,NM1
      DO 56 I=1,L
      PFSSTAR=FSSTAR(I,M,K)
      FSSTAR(I,M,K)=FF(I,MM1,K)/(1.-EE(I,MM1,K))
      COMPARE=ABS(FSSTAR(I,M,K)-PFSSTAR)/PFSSTAR
      IF (COMPARE.LT.0.001.OR.FSSTAR(I,M,K).EQ.PFSSTAR) GO TO 54
      IY=IY+1
C
C     INTERNAL NODES
C
 54   DO 55 J=1,MM2
      MB=M-J
      PFSSTAR=FSSTAR(I,MB,K)
      FSSTAR(I,MB,K)=EE(I,MB,K)*FSSTAR(I,MB+1,K)+FF(I,MB,K)
      COMPARE=ABS(FSSTAR(I,MB,K)-PFSSTAR)/PFSSTAR
      IF (COMPARE.LT.0.001.OR.FSSTAR(I,MB,K).EQ.PFSSTAR) GO TO 55
      IY=IY+1
 55   CONTINUE
```

```
1201          FSSTAR(I,1,K)=FSSTAR(I,2,K)
1202    56    CONTINUE
1203  C
1204  C       CALCULATIONS FOR ¤Z¤ NODE EQUAL TO 1
1205  C
1206          DO 59 I=1,L
1207          IF (I.LE.L2.AND.M.EQ.M2) GO TO 59
1208          PFSSTAR=FSSTAR(I,M,1)
1209          FSSTAR(I,M,1)=FF(I,MM1,1)/(1.-EE(I,MM1,1))
1210          COMPARE=ABS(FSSTAR(I,M,1)-PFSSTAR)/PFSSTAR
1211          IF (COMPARE.LT.0.001.OR.FSSTAR(I,M,1).EQ.PFSSTAR) GO TO 57
1212          IY=IY+1
1213    57    DO 58 J=1,MM2
1214          MB=M-J
1215          IF (I.LE.L2.AND.MB.LE.M2) GO TO 59
1216          PFSSTAR=FSSTAR(I,MB,1)
1217          FSSTAR(I,MB,1)=EE(I,MB,1)*FSSTAR(I,MB+1,1)+FF(I,MB,1)
1218          COMPARE=ABS(FSSTAR(I,MB,1)-PFSSTAR)/PFSSTAR
1219          IF (COMPARE.LT.0.001.OR.FSSTAR(I,MB,1).EQ.PFSSTAR) GO TO 58
1220          IY=IY+1
1221    58    CONTINUE
1222          IF (I.LE.L2) GO TO 59
1223          FSSTAR(I,1,1)=FSSTAR(I,2,1)
1224    59    CONTINUE
1225          IF (IY.EQ.0) GO TO 60
1226          ITERY=ITERY+1
1227          IF (ITERY.LT.2) GO TO 30
1228  C
1229  C       ¤Z¤ DIRECTION IMPLICIT -- USED FOR ALL REGIONS
1230  C
1231  C
1232  C       CALCULATE COEFFICIENTS FOR ¤Z¤ NODES BETWEEN 2 AND NM1 UTILIZING
1233  C       WEIGHTED AVERAGE BETWEEN OLD AND NEW VALUES OF F(I,J,K).  THE OLD
1234  C       VALUES ARE FSSTAR(I,J,K) AND THE NEW VALUES ARE AF(I,J,K) BOTH
1235  C       INSIDE AND OUTSIDE THE CRACK.  CALCULATE FOR ¤Y¤ NODES BETWEEN 1
1236  C       AND M WITH ¤X¤ NODES BETWEEN 1 AND L.  BOUNDARY NODES USE THE
1237  C       NEUMANN CONDITION IN BOTH ¤X¤ AND ¤Y¤ DIRECTIONS.
1238  C
1239    60    DO 61 I=1,L
1240          DO 61 J=1,M
1241          DO 61 K=1,NM1
1242          AF(I,J,K)=FSSTAR(I,J,K)
1243    61    CONTINUE
1244    62    DO 78 K=2,NM1
1245  C
1246  C       ¤X¤ DIRECTION NODE EQUAL TO ONE
1247  C
1248          DO 68 J=2,MM1
1249          IF (DTOT(J,K).GT.0.) GO TO 63
1250  C
1251  C       OUTSIDE THE CRACK
1252  C
1253          ETA(I,J,K)=THETA/SQRT(AF(I,J,K)+PRFUN)+THETA1/SQRT(FSSTAR(I,J,K)+P
1254         1RFUN)
1255          BB(I,J,K)=2.*ZKZ+DZ2*ETA(I,J,K)/DT2
1256          DD(I,J,K)=(2.*XKX*(FSTAR(2,J,K)-FSTAR(I,J,K))/(DX(2)*DX(2))+YKY*(F
1257         1SSTAR(I,J+1,K)-2.*FSSTAR(I,J,K)+FSSTAR(I,J-1,K))/DY2+ETA(I,J,K)*FS
1258         2STAR(I,J,K)/DT2)*DZ2
1259          GO TO 68
1260  C
```

```
C      INSIDE THE CRACK
C
   63   B1=0.
        B2=0.
        G1=0.
        G2=0.
        D1=0.
        D2=0.
        Z1=0.
        Z2=0.
        IF (ABS(AF(I,J+1,K)-AF(I,J-1,K)).LT.1.E-25) GO TO 64
        B1=THETA*(AF(I,J+1,K)-AF(I,J-1,K))/SQRT(2.*DY*ABS(AF(I,J+1,K)-AF(I
       1,J-1,K)))
        G1=THETA/SQRT(2.*ABS(AF(I,J+1,K)-AF(I,J-1,K)))/DY)
   64   IF (ABS(FSSTAR(I,J+1,K)-FSSTAR(I,J-1,K)).LT.1.E-25) GO TO 65
        B2=THETA1*(FSSTAR(I,J+1,K)-FSSTAR(I,J-1,K))/SQRT(2.*DY*ABS(FSSTAR(
       1I,J+1,K)-FSSTAR(I,J-1,K)))
        G2=THETA1/SQRT(2.*ABS(FSSTAR(I,J+1,K)-FSSTAR(I,J-1,K)))/DY)
   65   BETA(I,J,K)=B1+B2
        GAMMA(I,J,K)=CKYZ(J,K)*(G1+G2)
        IF (ABS(AF(I,J,K+1)-AF(I,J,K-1)).LT.1.E-25) GO TO 66
        D1=THETA*(AF(I,J,K+1)-AF(I,J,K-1))/SQRT(2.*DZ*ABS(AF(I,J,K+1)-AF(I
       1,J,K-1)))
        Z1=THETA/SQRT(2.*ABS(AF(I,J,K+1)-AF(I,J,K-1)))/DZ)
   66   IF (ABS(FSSTAR(I,J,K+1)-FSSTAR(I,J,K-1)).LT.1.E-25) GO TO 67
        D2=THETA1*(FSSTAR(I,J,K+1)-FSSTAR(I,J,K-1))/SQRT(2.*DZ*ABS(FSSTAR(
       1I,J,K+1)-FSSTAR(I,J,K-1)))
        Z2=THETA1/SQRT(2.*ABS(FSSTAR(I,J,K+1)-FSSTAR(I,J,K-1)))/DZ)
   67   DELTA(I,J,K)=D1+D2
        ZETA(I,J,K)=CKYZ(J,K)*(Z1+Z2)
        ETA(I,J,K)=0.5*(THETA/SQRT(AF(I,J,K)+PRFUN)+THETA1/SQRT(FSSTAR(I,
       1,K)+PRFUN))
        BB(I,J,K)=2.*ZETA(I,J,K)+DZ2*ETA(I,J,K)/DT2
        DD(I,J,K)=(0.5*BETA(I,J,K)*(CKYZ(J+1,K)-CKYZ(J-1,K))/DY+GAMMA(I,J,
       1K)*(FSSTAR(I,J+1,K)-2.*FSSTAR(I,J,K)+FSSTAR(I,J-1,K))/DY2+0.5*DELT
       2A(I,J,K)*(CKYZ(J,K+1)-CKYZ(J,K-1))/DZ+ETA(I,J,K)*FSSTAR(I,J,K)/DT2
       3)*DZ2
   68   CONTINUE
C
C      ¤Y¤ NODE EQUALS ¤M¤
C
        ETA(I,M,K)=THETA/SQRT(AF(I,M,K)+PRFUN)+THETA1/SQRT(FSSTAR(I,M,K)+P
       1RFUN)
        BB(I,M,K)=2.*ZKZ+DZ2*ETA(I,M,K)/DT2
        DD(I,M,K)=(2.*XKX*(FSTAR(2,M,K)-FSTAR(I,M,K))/(DX(2)*DX(2))+YKY*2.
       1*(FSSTAR(I,M-1,K)-FSSTAR(I,M,K))/DY2+ETA(I,M,K)*FSSTAR(I,M,K)/DT2
       2*DZ2
C
C      ¤Y¤ NODE EQUALS ONE
C
        IF (DTOT(I,K).GT.0.) GO TO 69
C
C      OUTSIDE THE CRACK
C
        ETA(I,1,K)=THETA/SQRT(AF(I,1,K)+PRFUN)+THETA1/SQRT(FSSTAR(I,1,K)+P
       1RFUN)
        BB(I,1,K)=2.*ZKZ+DZ2*ETA(I,1,K)/DT2
        DD(I,1,K)=(2.*XKX*(FSTAR(2,1,K)-FSTAR(I,1,K))/(DX(2)*DX(2))+YKY*2.
       1*(FSSTAR(I,2,K)-FSSTAR(I,1,K))/DY2+ETA(I,1,K)*FSSTAR(I,1,K)/DT2)*D
       2Z2
```

```
      GO TO 74
C
C     INSIDE THE CRACK
C
 69   B1=0.
      B2=0.
      G1=0.
      G2=0.
      D1=0.
      D2=0.
      Z1=0.
      Z2=0.
      IF (ABS(AF(I,2,K)-AF(I,1,K)).LT.1.E-25) GO TO 70
      B1=THETA*(AF(I,2,K)-AF(I,1,K))/SQRT(DY*ABS(AF(I,2,K)-AF(I,1,K)))
      G1=THETA/SQRT(ABS(AF(I,2,K)-AF(I,1,K))/DY)
 70   IF (ABS(FSSTAR(I,2,K)-FSSTAR(I,1,K)).LT.1.E-25) GO TO 71
      B2=THETA1*(FSSTAR(I,2,K)-FSSTAR(I,1,K))/SQRT(DY*ABS(FSSTAR(I,2,K)-
     1FSSTAR(I,1,K)))
      G2=THETA1/SQRT(ABS(FSSTAR(I,2,K)-FSSTAR(I,1,K))/DY)
 71   BETA(I,1,K)=B1+B2
      GAMMA(I,1,K)=0.5*CKYZ(I,K)*(G1+G2)
      IF (ABS(AF(I,1,K+1)-AF(I,1,K-1)).LT.1.E-25) GO TO 72
      D1=THETA*(AF(I,1,K+1)-AF(I,1,K-1))/SQRT(2.*DZ*ABS(AF(I,1,K+1)-AF(I
     1,1,K-1)))
      Z1=THETA/SQRT(2.*ABS(AF(I,1,K+1)-AF(I,1,K-1))/DZ)
 72   IF (ABS(FSSTAR(I,1,K+1)-FSSTAR(I,1,K-1)).LT.1.E-25) GO TO 73
      D2=THETA1*(FSSTAR(I,1,K+1)-FSSTAR(I,1,K-1))/SQRT(2.*DZ*ABS(FSSTAR(
     1I,1,K+1)-FSSTAR(I,1,K-1)))
      Z2=THETA1/SQRT(2.*ABS(FSSTAR(I,1,K+1)-FSSTAR(I,1,K-1))/DZ)
 73   DELTA(I,1,K)=D1+D2
      ZETA(I,1,K)=CKYZ(I,K)*(Z1+Z2)
      ETA(I,1,K)=0.5*(THETA/SQRT(AF(I,1,K)+PRFUN)+THETA1/SQRT(FSSTAR(I,1
     1,K)+PRFUN))
      BB(I,1,K)=2.*ZETA(I,1,K)+DZ2*ETA(I,1,K)/DT2
      DD(I,1,K)=(BETA(I,1,K)*(CKYZ(2,K)-CKYZ(1,K))/DY+GAMMA(I,1,K)*2.*(F
     1SSTAR(I,2,K)-FSSTAR(I,1,K))/DY2+0.5*DELTA(I,1,K)*(CKYZ(1,K+1)-CKYZ
     2(1,K-1))/DZ+ETA(I,1,K)*FSSTAR(I,1,K)/DT2)*DZ2
C
C     ¤X¤ DIRECTION INTERNAL NODES
C
 74   DO 75 J=2,MM1
      DO 75 I=2,LM1
C
C     ¤Y¤ DIRECTION INTERNAL NODES
C
      ETA(I,J,K)=THETA/SQRT(AF(I,J,K)+PRFUN)+THETA1/SQRT(FSSTAR(I,J,K)+P
     1RFUN)
      BB(I,J,K)=2.*ZKZ+DZ2*ETA(I,J,K)/DT2
      DD(I,J,K)=(2.*XKX*((FSTAR(I+1,J,K)-FSTAR(I,J,K))/DX(I+1)-(FSTAR(I,
     1J,K)-FSTAR(I-1,J,K))/DX(I))/(DX(I+1)+DX(I))+YKY*(FSSTAR(I,J+1,K)-2
     2.*FSSTAR(I,J,K)+FSSTAR(I,J-1,K))/DY2+ETA(I,J,K)*FSSTAR(I,J,K)/DT2)
     3*DZ2
 75   CONTINUE
C
C     ¤Y¤ NODE EQUALS ¤M¤
C
      DO 76 I=2,LM1
      ETA(I,M,K)=THETA/SQRT(AF(I,M,K)+PRFUN)+THETA1/SQRT(FSSTAR(I,M,K)+P
     1RFUN)
      BB(I,M,K)=2.*ZKZ+DZ2*ETA(I,M,K)/DT2
```

```
      DD(I,M,K)=(2.*XKX*((FSTAR(I+1,M,K)-FSTAR(I,M,K))/DX(I+1)-(FSTAR(I,
     1M,K)-FSTAR(I-1,M,K))/DX(I)))/(DX(I+1)+DX(I))+YKY*2.*(FSSTAR(I,MM1,K
     2)-FSSTAR(I,M,K))/DY2+ETA(I,M,K)*FSSTAR(I,M,K)/DT2)*DZ2
C
C     ¤Y¤ NODE EQUALS 1
C
      ETA(I,1,K)=1HETA/SQRT(AF(I,1,K)+PRFUN)+THETA1/SQRT(FSSTAR(I,1,K)+P
     1RFUN)
      BB(I,1,K)=2.*ZKZ+DZ2*ETA(I,1,K)/DT2
      DD(I,1,K)=(2.*XKX*((FSTAR(I+1,1,K)-FSTAR(I,1,K))/DX(I+1)-(FSTAR(I,
     11,K)-FSTAR(I-1,1,K))/DX(I)))/(DX(I+1)+DX(I))+YKY*2.*(FSSTAR(I,2,K)-
     2FSSTAR(I,1,K))/DY2+ETA(I,1,K)*FSSTAR(I,1,K)/DT2)*DZ2
 76   CONTINUE
C
C     ¤X¤ NODE EQUAL TO ¤L¤
C
      DO 77 J=2,MM1
      ETA(L,J,K)=THETA/SQRT(AF(L,J,K)+PRFUN)+THETA1/SQRT(FSSTAR(L,J,K)+P
     1RFUN)
      BB(L,J,K)=2.*ZKZ+DZ2*ETA(L,J,K)/DT2
      DD(L,J,K)=(XKX*2.*(FSTAR(LM1,J,K)-FSTAR(L,J,K))/'DX(L)*DX(L))+YKY*
     1(FSSTAR(L,J+1,K)-2.*FSSTAR(L,J,K)+FSSTAR(L,J-1,K))/DY2+ETA(L,J,K)*
     2FSSTAR(L,J,K)/DT2)*DZ2
 77   CONTINUE
C
C     ¤X¤ NODE EQUAL ¤L¤ AND ¤Y¤ NODE EQUAL ¤M¤
C
      ETA(L,M,K)=THETA/SQRT(AF(L,M,K)+PRFUN)+THETA1/SQRT(FSSTAR(L,M,K)+P
     1RFUN)
      BB(L,M,K)=2.*ZKZ+DZ2*ETA(L,M,K)/DT2
      DD(L,M,K)=(XKX*2.*(FSTAR(LM1,M,K)-FSTAR(L,M,K))/(DX(L)*DX(L))+YKY*
     12.*(FSSTAR(L,MM1,K)-FSSTAR(L,M,K))/DY2+ETA(L,M,K)*FSSTAR(L,M,K)/DT
     22)*DZ2
C
C     ¤X¤ NODE EQUALS ¤L¤ AND ¤Y¤ NODE EQUALS ONE
C
      ETA(L,1,K)=THETA/SQRT(AF(L,1,K)+PRFUN)+THETA1/SQRT(FSSTAR(L,1,K)+P
     1RFUN)
      BB(L,1,K)=2.*ZKZ+DZ2*ETA(L,1,K)/DT2
      DD(L,1,K)=(XKX*2.*(FSTAR(LM1,1,K)-FSTAR(L,1,K))/(DX(L)*DX(L))+YKY*
     12.*(FSSTAR(L,2,K)-FSSTAR(L,1,K))/DY2+ETA(L,1,K)*FSSTAR(L,1,K)/DT2)
     2*DZ2
 78   CONTINUE
C
C     CALCULATE EE(I,J,K) AND FF(I,J,K) FOR ¤Z¤ NODES BETWEEN 1 AND NM1.
C     USE NEUMANN CONDITION FOR K=1 (DFSSTAR/DZ=0.) IN REGION WHERE
C     AF(I,J,1) IS NOT SPECIFIED AS INPUT AND DIRICHLET CONDITION WHERE
C     AF(I,J,1) IS SPECIFIED EQUAL TO FSSTAR(I,J,1).  USE THE RECURSION
C     RELATIONSHIP FOR ALL OTHER ¤Z¤ NODES.
C
      DO 83 J=1,M
      DO 83 I=1,L
      IF (I.LE.L2.AND.J.LE.M2) GO TO 79
      EE(I,J,1)=1.
      FF(I,J,1)=0.
      GO TO 80
 79   EE(I,J,1)=0.
      FF(I,J,1)=FSSTAR(I,J,1)
 80   DO 82 K=2,NM1
      IF (DTOT(J,K).GT.0..AND.I.EQ.1) GO TO 81
```

```
1441 C
1442 C      OUTSIDE THE CRACK
1443 C
1444         DEN=BB(I,J,K)-ZKZ*EE(I,J,K-1)
1445         EE(I,J,K)=ZKZ/DEN
1446         FF(I,J,K)=(DD(I,J,K)+ZKZ*FF(I,J,K-1))/DEN
1447         GO TO 82
1448 C
1449 C      INSIDE THE CRACK
1450 C
1451   81    DEN=BB(I,J,K)-ZETA(I,J,K)*EE(I,J,K-1)
1452         EE(I,J,K)=ZETA(I,J,K)/DEN
1453         FF(I,J,K)=(DD(I,J,K)+ZETA(I,J,K)*FF(I,J,K-1))/DEN
1454   82    CONTINUE
1455   83    CONTINUE
1456 C
1457 C      CALCULATE VALUES OF AF(I,J,K) -- THE LAST VALUE OF F(I,J,K) AFTER
1458 C      COMPLETION OF ALL EXPLICIT AND IMPLICIT CALCULATIONS.  THE VALUE
1459 C      OF F(I,J,N) IS ALWAYS EQUAL TO ZERO.  COMPARE VALUES OF AF(I,J,K)
1460 C      WITH PREVIOUS VALUES AND ITERATE THROUGH ¤Z¤ DIRECTION
1461 C      CALCULATIONS IF CONVERGENCE NOT OBTAINED.
1462 C
1463 C
1464         IZ=0
1465         DO 85 J=1,M
1466         DO 85 I=1,L
1467         DO 84 K=1,NM2
1468         NB=N-K
1469         AAF=AF(I,J,NB)
1470         AF(I,J,NB)=EE(I,J,NB)*AF(I,J,NB+1)+FF(I,J,NB)
1471         COMPARE=ABS(AF(I,J,NB)-AAF)/AAF
1472         IF (COMPARE.LT.0.001.OR.AF(I,J,NB).EQ.AAF) GO TO 84
1473         IZ=IZ+1
1474   84    CONTINUE
1475         IF (I.LE.L2.AND.J.LE.M2) GO TO 85
1476         AF(I,J,1)=AF(I,J,2)
1477   85    CONTINUE
1478         IF (IZ.EQ.0) GO TO 86
1479         ITERZ=ITERZ+1
1480         IF (ITERZ.LT.2) GO TO 62
1481 C
1482 C      COMPARE TOTAL COMBINED ¤X¤, ¤Y¤, AND ¤Z¤ IMPLICIT LOOPS AND
1483 C      ITERATE THROUGH ALL IMPLICIT CALCULATIONS IF CONVERGENCE IS NOT
1484 C      OBTAINED.
1485 C
1486   86    IT=0
1487         DO 88 I=1,L
1488         DO 88 J=1,M
1489         DO 88 K=1,N
1490         IF (AF(I,J,K).GT.FMAX) GO TO 91
1491         COMPARE=ABS(AFF(I,J,K)-AF(I,J,K))/AFF(I,J,K)
1492         IF (COMPARE.LT.0.001.OR.AFF(I,J,K).EQ.AF(I,J,K)) GO TO 87
1493         IT=IT+1
1494   87    AFF(I,J,K)=AF(I,J,K)
1495   88    CONTINUE
1496         IF (IT.EQ.0) GO TO 89
1497         ITERT=ITERT+1
1498         IF (ITERT.LT.2) GO TO 6
1499 C
1500 C      UPDATE VALUES OF F IF CONVERGENCE IS SATISFACTORY
```

```
1501 C
1502  89    DO 90 J=1,M
1503        DO 90 I=1,L
1504        DO 90 K=1,NM1
1505        F(I,J,K)=AF(I,J,K)
1506  90    CONTINUE
1507        RETURN
1508  91    WRITE (59,92) I,J,K
1509        CALL EXIT(1)
1510 C
1511  92    FORMAT (65HCONVERGENCE FAILURE IN SUBROUTINE FLOW, REDUCE TIME STE
1512       1P, I,J,K= ,3I5)
1513        END
```

SAMPLE INPUT

```
2.25     0.0001    4.0        500000.   0.25     0.30     0.30     4.0
 10     5  100    7     5
13.5     0.02      0.1        1488.5    53.3     0.01     520.
1[illegible].     60.      0.700000361755.
```

SAMPLE OUTPUT

```
[illegible] EPS.FRAC[illegible]
 [illegible]  [illegible]E-04  4.00000E+00  5.00000E+0[illegible]  2.50000E-01  3.00000E-01  3.00000E-01  4.00000E+00
[illegible] NTOT.NYTIP1.NZTIP1*
 [illegible]  [illegible]  10  15  20  1[illegible]  2  100  7  5
[illegible] SIZE,TEMP*
 [illegible]  [illegible]E-02  1.00000E-01  1.48850E+03  5.33000E+01  1.00000E-02  5.20000E+02
[illegible]
 [illegible]  [illegible]E+0[illegible]  [illegible]E-07  1.[illegible]E+0[illegible]  3.35909E+02  5.74261E-06  3.74349E+03
[illegible]
 [illegible]  [illegible]E-0[illegible]  [illegible]E-01  7.03547E-01  1.66762E+00
 [illegible]  [illegible]E+0[illegible]  [illegible]E+01  4.44062E+0[illegible]  1.00000E+02
```

[illegible]	[illegible]	[illegible]	.94745	.94745	.94745	.94745	.94749	.94745	.94745
[illegible]	[illegible]	[illegible]	.94745	.94745	.94745	.94745	.94745	.94745	.94745
.94745	[illegible]	[illegible]	.94745	.94745	.94745	.94745	.94745	.94745	.94745
[illegible]	[illegible]	[illegible]	[illegible]	.55106	[illegible]	.00385	.00000	.00000	.00000
[illegible]	[illegible]	[illegible]	.55426	.47899	.21773	.00421	.00000	.00000	.00000
[illegible]	[illegible]	[illegible]	.50477	.41777	.12165	.00094	.00000	.00000	.00000
[illegible]	[illegible]	[illegible]	.45549	.36855	.07846	.00035	.00000	.00000	.00000
[illegible]	[illegible]	[illegible]	[illegible]	.32031	.04892	.00013	.00000	.00000	.00000
[illegible]	[illegible]	[illegible]	.35815	.25506	.02196	.00003	.00000	.00000	.00000
[illegible]	[illegible]	[illegible]	.27917	.13458	.00332	.00000	.00000	.00000	.00000
[illegible]	[illegible]	[illegible]	.04986	.00100	.00000	.00000	.00000	.00000	.00000
[illegible]	[illegible]	.00000	.00000	.00000	.00000	.00000	.00000	.00000	.00000
[illegible]	[illegible]	.00000	.00000	.00000	.00000	.00000	.00000	.00000	.00000
[illegible]	[illegible]	[illegible]	.00000	.00000	.00000	.00000	.00000	.00000	.00000
[illegible]	[illegible]	[illegible]	.00000	.00000	.00000	.00000	.00000	.00000	.00000

[illegible]	[illegible]	30115	.76429	.67434	[illegible]	.02209	.00150	.00143	.00149
[illegible]	[illegible]	.30114	[illegible]	.67434	.42776	.02209	.00150	.00149	.00149
[illegible]	[illegible]	[illegible]	[illegible]	.65360	.40630	.01977	.00150	.00149	.00149
[illegible]	[illegible]	.67296	[illegible]	.55106	[illegible]	.00885	.00000	.00000	.00000
[illegible]	[illegible]	[illegible]	.56426	.47999	.21773	.00421	.00000	.00000	.00000
[illegible]	[illegible]	[illegible]	.50477	.41777	.12165	.00094	.00000	.00000	.00000
[illegible]	[illegible]	.45951	.45549	.36855	.07846	.00035	.00000	.00000	.00000
[illegible]	[illegible]	.44591	[illegible]	.32031	.04892	.00013	.00000	.00000	.00000
[illegible]	[illegible]	[illegible]	.35815	.25506	.02196	.00003	.00000	.00000	.00000
[illegible]	[illegible]	.32978	.27917	.13468	.00332	.00000	.00000	.00000	.00000
[illegible]	[illegible]	.13337	.04986	.00100	.00000	.00000	.00000	.00000	.00000
[illegible]	.00000	.00000	.00000	.00063	.00000	.00000	.00000	.00000	.00000
[illegible]	.00000	.00000	.00000	.00000	.00000	.00000	.00000	.00000	.00000
[illegible]	[illegible]	.00000	.00000	.00000	.00000	.00000	.00000	.00000	.00000
[illegible]	[illegible]	.00000	.00000	.00000	.00000	.00000	.00000	.00000	.00000

[illegible]	[illegible]	[illegible]	.66941	.59166	.32964	.01121	.00000	.00000	.00000
[illegible]	[illegible]	[illegible]	.66941	.59166	.32964	.01121	.00000	.00000	.00000
[illegible]	[illegible]	[illegible]	.65404	.56632	.31410	.01007	.00000	.00000	.00000
[illegible]	.65490	.64001	.60541	.51999	.26416	.00671	.00000	.00000	.00000
[illegible]	[illegible]	.58467	.55030	.46716	.20334	.00358	.00000	.00000	.00000
.59412	[illegible]	.53257	[illegible]	.41021	.11224	.00077	.00000	.00000	.00000
[illegible]	.50115	.49626	.45131	.36456	.07623	.00033	.00000	.00000	.00000
.46474	.45815	.44283	.40682	.31764	.04804	.00013	.00000	.00000	.00000
.42158	.41578	.39668	.35617	.25399	.02197	.00003	.00000	.00000	.00000
[illegible]	[illegible]	.13012	.28870	.13934	.00370	.00000	.00000	.00000	.00000
[illegible]	[illegible]	[illegible]	[illegible]	.00226	.00000	.00000	.00000	.00000	.00000
[illegible]	[illegible]	[illegible]	.00000	.00000	.00000	.00000	.00000	.00000	.00000
[illegible]	[illegible]	[illegible]	.00000	.00000	.00000	.00000	.00000	.00000	.00000
[illegible]	[illegible]	.00000	.00000	.00000	.00000	.00000	.00000	.00000	.00000
[illegible]	[illegible]	.00000	.00000	.00000	.00000	.00000	.00000	.00000	.00000

P(I,J,4)=

.65175	.64413	.62938	.59498	.50994	.25313	.00606	.00000	.00000	.00000
.65053	.64408	.62930	.59498	.50994	.25313	.00606	.00000	.00000	.00000
.64121	.63474	.62011	.58589	.50125	.24382	.00556	.00000	.00000	.00000
.61517	.60978	.59435	.56057	.47687	.21650	.00420	.00000	.00000	.00000
[illegible]	.57102	.55760	.52431	.44163	.17462	.00250	.00000	.00000	.00000
.53745	.53007	.51600	.48111	.39428	.09579	[illegible]	.00000	.00000	.00000
.49687	.49026	.47545	.44068	.35453	.07095	.00029	.00000	.00000	.00000
.45713	.45035	.43506	.39914	.31023	.04979	.00011	.00000	.00000	.00000
.41549	.40744	.39093	.35063	.24944	.02179	.00003	.00000	.00000	.00000
[illegible]	.34962	.32901	.27977	.14130	.00392	.00000	.00000	.00000	.00000
.23977	.22420	.19098	.10609	.00467	.00000	.00000	.00000	.00000	.00000
.00001	.00001	.00001	.00000	.00000	.00000	.00000	.00000	.00000	.00000
.00000	.00000	.00000	.00000	.00000	.00000	.00000	.00000	.00000	.00000
.00000	.00000	.00000	.00000	.00000	.00000	.00000	.00000	.00000	.00000
.00000	.00000	.00000	.00000	.00000	.00000	.00000	.00000	.00000	.00000

P(I,J,5)=

.58813	.58115	.56700	.53293	.45179	.19131	.00321	.00000	.00000	.00000
.58747	.58112	.56700	.53293	.45179	.19131	.00321	.00000	.00000	.00000
.58192	.57569	.56161	.52862	.44677	.18615	.00298	.00000	.00000	.00000
.56705	.56086	.54655	.51415	.43283	.17066	.00247	.00000	.00000	.00000
.54292	.53677	.52291	.49041	.40978	.14767	.00161	.00000	.00000	.00000
.51260	.50637	.49230	.45933	.37750	.10127	.00062	.00000	.00000	.00000
.47900	.47264	.45712	.42409	.33994	.06609	.00026	.00000	.00000	.00000
.44707	.43715	.42186	.37595	.29724	.04064	.00009	.00000	.00000	.00000
.40541	.39799	.38102	.34001	.24004	.01984	.00002	.00000	.00000	.00000
.35411	.34493	.32458	.27594	.13391	.00352	.00000	.00000	.00000	.00000
.24985	.23473	.20225	.12131	.00636	.00001	.00000	.00000	.00000	.00000
.00001	.00001	.00001	.00000	.00000	.00000	.00000	.00000	.00000	.00000
.00000	.00000	.00000	.00000	.00000	.00000	.00000	.00000	.00000	.00000
.00000	.00000	.00000	.00000	.00000	.00000	.00000	.00000	.00000	.00000
.00000	.00000	.00000	.00000	.00000	.00000	.00000	.00000	.00000	.00000

P(I,J,6)=

.53374	.52730	.51365	.48170	.40231	.14062	.00157	.00000	.00000	.00000
.53332	.52715	.51365	.48170	.40231	.14062	.00157	.00000	.00000	.00000
.53007	.52400	.51036	.47847	.39910	.13673	.00147	.00000	.00000	.00000
[illegible]	[illegible]	.50125	.46947	.39049	.12611	.00121	.00000	.00000	.00000
.50402	.49681	.48524	.45246	.37464	.11015	.00090	.00000	.00000	.00000
.48263	.47652	.46213	.43042	.35041	.08575	.00047	.00000	.00000	.00000
[illegible]	.44947	.43597	.40173	.31812	.05510	.00015	.00000	.00000	.00000
.42570	.41890	.40353	.36740	.27821	.03335	.00007	.00000	.00000	.00000
.38118	.37363	.35661	.32674	.22447	.01643	.00002	.00000	.00000	.00000
.34577	.33602	.31583	.26769	.13308	.00355	.00000	.00000	.00000	.00000
[illegible]	.23576	.20754	.12381	.00679	.00001	.00000	.00000	.00000	.00000
.00001	.00001	.00001	.00000	.00000	.00000	.00000	.00000	.00000	.00000
.00000	.00000	.00000	.00000	.00000	.00000	.00000	.00000	.00000	.00000
.00000	.00000	.00000	.00000	.00000	.00000	.00000	.00000	.00000	.00000
.00000	.00000	.00000	.00000	.00000	.00000	.00000	.00000	.00000	.00000

P(I,J,7)=

.49626	.48001	.46668	.43549	.35816	.09354	.00073	.00000	.00000	.00000
.48583	.48000	.46668	.43549	.35816	.09354	.00073	.00000	.00000	.00000
.48374	.47785	.46459	.43337	.35609	[illegible]	.00070	.00000	.00000	.00000
.47756	.47177	.45842	.42713	.34995	.08167	.00060	.00000	.00000	.00000
[illegible]	.46015	.44712	.41566	[illegible]	.07001	.00044	.00000	.00000	.00000
.45006	.44395	.43017	.39789	.31827	.06223	.00025	.00000	.00000	.00000
.42832	.42238	.40786	.37379	.28989	.04250	.00011	.00000	.00000	.00000
.40336	.39645	.38082	.34405	.25280	.02588	.00004	.00000	.00000	.00000
.37283	.36517	.34786	.30683	.20156	.01235	.00001	.00000	.00000	.00000
.33180	.32284	.30273	.25477	.11894	.00276	.00000	.00000	.00000	.00000
.24884	.23410	.20214	.12266	.00664	.00001	.00000	.00000	.00000	.00000
.00001	.00001	.00001	.00000	.00000	.00000	.00000	.00000	.00000	.00000
.00000	.00000	.00000	.00000	.00000	.00000	.00000	.00000	.00000	.00000
.00000	.00000	.00000	.00000	.00000	.00000	.00000	.00000	.00000	.00000
.00000	.00000	.00000	.00000	.00000	.00000	.00000	.00000	.00000	.00000

P(I,J,8)=

.44316	.43700	.42364	.39235	.31516	.06529	.00029	.00000	.00000	.00000
.44290	.43699	.42364	.39235	.31516	.06529	.00029	.00000	.00000	.00000
.44140	.43548	.42213	.39085	.31369	.06446	.00028	.00000	.00000	.00000
.43707	.43112	.41766	.38614	.30844	.06016	.00024	.00000	.00000	.00000
.42692	.42287	.40916	.37713	.29822	.05255	.00018	.00000	.00000	.30000
.41638	.41009	.39588	.36254	.28048	.04081	.00011	.00000	.00000	.00000
.39935	.39269	.37764	.34222	.25463	.02831	.00005	.00000	.00000	.00000
.37783	.37068	.35449	.31622	.21986	.01718	.00002	.00000	.00000	.00000
.35100	.34311	.32525	.28269	.17004	.00772	.00001	.00000	.00000	.00000
.31439	.30540	.28519	.23675	.09629	.00167	.00000	.00000	.00000	.00000
.23956	.22498	.19324	.11324	.00552	.00001	.00000	.00000	.00000	.00000
.00001	.00001	.00001	.00000	.00000	.00000	.00000	.00000	.00000	.00000
.00000	.00000	.00000	.00000	.00000	.00000	.00000	.00000	.00000	.00000
.00000	.00000	.00000	.00000	.00000	.00000	.00000	.00000	.00000	.00000
.00000	.00000	.00000	.00000	.00000	.00000	.00000	.00000	.00000	.00000

P(I,J,9)=

.40315	.39677	.38267	.34965	.26840	.03720	.00009	.00000	.00000	.00000
.40294	.39673	.38267	.34965	.26840	.03720	.00009	.00000	.00000	.00000
.40151	.39560	.38156	.34858	.26743	.03698	.00009	.00000	.00000	.00000
.39855	.39236	.37805	.34465	.26240	.03431	.00008	.00000	.00000	.00000
.39229	[illegible]	.37139	.33771	.25297	.02997	.00006	.00000	.00000	.00000
.38236	[illegible]	[illegible]	.32477	.23999	.02313	.00004	.00000	.00000	.00000
.36877	.36133	.34533	.30748	.21196	.01607	.00002	.00000	.00000	.00000
.34999	.34245	.32537	.28456	.17798	.00925	.00001	.00000	.00000	.00000
.32626	.31909	.29958	.25512	.13059	.00379	.00000	.00000	.00000	.00000
.29271	.28357	.26301	.21392	.06611	.00068	.00000	.00000	.00000	.00000
.22163	.20716	.17551	.09370	.00359	.00000	.00000	.00000	.00000	.00000
.00001	.00001	.00000	.00000	.00000	.00000	.00000	.00000	.00000	.00000
.00000	.00000	.00000	.00000	.00000	.00000	.00000	.00000	.00000	.00000
.00000	.00000	.00000	.00000	.00000	.00000	.00000	.00000	.00000	.00000
.00000	.00000	.00000	.00000	.00000	.00000	.00000	.00000	.00000	.00000

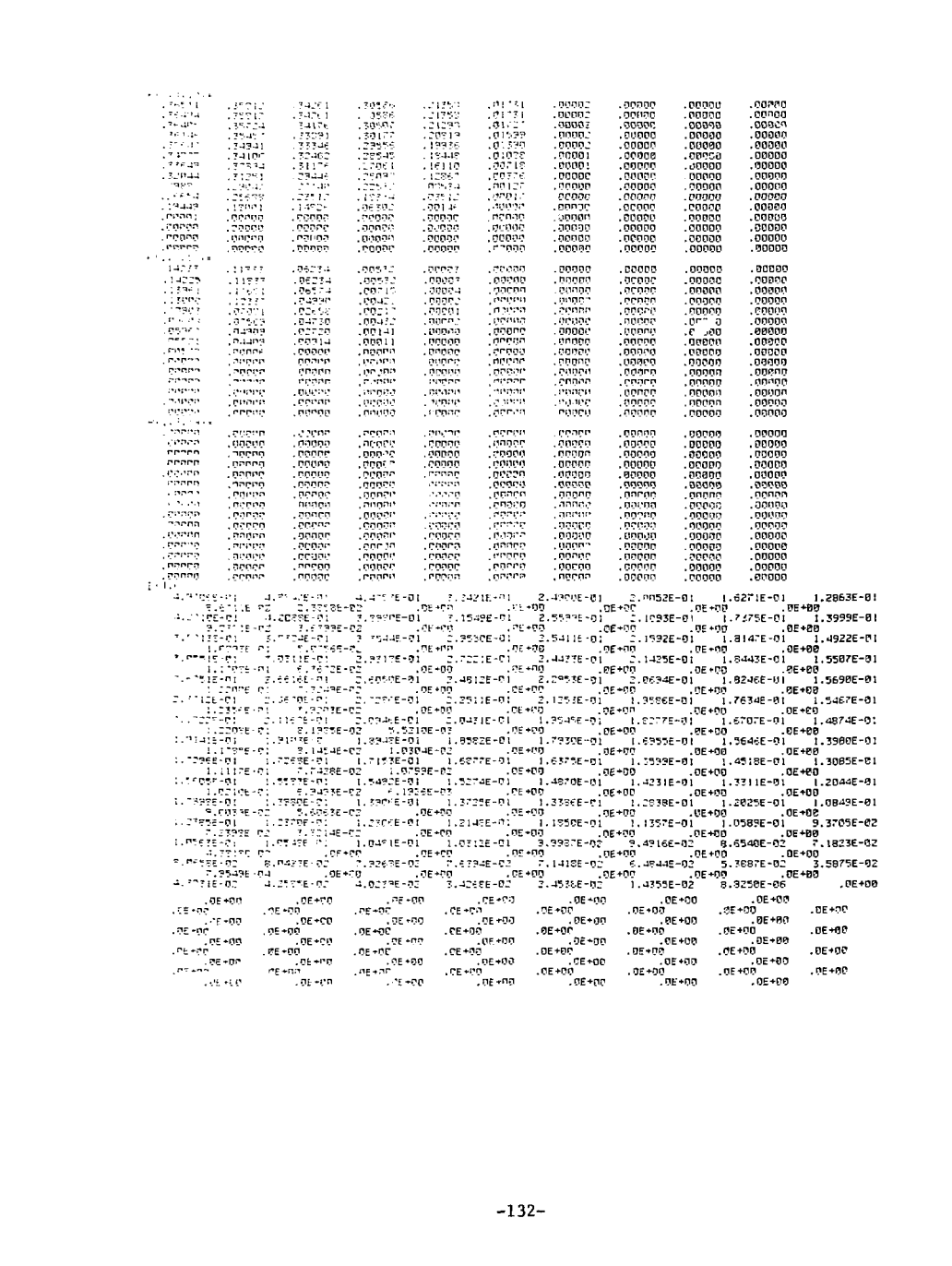

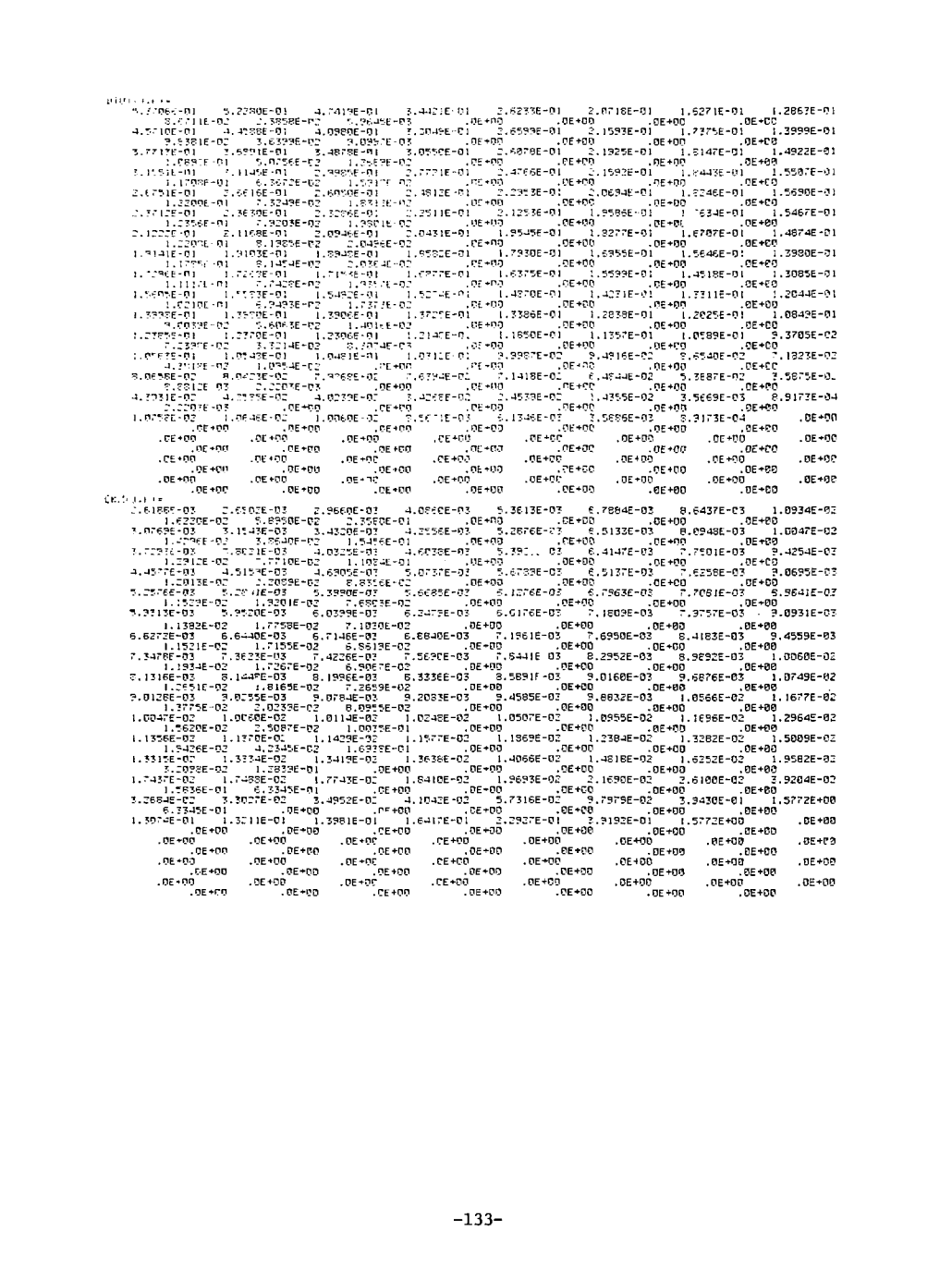

```
[illegible]
 [illegible]     [illegible]     [illegible]     [illegible]     [illegible]     [illegible]     4.0794E+07     2.562[illegible]E+07
     [illegible]     2.4848E+06     [illegible]     .0E+00     .0E+00     .0E+00     .0E+00
 4.41[illegible]     4.4[illegible]     4.629[illegible]     [illegible]     [illegible]     7.5627E+07     4.6517E+07     3.0001E+07
     1.7195E+07     4.6945E+06     [illegible]     .0E+00     .0E+00     .0E+00     .0E+00
 [illegible]     [illegible]     2.6[illegible]     1.5[illegible]     1.21[illegible]     7.9166E+07     5.1471E+07     3.4307E+07
     [illegible]     [illegible]     [illegible]     .0E+00     .0E+00     .0E+00     .0E+00
 [illegible]     [illegible]     [illegible]     [illegible]     [illegible]     [illegible]     5.7369E+07     3.7190E+07
     [illegible]     [illegible]     [illegible]     .0E+00     .0E+00     .0E+00     .0E+00
 [illegible]     [illegible]     1.1247E+08     [illegible]     [illegible]     6.7334E+07     5.1[illegible]     3.7629E+07
     [illegible]     1.1[illegible]     [illegible]     .0E+00     .0E+00     .0E+00     .0E+00
 [illegible]     [illegible]     9.13[illegible]     [illegible]     [illegible]     5.67[illegible]     4.7026E+07     3.6213E+07
     [illegible]     1.2[illegible]     1.[illegible]     .0E+00     .0E+00     .0E+00     .0E+00
 6.[illegible]     [illegible]     6.1444E+07     [illegible]     5.5[illegible]     4.[illegible]     4.0541E+07     3.2[illegible]
     [illegible]     1.[illegible]     [illegible]     .0E+00     .0E+00     .0E+00     .0E+00

 4.711[illegible]E+07     4.7[illegible]E+07     4.7341E+07     4.[illegible]     4.4231E+07     4.0184E+07     3.4726E+07     2.9399E+07
     2.13[illegible]     1.2518E+07     1.7[illegible]     .0E+00     .0E+00     .0E+00     .0E+00
 [illegible]     3.6[illegible]E+07     3.6974E+07     3.[illegible]E+07     3.5304E+07     3.2643E+07     2.9519E+07     2.4225E+07
     1.6[illegible]E+07     1.1176E+07     1.[illegible]15E+06     .0E+00     .0E+00     .0E+00     .0E+00
 2.[illegible]E+07     2.9[illegible]E+07     2.9034E+07     2.8793E+07     2.7932E+07     2.6212E+07     2.3589E+07     2.0082E+07
     1.[illegible]30E+07     9.2808E+06     1.2[illegible]E+06     .0E+00     .0E+00     .0E+00     .0E+00
 2.2[illegible]E+07     2.2639E+07     2.2734E+07     2.2562E+07     2.1995E+07     2.0748E+07     1.9629E+07     1.6134E+07
     [illegible]     6.7517E+06     8.71[illegible]E+05     .0E+00     .0E+00     .0E+00     .0E+00
 1.[illegible]     1.75[illegible]E+07     1.7594E+07     1.7447E+07     1.[illegible]E+07     1.5073E+07     1.4536E+07     1.2324E+07
     8.7[illegible]E+06     3.2014E+06     3.4072E+05     .0E+00     .0E+00     .0E+00     .0E+00
 1.3201E+07     1.3[illegible]E+07     1.3170E+07     1.[illegible]E+07     1.2546E+07     1.1695E+07     1.0313E+07     9.1426E+06
     4.7809E+06     5.6779E+05     .0E+00     .0E+00     .0E+00     .0E+00     .0E+00
 8.6698E+06     8.6[illegible]E+06     8.5590E+06     8.3133E+06     7.95[illegible]     6.9342E+06     5.5874E+06     3.1920E+06
     3.8146E+05     3.0205E+04     .0E+00     .0E+00     .0E+00     .0E+00     .0E+00
 3.2490E+06     3.2275E+06     3.0926E+06     2.5166E+06     1.5187E+06     6.7220E+05     7.7811E+04     8.531[illegible]
     2.2935E+04     .0E+00     .0E+00     .0E+00     .0E+00     .0E+00     .0E+00
 2.9221E+05     2.9973E+05     2.6695E+05     2.0020E+05     1.0307E+05     4.0445E+04     3.2814E+03     .0E+00
     .0E+00     .0E+00     .0E+00     .0E+00     .0E+00     .0E+00     .0E+00
 .0E+00     .0E+00     .0E+00     .0E+00     .0E+00     .0E+00     .0E+00     .0E+00
     .0E+00     .0E+00     .0E+00     .0E+00     .0E+00     .0E+00     .0E+00
 .0E+00     .0E+00     .0E+00     .0E+00     .0E+00     .0E+00     .0E+00     .0E+00
     .0E+00     .0E+00     .0E+00     .0E+00     .0E+00     .0E+00     .0E+00
 .0E+00     .0E+00     .0E+00     .0E+00     .0E+00     .0E+00     .0E+00     .0E+00
     .0E+00     .0E+00     .0E+00     .0E+00     .0E+00     .0E+00     .0E+00
N,TIE(J)=
     16     15     16     16     16     16     16     15     15     13
      0      0      0      0      0
 TIME,DT=     1.600E+00     1.000E-04
```


GPO 690-431/202